

UCSF

UC San Francisco Electronic Theses and Dissertations

Title

Regulatory interactions at the dimer interface of Kaposi's Sarcoma-associated herpesvirus protease

Permalink

<https://escholarship.org/uc/item/4rk244p1>

Author

Pray, Todd Richard

Publication Date

2000

Peer reviewed|Thesis/dissertation

Regulatory Interactions at the Dimer Interface of Kaposi's Sarcoma-
Associated Herpesvirus Protease

by

Todd Richard Pray

DISSERTATION

Submitted in partial satisfaction of the requirements for the degree of

DOCTOR OF PHILOSOPHY

in

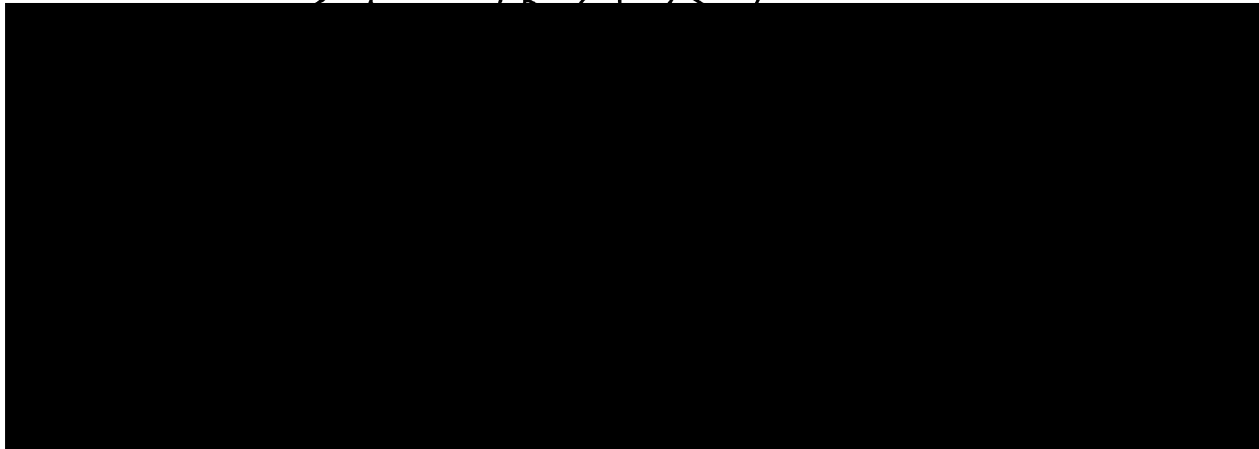
BIOPHYSICS

in the

GRADUATE DIVISION

of the

UNIVERSITY OF CALIFORNIA SAN FRANCISCO



Date

University Librarian

Degree Conferred:

copyright 2000

by

Todd Richard Pray

This manuscript is dedicated to Meilee Chen, to whom I owe an incredible debt of gratitude for her many years of love, care, compassion and support. There will always be a special place for her in my heart and soul, no matter how many miles separate us.

It is also dedicated to my friends; in particular Kinkead Reiling, Sandy Waugh and Andrew Bogan; and family; especially my brother Mickey Pray and sister Laura Schroeder, who helped me so much through the troubles of this past year.

Finally, I would like to thank Laura Koo for her friendship, companionship, advice and encouragement. She has helped me realize what it is to be happy again.

Preface

As with any body of work, this one has not been a solitary labor. I have been lucky enough to toil with some incredible collaborators over these past four years, and must thank them all.

The project I have been involved in, studying the relationship between the structure and function of the protease encoded by Kaposi's sarcoma-associated herpesvirus (KSHV), was borne out of a collaboration between the Craik lab and Prof. Don Ganem. Don, a member of my thesis committee, has provided innumerable pieces of advice and encouragement over the years, and it has been a privilege to have met and interacted with him. His post-doc, Dr. Michael Lagunoff, has been a friend for many years, beginning back in my college days, and has also helped along the way with countless conversations on both technical and personal issues. Dr. Jean Chang, a former student in the Ganem lab, also provided insight into aspects of this work. I must also extend my warmest thanks to all of the Ganem lab members, for both their friendship and the knowledge they have imparted to me regarding KSHV and virology in general.

The second research group with whom I have had the pleasure to work with is that of Prof. Paul Ortiz de Montellano. Paul's enthusiasm for the KSHV protease (KSHV Pr) project continues, and four of his coworkers have had an impact on the search for inhibitors of KSHV Pr. Drs. Zhou-Peng Zhang, Patricia Traylor and Alex Aranov were involved in the earlier stages of the development of possible anti-KSHV Pr compounds. Alan Marnett, a joint student with the Craik lab, continues this work with great diligence, between hilarious, smart-assed comments, focusing on an interesting blend of structure-

based and combinatorial screening methods. I wish him the best of luck in the coming years.

A third group which with we have a most fruitful collaboration is that of Prof. Robert Stroud. Bob has contributed not only to the KSHV Pr project through conversations and the commitment of resources to solving the crystal structure of the enzyme, but also through his enthusiasm and constructive criticism as a member of my thesis committee. Kinkead Reiling, his student and one of my best friends, was incredibly persistent, diligent, and clever in refining the KSHV Pr structure. It has been an absolute joy and blessing to work with them both.

And last but not least is the Craik group itself. Every member of the lab, from Charly on down, have helped in some way over the past four years. I am afraid I may neglect to mention a few important names, but all should know that graduate school would not have been the same without them for me. After having worked in number of labs earlier in my career, I can honestly say that I have never seen such a collegial, supportive, goofy and intelligent group of people in a single lab. Dr. Ayçe Ünal, one of the sweetest people I have ever met, was the post-doc responsible for initiating the KSHV Pr project, and was a pleasure to work with on the early stages of our studies. Anson Nomura, who was a rotation student with me in my second year at UCSF, made a great contribution to the project, and has since joined Charly's lab. He continues to make headway in his most difficult project in collaboration with Prof. Volker Dötsch, and I wish him the best of luck. Berj Demirjian, a summer student from UCLA in the summer of 1999, was also a true joy to work with during his 10 weeks in the lab, during which time he accomplished a great deal. Dr. Stephen Todd, a post-doc in the lab, began some

studies with KSHV Pr which were not fortunate enough to be successful, but he helped along the way with some good insight into Ayçe's and my work.

There are many others in the lab whom should be acknowledged, as well. I should thank my bay-mate, Dr. Teaster Baird, Jr., for entertaining me with his great MP-3 library. Deborah Dauber, Dr. Jennifer Harris, Dr. Martha Laboissiere and Dr. Toshi Takeuchi all provided good advice and expertise regarding different aspects of the project, and Anh Le contributed her technical support early on. Everyone else, except maybe Ibo (just kidding - haha...), have also contributed remarkably to the atmosphere of the lab, whether during group meeting, at a lab lunch, or just hanging out in the lunchroom. I will miss each and every one of them. I guess I'm beginning to already, even though I'll be in the lab for another month or so.

Two other important groups of people deserving my thanks are my orals and thesis committees. Profs. Frances Brodsky, Ken Dill, Volker Dötsch and Wendell Lim provided some great early input on the KSHV Pr project during my oral exam. Without their advice, questions, criticisms and suggestions, things might not have coalesced quite so fast with my work. Charly, Don Ganem and Bob Stroud, the three members of my thesis committee, have been absolutely invaluable in my development as a scientist. As a committee, their tough stance on some issues and their encouragement on others was always appropriate and constructive. I thank them for their time, effort and humor along the way, and truly hope to be able to work with them again.

The most important individual to thank at this point, of course, is one's advisor, and in a way I feel like the child of *three* scientific fathers. Prof. Laimonis (Lou) Laimins, now at Northwestern University, provided me with the initial excitement and

training in molecular biology and virology during and immediately after college at the University of Chicago. His continued support is incredibly generous and much appreciated, as are the free lunches every time I visit Chicago. Prof. Gary Ackers, whose lab I joined at the Washington University School of Medicine during my first two years of graduate training, instilled in me the need to be rigorous and conscientious in experimental design, execution and interpretation. His willingness and ability to help me relocate and transfer graduate programs was most gracious and is still appreciated by me to this day, as is his continued support in my career. And Charles Craik, my current and soon-to-be previous advisor, certainly deserves a paragraph of his own, so just hold on...

Charly has at times been inspirational, at times frustrating, at times funnier than hell, and at others incredibly understanding. Through all he has been helpful, conscientious and devoted. He has been a great mentor, not just in terms of what it takes to become accomplished scientifically, but also in helping me find a great job and in certain personal matters. His compassion and thoughtfulness come to mind now. In letting me take a LOT of time off after my separation he helped me realize that it was okay to be human, to spend time straightening my life out. I will always remember him for that, and for the night he and Nancy invited me to their home for dinner with their family. One last thing which I will also always remember is Charly's ability to apologize. We are all human, but many PI's (and bosses in general) are unable to admit fault. Charly does not suffer from this weakness. His willingness to accept responsibility for his mistakes, *faux pas* and occasional impatience are the greatest lesson I take from his lab. I only hope that I can be so honest and forthright in my career and with my colleagues.

Abstract

Regulatory Interactions at the Dimer Interface of Kaposi's Sarcoma-associated Herpesvirus Protease

Todd Richard Pray

The structural and functional linkage between the dimer interface and active sites of the protease encoded by Kaposi's sarcoma-associated herpesvirus (KSHV) has been investigated. KSHV, also known as human herpesvirus-8, causes the most common neoplasm among individuals with AIDS, and is a recently identified viral pathogen. Herpesviral serine proteases, dimeric enzymes, are essential for the replication of these viruses, and are of interest as chemotherapeutic targets. Initial studies of KSHV protease (KSHV Pr), involved the establishment of an expression system and activity assay for the enzyme. It was first cloned from the viral genome in collaboration with the Ganem laboratory, and expressed and purified from inclusion bodies in *Escherichia coli*. A fluorescence-based kinetic assay for the cleavage of synthetic oligopeptide substrates was developed. In order to produce material for further studies, a soluble expression and purification protocol was developed for active KSHV Pr.

These studies led to the identification of a novel inactivation strategy among herpesviral proteases, and to the elucidation of the enzyme's crystal structure. An autolysis site within the predicted dimer interface of KSHV Pr was observed. Cleavage at this site, seen both in *E. coli* and virally infected human cells, inactivated the enzyme

UCSF LIBRARY
MAY 17 1990

and induced large conformational changes, detected with circular dichroism and fluorescence spectroscopies. The concurrent loss of dimerization by the truncated protein, KSHV Pr delta, was verified by gel-filtration chromatography and analytical ultracentrifugation. The 2.2 Angstrom crystal structure of the full-length dimeric enzyme, solved in collaboration with the Stroud laboratory, indicated key functional regions and possible modes of structural plasticity upon dimer interface autolysis.

A final study confirmed the functional role of KSHV Pr dimerization. The activation of KSHV Pr upon oligomerization was observed, as well as the appearance of subtle conformational changes. These spectroscopically detected events, less dramatic than seen in the KSHV Pr to Pr delta conversion, are perhaps responsible for the ordering of the enzyme's independent active sites. The dimer interface of KSHV Pr is thus responsible for both the negative and positive autoregulation of the enzyme's activity.

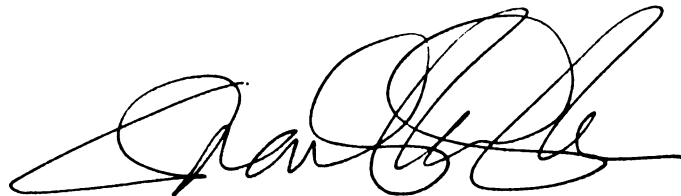
A handwritten signature in black ink, appearing to read 'Paul D. ...', with a stylized, cursive script.

Table of Contents

Chapter 1	page 1
Introduction	
Chapter 2	page 13
The protease and the assembly protein of Kaposi's sarcoma-associated herpesvirus protease (human herpesvirus-8).	
Chapter 3	page 43
Auto-inactivation by cleavage within the dimer interface of Kaposi's sarcoma-associated herpesvirus protease.	
Chapter 4	page 59
Functional consequences of the Kaposi's sarcoma-associated herpesvirus protease structure: Regulation of activity and dimerization by conserved structural elements.	
Chapter 5	page 95
Conformational change coupling the dimerization and activation of Kaposi's sarcoma-associated herpesvirus protease.	
Chapter 6	page 135
Future Directions	

List of Tables

Table 2-1	page 42
k_{cat}/K_m values for herpesviral proteases and trypsins	
Table 3-1	page 58
Summary of kinetic data and apparent secondary structure.	
Table 4-1	page 80
Crystallographic statistics.	

List of Figures/Illustrations

- Figure 1-1 page 11
Sequence features of KSHV Pr/AP.
- Figure 1-2 page 12
Role of herpesviral proteases in replication.
- Figure 2-1 page 37
Schematic of partial genome of KSHV and location of ORF 17.
- Figure 2-2 page 38
Alignment of herpesvirus Pr's and AP maturation sites.
- Figure 2-3 page 39
SDS-polyacrylamide gel electrophoresis and immunoblot analysis of KSHV Pr expression and purification.
- Figure 2-4 page 40
Northern blots of BCBL-1 RNA hybridized to probes from Pr or Pr/AP.
- Figure 2-5 page 41
DNA sequence of KSHV Pr/AP.

Figure 3-1	page 55
Identification of an autolysis site within KSHV Pr.	
Figure 3-2	page 56
Effect of D-site cleavage on KSHV Pr dimerization.	
Figure 3-3	page 57
Spectroscopic detection of structural changes within KSHV Pr upon D-site cleavage.	
Figure 4-1	page 81
Schematic of KSHV Pr structure viewed along dimer two-fold axis.	
Figure 4-2	page 83
Structural divergence of dimer interface helices of herpesviral proteases.	
Figure 4-3	page 85
Mapping sequence conservation to the KSHV Pr structure reveals clusters of residues conserved in both primary sequence and tertiary fold.	
Figure 4-4	page 87
The catalytic triad and oxyanion loop shown with a model substrate based on the inhibitor-bound hCMV Pr structure.	

Figure 4-5 page 89

Further characterization of KSHV Pr dimer interface helical packing.

Figure 4-6 page 91

Unfavorable electrostatic consequences of burying Arg209 within the dimer interface.

Figure 4-7 page 93

Solvent accessibility of herpesviral protease active sites.

Figure 5-1 page 119

Stimulation of KSHV Pr specific activity upon dimerization.

Figure 5-2 page 121

Linkage between structural changes and KSHV Pr's dimerization enhanced activity.

Figure 5-3 page 123

Temperature dependence of the fluorescence emission spectrum of KSHV Pr.

Figure 5-4

page 125

Schematic of KSHV Pr dimer structure and position of Trp residues and mutagenized positions.

Figure 5-5

page 127

Perturbation of dimerization and activity of KSHV Pr by point mutations within its dimer interface.

Figure 5-6

page 129

Putative alterations in the secondary structure of KSHV Pr upon point mutation within the dimer interface correlate with the monomer-dimer transition of the active enzyme.

Figure 5-7

page 131

Deactivating dimer interface substitutions within KSHV Pr mimic the fluorescence emission spectrum of heat-inactivated monomers of the active enzyme.

Figure 5-8

page 133

Autolysis of KSHV Pr within its dimer interface during viral replication.

Figure 6-1

page 143

Gel filtration of KSHV AP showing apparent trimerization.

Figure 6-2

page 144

Specific immunoreactivity of anti-KSHV mAP serum against recombinant and virally produced AP.

Figure 6-3

page 145

Analysis of Pr/AP processing in viral capsid species by sucrose gradient separation.

Chapter 1

Introduction

Kaposi's sarcoma (KS) was the earliest visible harbinger of the devastating AIDS epidemic in the 1970s and early 1980s (reviewed in Ganem, 1998). KS, the most common cancer among gay and bisexual HIV positive males, exhibits both outward lesions and severe internal neoplasms. The search for the cause of KS led to the discovery of the eighth human herpesvirus, KS-associated herpesvirus (KSHV), which is present in cells in all KS lesions (Chang *et al.*, 1994). The first identification of herpesviral DNA in these lesions led, in short order, to the elucidation of its complete genomic sequence (Russo *et al.*, 1996) and organization (Lagunoff & Ganem, 1997).

The Role of Proteases in the Replication of Herpesviruses

An important class of molecules in many viral infections are proteases (Babe & Craik, 1997), enzymes responsible for the specific and regulated cleavage of peptide bonds in other protein molecules, or substrates; all herpesviruses, in fact, encode an homologous protease in their genome (Liu & Roizman, 1992; Gao *et al.*, 1994; Preston *et al.*, 1983). These proteases are synthesized as N-terminal cotranslational fusion molecules with their only known substrates, the capsid's scaffold assembly protein (AP), to yield a precursor protease-AP (Pr/AP) species (Figure 1-1). The AP portion of the Pr/AP ORFs of herpesviruses, such as ORF17 of KSHV, are also independently transcribed from an internal promoter (Chang & Ganem, 2000) at roughly 10-fold higher molar levels than the 3' coterminal Pr/AP message (Ünal *et al.*, 1997).

The role of these protease domains is to specifically liberate AP from the interior of the spherical procapsid in infected cells, after the nuclear import of AP-major capsid protein (MCP) and Pr/AP-MCP complexes (Figure 1-2). First, cleavage of the KSHV Pr domain from AP at the release site (R-site) occurs, followed by the further processing of the maturation site (M-site) of the remaining AP molecules. M-site cleavage releases the small MCP-binding domain, predicted to be an α -helix, from the C-terminus of AP. The disassembly of the scaffold from the inner shell of the spherical procapsid induces a morphological change - angularization and attainment of an icosahedral structure -which is then competent for expulsion of the cleaved AP and the pursuant incorporation of newly synthesized genomic KSHV DNA (Nealon *et al.*, 2000 and references therein, reviewed by Roizman and Sears, 1996 and Gibson, 1996). The cleavage of the R-site and M-site thus appear to be critical regulatory steps in viral replication, a conclusion borne out by cell culture studies of protease knock-out and temperature sensitive virus strains in herpes simplex virus-1 (HSV-1). Thus, the importance of studying the proteases of all herpesviruses is clear as they are potential points of control and inhibition of these virus' life cycles (Waxman & Darke, 2000). The protease of KSHV in particular, presumed to be a key regulatory step in the development of an AIDS-related neoplasm, garners much interest. This interest forms the basis for the work presented in this thesis regarding the structure and function of KSHV Pr, as well for the relationship of this enzyme's *in vitro* behavior to its *in vivo* role.

Dimerization and Conformational Change of Herpesvirus Proteases

The hypothesis which has driven our work on KSHV Pr is simple, namely that its dimerization plays a key role in the control of its structure and function. In essence, this single protein-protein interaction between two KSHV Pr monomers can be thought of as a necessary, although not sufficient, regulatory event in the course of viral replication. This hypothesis, certainly not ours alone, came from some very interesting, preliminary biochemical characterization of related proteases from herpesviruses such as HSV-1 and human cytomegalovirus (HCMV). HCMV Pr was shown to dimerize by a number of methods, including chemical crosslinking of monomers to one another in solution and by dynamic light scattering (Margosiak *et al.*, 1996), analytical ultracentrifugation (Cole, 1996), and gel-filtration chromatography (Darke *et al.*, 1996). A correlation between the dimerization behavior observed in the gel-filtration study with an increase in the proteolytic activity of HCMV Pr led researchers to postulate that oligomerization is linked to activity, and that monomers of HCMV Pr are inactive (Darke *et al.*, 1996). This assertion was supported by the observation of similar behavior in the related protease from HSV-1 (Schmidt & Darke, 1997).

These biochemical data, linking dimerization to proteolytic activity of this class of enzymes, have been confirmed in high resolution structural detail. The crystal structures of dimers of the proteases from HCMV (Qiu *et al.*, 1996; Tong *et al.*, 1996; Shieh *et al.*, 1996; Chen *et al.*, 1996), HSV-1 and -2 (Hoog *et al.*, 1997), and VZV (Qiu *et al.*, 1997) have all been reported. These crystal structures reveal unambiguously the unusual catalytic triad of these enzymes, all of which are composed of a Ser-His-His residue set. Interestingly, the His residue distal from the nucleophilic Ser side chain aligns in

structure very well with the conserved Asp residue found in the canonical serine proteases of the chymotrypsin and subtilisin folds, demonstrating what is likely a case of convergent evolution of the protease active site on a new, dimeric scaffold.

Dimerization itself is one part of the picture, but there must be some sort of concrete rationale for its linkage to activity. By necessity, there must be some mechanism whereby herpesviral proteases, and KSHV Pr in particular, change their conformation in order to orient properly its two otherwise independent active sites and/or substrate binding determinants. Once again, enticing but preliminary evidence of subtle conformational change arose out of work with HCMV Pr. First, the spectroscopic detection of possible structural changes upon peptidomimetic inhibitor binding emerged (Bonneau *et al.*, 1997). The changes in the fluorescence and near-UV CD spectra, due apparently to changes around Trp 42, were given high-resolution structural definition in a later manuscript which presented the crystal structure of an HCMV Pr-inhibitor complex (Tong *et al.*, 1998). This structure revealed subtle shifts in the packing and orientation of the enzyme's dimer interface α -helices. Interestingly, the binding of a smaller, non-peptidomimetic inhibitor, diisopropyl fluorophosphate (DIP), to the active site of HSV-2 Pr did not induce any such detectable structural change (Hoog *et al.*, 1997). This could be due simply to the low sequence identity, and thus different mechanistic requirements for substrate recognition, between the β -herpesviral protease from HCMV and the α -herpesviral protease from HSV-2. It is tempting to speculate, however, that the lack of detectable structural change upon binding the smaller molecule is an indication of how these enzymes recognize their extended substrate sequences, and that conformational plasticity may play a role in the regulation of such events.

Substrate Specificity of Herpesviral Proteases

Related to this issue of conformational change associated with substrate binding is the question of what, in fact, are the determinants of substrate specificity for herpesviral proteases, including KSHV Pr. Once again, prior to the initiation of our studies a preliminary body of work on related enzymes had accumulated regarding their substrate specificity. The first careful study of the requirements of substrate binding and turnover for herpesviral proteases indicated that extended determinants, spanning residues from P9 to P9', could greatly affect cleavage of synthetic peptides (DiIanni *et al.*, 1993). HSV-1 substrate phage display studies indicated the possibility that these longer substrates could be substantially trimmed if optimized, to the point where residues to the primed side of the scissile bond are unnecessary, under certain conditions, to detect enzyme activity (O'Boyle *et al.*, 1997). Atomic resolution information regarding substrate and inhibitor binding has recently begun to emerge for HSV-1 Pr, demonstrating the active site cavity complexed to DIP in a cocrystal structure (Hoog *et al.*, 1997). In addition, it has been shown by solution phase NMR that HCMV Pr P5-P1 substrate residues bind in an extended conformation as with other types of proteases (LaPlante *et al.*, 1998). These HCMV Pr studies have been extended to analyze the cocrystal structure of a P4-P1' peptidomimetic compound bound to the enzyme, as mentioned above, giving detailed information regarding the molecular determinants of these binding subsites on the protease (Tong *et al.*, 1998). Perhaps the most interesting and least understood aspect of herpesviral protease substrate recognition is the pronounced preference for binding and cleavage of their macromolecular AP substrates (Pinko *et al.*, 1996). Perhaps this fact is

an indication of large regions of additional protease-substrate contact, beyond the immediate vicinity of the active site, which could be possible targets for chemotherapeutic development. A very thorough discussion of these and other aspects of substrate specificity, as pertaining to inhibitor discovery for herpesviral proteases has recently been presented (Waxman & Darke, 2000).

Autolysis and Inactivation of Herpesviral Proteases

Having dealt with an introduction, first to the activation by dimerization, and second to the various aspects of the extended substrate specificity of herpesviral proteases, a final category of study for these enzymes and proteases in general is deactivation, an event which often occurs following autolysis. Early studies of HCMV Pr noted that the enzyme was capable of cleaving itself at one or two internal sites (I-sites) within the Pr catalytic domain, distinct from the R-site and M-site found in the Pr/AP precursor molecule. At first it was thought that cleavage at least at one of these sites, which was observed both *in vitro* and in cell culture, inactivated the enzyme (Baum *et al.*, 1993). Later, however, it was shown that this inactivation did not occur upon autolysis, and that the cleaved protein was active as a two fragment, 16 + 13 kD complex (O'Boyle *et al.*, 1995). Crystallization of HCMV Pr required that these sites be changed in order to avoid autolysis, but it was seen that they exist in two exposed surface loops of the enzyme (Qiu *et al.*, 1996; Tong *et al.*, 1996; Shieh *et al.*, 1996; Chen *et al.*, 1996). It appears, then, that HCMV Pr I-site autolysis does not play a regulatory role in the sense of modulating enzyme activity. A formal possibility exists, however, that cleavage at

these sites could modulate the structure of important protein-protein interaction surfaces of the protease which could play an as-of-yet undetermined role *in vivo*.

KSHV Protease: A Novel Molecule in the Context of a Novel Family of Enzymes

These three issues which have been introduced, and the preliminary evidence pertaining to all of them, are the factors which have served as the main driving forces of our study. Each of them - the role of dimerization in the positive regulation of KSHV Pr, the structural basis of substrate specificity and enzymatic activity, and the possible existence and role of autolysis within the KSHV Pr catalytic domain - and their linkage to whatever *in vivo* role KSHV Pr may play, have been addressed experimentally in this thesis. In brief, here is what follows in the following chapters, 2 - 5.

Chapter 2, a manuscript co-first authored by Ayçe Ünal and myself, describes our first efforts to express, isolate and characterize KSHV Pr (Ünal *et al.*, 1997). The gene for KSHV Pr was identified in a cDNA subclone of a portion of the KSHV genome by its homology to related ORFs in other herpesviruses. It was then sequenced, and the catalytic domain of the Pr/AP ORF amplified by PCR and cloned into an expression vector containing an in-frame poly-His tag. In order to characterize its activity, this protein was expressed in *Escherichia coli* and isolated from inclusion bodies by purification using metal-chelate chromatography. This protein had very low catalytic activity in a continuous fluorescence based assay we developed against both a commercially available HCMV Pr M-site substrate and a newly synthesized KSHV R-site substrate, provided by Dr. Michael Pennington of BACHEM Biosciences. This activity, however, was judged to be authentic since an active site mutant, KSHV Pr

S114A, exhibited no such cleavage. In collaboration with Dr. Michael Lagunoff in the Ganem lab, the expression of the KSHV Pr/AP ORF was also analyzed. Northern blot analysis indicated that the Pr/AP and AP mRNA species were only present upon the induction of lytic viral replication, as seen with other viral late genes. In addition, we were able to generate a potent and very specific polyclonal antiserum to KSHV Pr, which has been very useful in all subsequent studies.

Chapter 3 deals with the negative auto-regulation of KSHV Pr by cleavage within one of its dimer interface α -helices (Pray *et al.*, 1999). In order to obtain more active, perhaps, as well as more readily crystallized protein for structural studies, we were attempting to express soluble, non-His tagged KSHV Pr in *E. coli*. Autolysis of KSHV Pr was first noted during these studies, and was detected using the polyclonal antiserum made against the His-tagged material noted above. Based on the estimated size of the cleavage product, the autolysis site was predicted to occur 27 residues from the C-terminus of the 230 amino acid protein. The P1' Ser204 residue was changed to Gly (KSHV Pr S204G), and a three-column purification protocol developed to isolate the soluble, non-tagged enzyme in order to characterize its activity. Unlike the autolysis at the I-sites within HCMV Pr which do not affect this enzyme's activity, cleavage at the D-site of KSHV Pr has profound effects upon both its structure and function. The 22 kD cleavage product of this autolysis, KSHV Pr Δ , although soluble and stable in solution, is completely inactive and monomeric. It also exhibits stark structural differences as detected by CD and fluorescence spectroscopies, when compared to the full-length, dimeric wild-type and KSHV Pr S204G molecules. In addition, by stabilizing KSHV Pr

to autolysis without perturbing its apparent structure and proteolytic activity, we were able to facilitate the crystallization and structural characterization of this enzyme.

Chapter 4 details the crystal structure determination of this stabilized dimer, indicating important common features between KSHV Pr and other proteases of this class and protein fold (Reiling *et al.*, 2000). Kinkead Reiling was first author on this manuscript, and it was great working with him to crystallize KSHV Pr and analyze its structure in a functional context. The 2.2 Å resolution crystal structure revealed important structural similarities and differences relative to the other herpesviral protease structures in the literature. Information regarding the active site and substrate binding pockets of KSHV is presented, as is a wealth of analysis of its dimer interface. This protein-protein interaction surface exhibits interesting and not-so-subtle differences between KSHV Pr and its related proteases, and may provide a model system for studying the structural basis of allosteric regulation and macromolecular recognition for this family and fold of proteins.

Chapter 5, in a sense, is a study which attempts to tie together the previous chapters, and serves as the culmination of what may be considered the very beginning of a number of possible studies of KSHV Pr. Using activating assay conditions for the enzyme, developed with the enthusiastic assistance of Berj Demirjian, we have detected the stimulation of the activity of KSHV Pr as it dimerizes. This activation corresponds with conformational changes, seen spectroscopically with fluorescence and circular dichroism, within the KSHV Pr monomers as they associate. The spectral differences observed are not as pronounced as those described in chapter 3, which occur upon autolysis of KSHV Pr within its dimer interface. However, they do indicate that even in

the normal monomer → dimer transition we are able to detect the differences in structure which must be responsible, in the strictest sense, for this activation phenotype. In addition, it emphasizes that subtle changes likely govern the allostery of KSHV Pr, and that detailed, further structural information is necessary to fully understand the regulation of the isolated catalytic protease domain. This goal may be facilitated by the discovery and characterization of designed KSHV Pr monomers which are capable of dimerizing. Using site-directed mutagenesis, we were able to selectively perturb the dimer interface of KSHV Pr. The mutations discussed do not appear to greatly distress the overall structure of the KSHV Pr monomer, as judged by our spectroscopic assays, but do attenuate any detectable proteolytic activity. The study of these engineered monomers, along with that of KSHV Pr Δ which Anson Nomura is currently undertaking, will hopefully lead to an unprecedented resolution in the role of dimerization for herpesviral proteases.

Figure 1-1: Sequence features of KSHV Pr/AP.

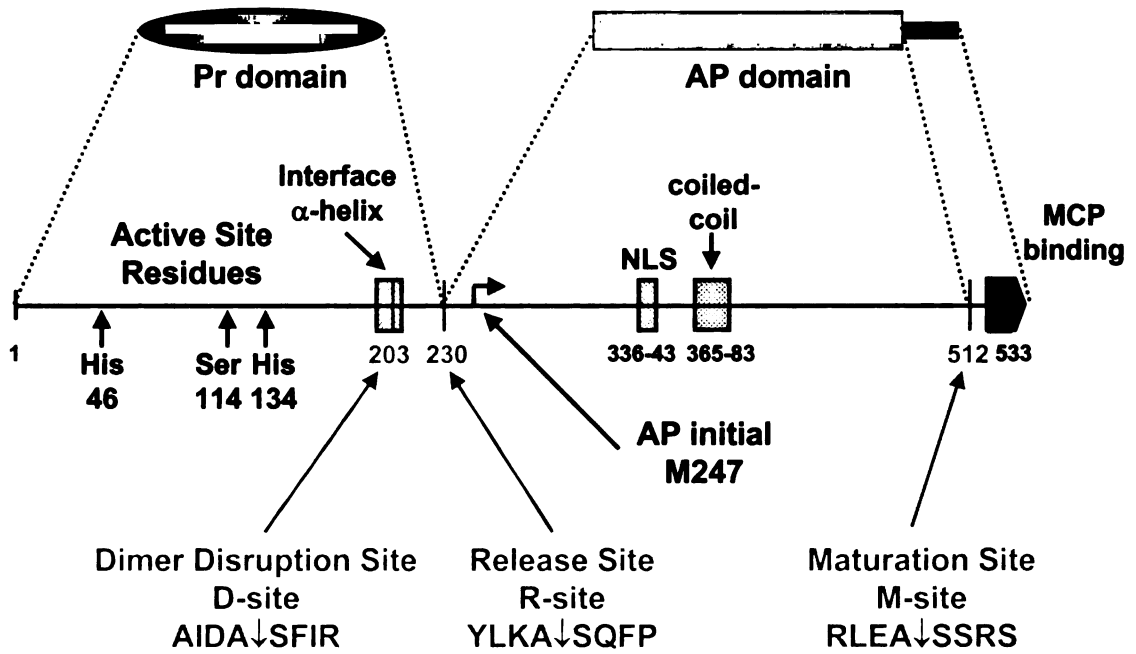
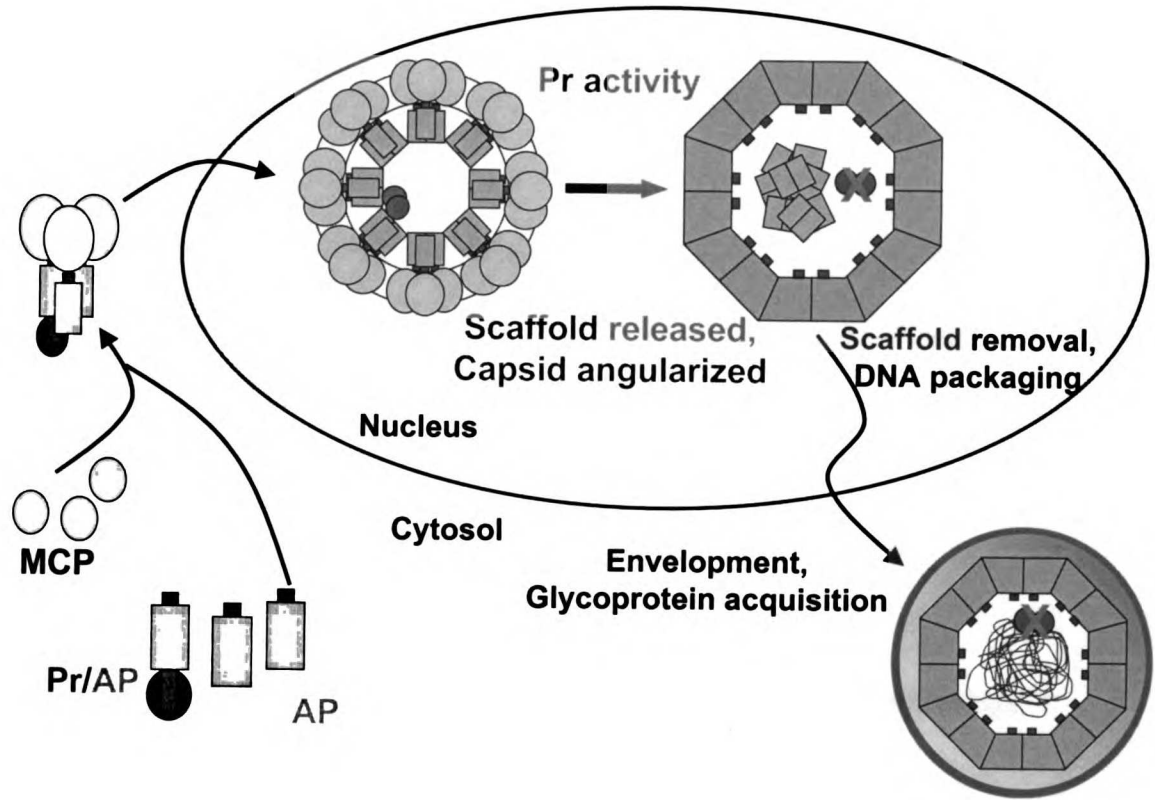


Figure 1-2: Role of herpesviral proteases in replication



Chapter 2

The Protease and Assembly Protein of Kaposi's Sarcoma-Associated Herpesvirus (Human Herpesvirus 8)

Ayçe Ünal¹, Todd R. Pray², Michael Lagunoff³, Don Ganem³ and Charles S. Craik^{1,2}

¹Department of Pharmaceutical Chemistry

²Graduate Group in Biophysics

*Howard Hughes Medical Institute and Department of Microbiology

University of California

San Francisco, CA 94143

T.R.P. and A.U. contributed equally to the preparation of this manuscript.

This chapter is reprinted with permission from the *Journal of Virology*.

J. Virol. (1997). **71**: 7030-7038.

ABSTRACT

A genomic clone encoding the protease and the assembly protein of Kaposi's sarcoma-associated herpesvirus (KSHV, also called human herpesvirus 8) has been isolated and sequenced. As with other herpesviruses, the protease and assembly protein coding regions are present within a single long open reading frame. The mature KSHV protease (KSHV Pr) and assembly protein polypeptides are predicted to contain 230 and 283 residues, respectively. The amino acid sequence of KSHV protease shares 56% identity with that of herpesvirus saimiri, the most similar virus by phylogenetic comparison. KSHV Pr is expressed in infected human cells as a late viral gene product, as suggested by RNA analysis of KSHV-infected BCBL-1 cells. Expression of the KSHV Pr domain in *Escherichia coli* yields an enzymatically active protease, as determined by cleavage of synthetic peptide substrates, while an active-site mutant of this same domain yields minimal proteolytic activity. Sequence comparisons with human cytomegalovirus (HCMV) protease permitted the identification of the catalytic residues, Ser114, His46 and His134, based on the known structure of the HCMV enzyme. The amino acid sequence of the release site of KSHV protease (Tyr-Leu-Lys-Ala*Ser-Gln-Phe-Pro) and the maturation site (Arg-Leu-Glu-Ala*Ser-Ser-Arg-Ser) show that the extended substrate binding pocket differs from that of other members of the family. The conservation of amino acids known to be involved in the dimer interface region of HCMV protease suggests that the KSHV Pr assembles in a similar fashion. These features of the viral protease provide opportunities to develop specific inhibitors of its enzymatic activity.

INTRODUCTION

Kaposi's sarcoma (KS), once considered a rare tumor largely confined to elderly Mediterranean and African men, has recently re-emerged as the most common neoplasm of patients with the acquired immunodeficiency syndrome (AIDS): 15-25% of such patients will develop this tumor in the course of their human immunodeficiency virus (HIV) infection. While HIV infection is an important risk factor in KS development (Ensoli *et al.*, 1991; Ganem, 1994), epidemiologic studies indicate that it is not sufficient to explain the etiology of the disease (Beral, 1991; Beral *et al.*, 1990). For example, KS is far more prevalent in AIDS patients who acquire their HIV infection by sexual routes than in those who contract HIV by percutaneous inoculation or vertical transmission. These findings suggest that a second, sexually transmitted cofactor may be required for KS development. Recently, DNA sequences of a novel human herpesvirus (KS-associated herpesvirus [KSHV], also called human herpesvirus 8 [HHV-8]) have been identified in KS tumors (Chang *et al.*, 1994). A growing body of evidence suggests an important role for this virus in KS pathogenesis: (i) infection precedes tumorigenesis and is associated with a striking increase in the risk of subsequent KS development (Moore *et al.*, 1995; Whitby *et al.*, 1995); (ii) the distribution of infection among HIV-positive patients parallels known KS risk (Gao *et al.*, 1996; Kedes *et al.*, 1996); (iii) all forms of KS, whether HIV-positive or HIV-negative, are strongly associated with KSHV infection (Ambroziak *et al.*, 1995; Chang *et al.*, 1994; Chuck *et al.*, 1996; Huang *et al.*, 1995; Moore & Chang, 1995; Schalling *et al.*, 1995; Soulier *et al.*, 1995); and (iv) infection is targeted to the endothelial (spindle) cells, thought to be central to KS pathogenesis (Boshoff *et al.*, 1995). These findings raise the important possibility that prevention or

suppression of KSHV infection could reduce the risk of KS development. Here we report the cloning, expression and initial biochemical characterization of a KSHV gene product with the potential to be a target for specific antiviral therapy.

Herpesviruses mature through a common assembly pathway, best studied using herpes simplex virus (HSV). Viral capsids assemble in the nucleus late in infection. Immature capsids lack DNA but contain an abundant internal polypeptide, the assembly protein (AP), that is not found in the mature, DNA-containing particles (Gibson, 1981; Gibson & Roizman, 1972; Irmiere & Gibson, 1985; O'Callaghan & Randall, 1976; Rixon *et al.*, 1988). This protein is known to interact, through its carboxy-terminus, with the major capsid protein (MCP) (Hong *et al.*, 1996; Wood *et al.*, 1997). This interaction is required for nuclear transport of the MCP (Nicholson *et al.*, 1994) and has also been proposed to act as a scaffold to facilitate the assembly of the capsid shell. Following immature capsid assembly, the AP undergoes proteolytic processing at the so-called "maturation" site (M-site) near its carboxy-terminus, which removes the last 25 amino acids (Gibson *et al.*, 1990). This proteolysis is mediated by a virally-encoded serine protease (Pr) (Liu & Roizman, 1992; Preston *et al.*, 1992; Welch *et al.*, 1991). Herpesvirus Pr molecules show clear homology, ranging from 90% amino acid sequence identity among closely related viruses, to 30% identity between distantly related viruses. These sequences are unrelated to the two major classes of presently characterized cellular serine proteases - the chymotrypsin and subtilisin families (Perona & Craik, 1995). The viral enzymes display similar substrate specificities, preferring an alanine residue at P1 and serine at P1' (see Schechter *et al.*, 1968 for nomenclature). Cleavage of AP by the viral Pr is essential for viral growth; HSV mutants bearing an inactive Pr accumulate

capsids lacking viral DNA (Desai *et al.*, 1994; Gao *et al.*, 1994; Preston *et al.*, 1994; Preston *et al.*, 1983; Sherman & Bachenheimer, 1988; Thomsen *et al.*, 1994). Presumably, cleavage of AP is required to allow its release from the capsid and permit the packaging of newly replicated viral DNA.

The coding strategy for the protease and assembly protein is similar in all well-characterized herpesvirus family members. The Pr and AP coding sequences are found in a single large open reading frame (ORF) (Figure 2-1) encoding a polyprotein (Pr/AP) whose amino-terminal domain represents Pr, and the carboxy-terminal portion AP. Active Pr excises itself from Pr/AP by cleavage at the so-called release site (R-site) and can then cleave AP at the M-site. Most AP, however, is not generated by Pr/AP cleavage; rather, a separate mRNA initiated within the ORF directs AP translation from an internal AUG codon. As expected for virion structural components, Pr- and Pr/AP-encoding transcripts are expressed as late viral genes in the lytic cycle, and presumably are not expressed during latent infection.

Recent success with protease inhibitors in antiviral therapy for HIV provides a precedent for a similar strategy for anti-KSHV therapeutics (Condra *et al.*, 1995). Defining the protease target of KSHV and its natural substrates is an essential step in achieving this goal. In this report we present the cloning and purification of the KSHV Pr, as well as a preliminary investigation of its enzymatic activity. In addition, evidence for the *in vivo* expression of Pr and Pr/AP as late viral gene products is presented, along with an analysis of their relationship to other herpesvirus Pr and precursor Pr/AP gene products.

MATERIALS AND METHODS

Sequencing studies

A partial KS genome had been previously subcloned from a pulmonary KS tumor as 10-15 kb overlapping segments in λ phage (Zhong *et al.*, 1996). DNA was prepared from a clone known to encode the thymidine kinase (TK) gene from which a 5.8 kb *Bam*H I-*Hind* III DNA fragment was subcloned into Bluescript II KS (Stratagene). A *Hind* III, *Sac* I digest resulted in four KS-specific DNA fragments of 1.9 kb, 1.5 kb, 1.1 kb and 0.8 kb. These fragments were subcloned into Bluescript and sequenced using T3 and T7 primers. The 1.5 kb and 0.8 kb fragments contained DNA sequences that encoded a protein that aligned with herpesvirus saimiri (HVS) Pr sequences. The nucleotide sequence of these fragments was determined by sequencing both strands of the DNA. Synthetic oligonucleotide primers were used to generate overlapping sequences of the entire insert. The primers were synthesized on an Applied Biosystems 391 DNA synthesizer. Automated DNA sequencing was carried out using an Applied Biosystems 377 Prism sequencer, and manual DNA sequencing was carried out using standard conditions.

Construction of Expression Vectors

A linear DNA fragment containing the KSHV Pr domain was amplified from the plasmid pBS1.5 (see Figure 2-1) using the polymerase chain reaction (PCR). The 5' primer for this amplification was 5'-GG GGG TCC GGA CAG GGC CTG TAC GTC GGA-3', and the 3' primer 5'-GG GGG AAG CTT CTA GGC CTT TAA ATA CAC CGG-3'.

In order to create a bacterial expression vector for KSHV Pr, the product of the PCR reaction was digested with the restriction endonucleases *BamH* I and *Hind* III prior to ligation into similarly treated pQE30 DNA (Qiagen). This construct (pHis₆-KSP), designed to over-express the wild-type Pr with the amino acid sequence Met-Arg-Gly-Ser-His₆-Gly-Ser replacing the initiating Met residue (His₆-Pr), allows for affinity purification of the His-tagged enzyme through the use of metal chelate chromatography. This plasmid was propagated in the *E. coli* strain XL1-Blue (Stratagene) to alleviate DNA degradation and rearrangement.

The substitution of Ser114, encoded by TCT, to Ala (GCC) was performed by PCR-mediated site-directed mutagenesis of the Pr ORF (Ausebel *et al.*, 1990). The DNA oligonucleotides 5'-CTC CCG GGG CTG GCC TTA TCG TCC ATA C-3' and 5'-TAT GGA CGA TAA GGC CAG CCC CGG GAG-3', corresponding to the mutated upper and lower strands, respectively, were used to introduce the substitutions into the Pr ORF (the mismatched bases are underlined). These PCR products were gel-purified and subjected to a second round of PCR in order to construct the full-length coding sequence of His₆-Pr(S132A). The presence of the correct substitution was verified by DNA sequence analysis, subsequent to insertion into the *BamH* I and *Hind* III restriction sites of pQE30 to construct the plasmid pHis₆-KSP(S114A).

Bacterial Growth and Protein Expression

The above plasmids were separately transformed into the *E. coli* strain X-90 to afford high-level expression of recombinant protease gene products (Evnin *et al.*, 1990). Bacterial cultures were grown at 37 °C in LB medium to an OD₆₀₀=0.8, and isopropyl β-

D-thiogalactopyranoside (IPTG) was added to a concentration of 0.2 mM. Cultures were then grown for 3 hours to allow for protein expression, and harvested by centrifugation.

Protein Purification

Cell pellets were resuspended in sonication buffer [50 mM Tris-HCl (pH 8.0), 0.5 M KCl, 10% (v/v) glycerol, 1 mM β -mercaptoethanol], and sonicated on ice. Lysates were then pelleted at 10,000 x g, and the insoluble matter resuspended in denaturing buffer [50 mM Tris-HCl (pH 8.0), 100 mM NaCl, 1 mM β -mercaptoethanol], containing 6 M deionized urea, by slowly stirring on ice for 30 minutes. The resuspended pellet was then centrifuged as above, and the supernatant incubated with 3 to 4 ml Ni-NTA agarose (Qiagen), which had been equilibrated in denaturing buffer/urea, by slow stirring on ice for 1 hour. This slurry was packed into a column reservoir, and subjected to a 1 L reverse urea gradient, from 6 M to 0 M, in denaturing buffer. The refolded, Ni-bound proteins were then washed in column buffer [50 mM Tris-HCl (pH 8.0), 500 mM KCl, 1 mM β -mercaptoethanol, 10% glycerol] containing 0.01% (v/v) Tween-20 and 10 mM imidazole, before equilibrating the column in the absence of Tween-20. Bound protein was then eluted using a 10 mM - 0.5 M imidazole gradient in column buffer. Protein-containing fractions were pooled and dialyzed against storage buffer [50 mM Tris-HCl (pH 8.0), 100 mM KCl, 10% glycerol, 0.1 mM DTT] before aliquoting and freezing at -80 °C. Protein concentrations were estimated using a calculated ϵ_{280} of 0.9 ml \cdot mg $^{-1}$ \cdot cm $^{-1}$.

Antibody Production & Immunoblot Analysis

Polyclonal antiserum was raised in rabbits against purified KSHV His₆-Pr (Animal Pharm Services, Inc., Healdsburg, CA). For immunoblot analysis, protein samples were run on a 10% polyacrylamide-SDS gel and transferred to a nitrocellulose membrane (Schleicher & Schuell). The membrane was treated with Tris-buffered saline with 0.1% (v/v) Triton X-100 (TBST) containing 5% (w/v) nonfat dry milk, washed with TBST containing 1% milk, and probed with a 1:250 dilution of the anti-protease (α -KSP) polyclonal serum in the same buffer. After washing as above, a 1:5000 dilution of goat anti-rabbit horseradish peroxidase-conjugated serum (Pierce) was then applied in TBST/1% milk. Antibody-bound protein bands were detected by enhanced chemiluminescence (Amersham).

Synthesis and chemical characterization of the KSHV M-site synthetic substrate

The KSHV M-site substrate, Mca- γ Abu-Asn-Arg-Leu-Glu-Ala-Ser-Ser-Arg-Ser-Lys(Dnp)-NH₂, was synthesized by using standard amino acids, 7-methoxycoumarin-4-acetyl (Mca), and 2,4-dinitrophenyl (Dnp)-Lys. 9-Fluorenylmethoxycarbonyl (Fmoc) amino acids and Fmoc-amide resin were obtained from Bachem Feinchemikalien (Bubendorf, Switzerland). The Fmoc-Lys (Dnp)-OH was prepared by the method of Nagase *et al.* (Nagase *et al.*, 1996). Peptide synthesis was performed on a semiautomated Labortec SP4000 synthesizer. All couplings were mediated by dicyclohexylcarbodiimide and 2 equivalents of 1-hydroxybenzotriazole. Colorimetric analyses (Kaiser *et al.*, 1970) of Fmoc deblocking and acylation steps were routinely performed. 7-Methoxycoumarin 4-acetic acid was coupled as the succinimide ester. Following completion of solid-phase

assembly, the peptide was cleaved from the resin and simultaneously deprotected with reagent K (King *et al.*, 1990). The product was purified by preparative reverse-phase high-performance liquid chromatography on a Rainin Dynamax octyldecyl silane column. Pure fractions were collected and lyophilized. The product was characterized as follows by electrospray ionization mass spectrometry: (M + H) = 1701 (observed) (theory, 1701). The amino acid composition was consistent with theory.

Fluorometric Enzyme Assays

Protease assays were performed with two fluorogenic peptide substrates. The first contained the KSHV M-site, Mca- γ Abu-Asn-Arg-Leu-Glu-Ala-Ser-Ser-Arg-Ser-Lys(Dnp)-COOH. The second, for comparative purposes, contained its related M-site from human cytomegalovirus (HCMV), NH₂-DABCYL-Arg-Gly-Val-Val-Asn-Ala-Ser-Ser-Arg-Leu-Ala-EDANS-COOH (BACHEM, King of Prussia, PA), where DABCYL represents 4-(4'-Dimethylaminophenylazo)benzoic acid, and EDANS signifies (2'-aminoethylamino)-naphthalene-1-sulfonic acid. Reaction progress curves were monitored optically by a Perkin-Elmer LS-5B luminescence spectrophotometer interfaced with a Macintosh SE-30 computer. His₆-Pr and His₆-Pr(S132A) were diluted 10-fold from storage buffer into assay buffer (50 mM potassium phosphate [pH 7.0], 150 mM NaCl, 25% [vol/vol] glycerol, 1 mM β -mercaptoethanol), equilibrated to 37 °C for 5 minutes in thermostatted quartz cuvettes, and manually mixed with substrate. The final KSHV Pr concentrations were 430 nM, and the substrate concentration range was kept below 25 μ M for the HCMV M-site substrate and 5 μ M substrate for the KSHV oligopeptide, due to solubility and inner filter concerns. Time-evolved fluorescence enhancement was

followed by exciting the KSHV M-site peptide at 325 nm and detecting emission at 393 nm; the HCMV substrate samples were excited at 355 nm, and their emissions were detected at 495 nm. Trypsin and its D102N variant (Craik *et al.*, 1987) were diluted into the same assay buffer to final concentrations of 1 nM and 430 nM, respectively, and treated identically to the KSHV enzymes.

Kinetics

The increase in fluorescence intensity during substrate cleavage was recorded as a function of time. The initial velocity, measured as fluorescence intensity per unit time, was calculated from the slope during the linear phase of cleavage by using Kaleidograph operating software. The inner filter effect was negligible in the range of substrate concentrations used, as measured by the linearity of fluorescence with respect to substrate concentration. On the basis of standard compound fluorescence extinction data, initial velocities were converted from fluorescence units to product concentration, and these data were fitted to the Michaelis-Menten equation to determine specificity constants, k_{cat}/K_m (where k_{cat} is the catalytic constant and K_m is the Michaelis constant), for each enzyme-substrate combination.

Northern Blot analysis

BCBL-1 cells (Renne *et al.*, 1996) were treated with phosphoroformic acid (PFA) at a concentration of 500 μM for at least 3 days prior to induction. Untreated and PFA treated cells were then split into identical flasks, at 3×10^5 cells/ml, and left

unstimulated or induced with 12-*O*-tetradecanoyl phorbol-13-acetate (TPA) at a concentration of 20 ng/ml. After 48 hours, total RNA was harvested using RNazol B as recommended by the manufacturer (Tel-Test, Friendwood, TX). To enrich the polyadenylated RNA fraction, 300 µg RNA samples, uninduced and induced with TPA, and with and without PFA treatment, were affinity purified using the Oligotex mRNA purification system (Qiagen). RNA was separated on a 1% agarose, 17% formaldehyde gel, transferred to Hybond-N nylon membrane in 10X SSC (1X SSC is 0.15 M NaCl plus 0.015 M sodium citrate) for 5 hours, and UV-crosslinked. For the double stranded Pr/AP probe, the 1.5 kb insert from pBS1.5 was gel purified and labeled using the rediPrime random Prime kit (Amersham). For the antisense single-stranded probes, either the plasmid containing the 1.5 kb SacI fragment or the plasmid containing the 0.8 kb SacI fragment was digested with EcoRI and phenol extracted and RNA was made with T3 RNA polymerase in the presence of radiolabeled UTP, followed by DNase treatment. Hybridization was performed as before (Renne *et al.*, 1994), and the blot exposed to Kodak XAR5 film.

RESULTS

The Pr/AP coding region of KSHV

The closest known relative of KSHV is herpesvirus saimiri (HVS), a T-lymphotropic herpesvirus which infects monkeys (Albrecht *et al.*, 1992). Previous work has shown that HSV and KSHV genomes are of similar size and display substantial regions of colinearity in the organization of ORFs. ORF 17 of HVS encodes the viral Pr and resides near the TK gene encoded by ORF 21. In earlier sequencing of phage λ clones from a KS-derived genomic library, we identified the KSHV TK gene within a clone of 13 kb (Figure 2-1) (Zhong *et al.*, 1996). The high degree of colinearity between KSHV and HVS genomes in this region (Moore *et al.*, 1996) suggested that the gene encoding the KSHV Pr/AP would likely reside nearby. Subsequent mapping and DNA sequencing of adjacent fragments from this region identified a KSHV ORF encoding a protein with striking homology to the HVS Pr. This presumptive KSHV Pr region resides at the 5' end of a larger coding region whose 3' portion displays evident homology to the AP gene of HVS, further suggesting that this ORF is indeed the gene encoding for the Pr/AP functions of KSHV.

The DNA sequence of this ORF reveals an Ala/Ser dipeptide at a position corresponding to the R-site in other herpesviruses. Thus, KSHV Pr is predicted to be a 230 amino acid polypeptide when released from the precursor (Figure 2-1). Figure 2-2 shows the alignment of the putative KSHV Pr sequence with those of other herpesviruses. The highest sequence identity (56% overall) was observed with HVS Pr. The seven conserved domains (CDs) previously found in other herpesvirus proteases were also

identified in the KSHV sequence (Loutsch *et al.*, 1994; Welch *et al.*, 1993) . These domains span Leu5 to Ser15 (CD5), Leu40 to Thr55 (CD2), Gly64 to Ser73 (CD4), Trp109 to His119 (CD3), Val135 to Tyr150 (CD1), Phe161 to Val164 (CD6) and Leu196 to Ile222 (CD7). Previous studies of HCMV Pr have identified Ser132, His63 (DiIanni *et al.*, 1993; Gibson *et al.*, 1994; Holwerda *et al.*, 1994; Welch *et al.*, 1993), and His157 (Chen *et al.*, 1996; Qiu *et al.*, 1996; Shieh *et al.*, 1996; Tong *et al.*, 1996) as members of the catalytic triad. These amino acid residues are absolutely conserved among all herpesvirus proteases, and the corresponding residues in KSHV enzyme are Ser114, His46 and His134, respectively. The release site residues Tyr-Leu-Lys-Ala*Ser-Gln-Phe-Pro in KSHV, are identical in the P1 and P1' positions but vary in the flanking positions when compared to the other members of the family. The oxyanion stabilization signature sequence containing Gly-Arg-Arg-X-Gly-Thr was identified between residues 136 to 150; this sequence is absolutely conserved in all 14 known amino acid sequences of herpesvirus proteases (Welch *et al.*, 1993). This region in KSHV is identical to that in HVS. These findings suggest that the KSHV gene product has the sequence features of a functional protease.

The DNA sequence of the assembly protein predicts a 309 amino acid protein. Unlike that of Pr, the amino acid sequence of KSHV AP is only weakly homologous to that of HVS. The predicted M-site is composed of Arg-Leu-Glu-Ala*Ser-Ser-Arg-Ser (Figure 2-2). M-site residues of herpesvirus assembly proteins show more variety than R-site sequences; except for P1 and P1', none of the other residues of the site is conserved. Cleavage of AP at the M-site by Pr would release the 283 amino acid, mature AP from the 26 amino acid carboxy-terminal fragment.

UCSF LIBRARY

Purification of KSHV protease and specific immuno-reactivity

The portion of the KSHV ORF corresponding to the viral Pr was subcloned into an *E. coli* expression vector transcriptionally regulated by an IPTG-inducible promoter (see Materials and Methods). An amino-terminal His₆ tag was incorporated into the Pr ORF to facilitate purification. A variant was also constructed in which Ser114 was converted to Ala (S114A). Following overexpression of His₆-Pr and His₆-Pr(S114A), these proteins were subjected to metal-chelate affinity chromatography under denaturing conditions, refolded, and eluted. Purified protein, as well as samples from throughout expression and purification, was analyzed by SDS-PAGE and deemed greater than 90% pure (Figure 2-3). A protein yield of roughly 10 mg from 1-liter bacterial cultures was obtained.

Expression of KSHV Pr and the S114A variant in *E. coli* yielded bands which migrated near 31 kDa, corresponding to the full-length translated Pr domain, terminating at the putative R-site alanine residue (Figure 2-3). This apparent size, slightly larger than the expected 27 kD, is most likely due to incorporation of the His₆ tag. Two faster-migrating proteolytic fragments were also observed that may have resulted from autoproteolysis. The S114A variant is significantly more homogenous, perhaps due to lower levels of autoproteolysis (Figure 2-3A, lanes 6 and 7). In order to verify that the extra bands are not contaminating *E. coli* polypeptides, the products were examined by immunoblotting with an antibody raised to the recombinant, full-length Pr. A control bacterial extract was analyzed on the same immunoblot as the purified His₆-Pr material, and gave rise to no significant, specific hybridization of the same bands in the purified fraction of His₆-Pr (Figure 2-3B). These results indicate the purity of the protein

UCSF LIBRARY

fractions and the specificity of the antibody, α -KSP, for KSHV Pr. As a further control, a parallel immunoblot was assayed with a commercially available monoclonal antibody (Qiagen) directed against the amino-terminal Arg-Gly-Ser-His₄ epitope of His₆-Pr (data not shown). This experiment yielded essentially the same set of bands as α -KSP. The additional protein species thus contain the amino-terminal His₆-tag, and have arisen due to proteolysis during expression and/or purification by either an endogenous bacterial enzyme, or to autodigestion of KSHV His₆-Pr at as-yet-uncharacterized sites.

Kinetic properties of purified KSHV protease domain variants

To determine whether the recombinant protease was catalytically active, the ability of the His₆-Pr and His₆-Pr(S114A) proteins to cleave a synthetic peptide substrate were examined. The substrates, containing either the KSHV or HCMV M-site peptide sequences flanked by a fluorogenic donor-acceptor pair, allow continuous monitoring of peptide hydrolysis due to fluorescence enhancement arising from donor-acceptor separation (Holskin *et al.*, 1995). Since the substrate specificity among the herpesvirus family of proteases is not strict, we expected KSHV Pr to recognize the HCMV M-site substrate. Both substrates contain internal Arg residues, allowing for cleavage by trypsin, an extremely well-characterized serine protease. We can thus obtain preliminary information regarding the KSHV enzyme's substrate specificity, as well as perform a comparative analysis of its catalytic efficiency *versus* that of selected trypsin variants of differing activity.

There is indeed a difference in proteolysis catalyzed by KSHV Pr and the active-site variant. Both the KSHV and HCMV substrates demonstrate minimal hydrolysis by

UCSF LIBRARY

the S114A variant over 1 h, perhaps due to some residual proteolytic activity (for which kinetic parameters were not able to be resolved in the present assay). On the other hand, which native KSHV Pr has a low absolute velocity, the k_{cat}/K_m values indicated for this enzyme are comparable to those for its related herpesviral maturational Pr's (Table 2-1). Such values have shown significant enhancement under various conditions for the HSV Pr (Hall & Darke, 1995) and will likely do so for KSHV Pr in further biochemical studies as well. In addition, our k_{cat}/K_m values could be higher upon the consideration of dimerization and the fact that we may be slightly below this assembly threshold. Darke *et al.*, by careful enzymatic analysis, demonstrated apparent HCMV Pr K_d values very near our experimental KSHV Pr concentrations (Darke *et al.*, 1996), and Cole observed slightly higher values in sedimentation studies (Cole, 1996). In any case, there is specific cleavage of a KSHV substrate by the purified KSHV Pr as well as apparent cross-species reactivity with a related HCMV site.

Due to its low velocity, the proteolytic activity of this newly identified protease was compared with that of trypsin and trypsin D102N (Craik *et al.*, 1987). Trypsin has an extremely high rate of catalytic turnover, and has served as a paradigm for the understanding of site-specific enzyme-directed peptide hydrolysis. Trypsin D102N, in which the active site Asp residue has been replaced with Asn, has a catalytic efficiency orders of magnitude lower than trypsin, depending on solution conditions (in our assay roughly 10,000-fold lower). We reasoned that these two proteases would provide a sound basis for comparison with the KSHV Pr, which lacks an Asp within its catalytic triad. Indeed, 1 nM trypsin hydrolyzes the HCMV substrate at a much higher rate than 430 nM KSHV Pr, indicating that trypsin is substantially more active than the KSHV

WUST LIBRARY

enzyme (Table 2-1). On the other hand, D102N and KSHV Pr have similar kinetic profiles at identical enzyme concentrations (Table 2-1). Thus, the lack of an active site Asp, with conservation of the other two catalytic triad members, His and Ser, results in similar rates of peptide hydrolysis by two unrelated serine proteases, whether engineered as in trypsin, or naturally occurring, as in KSHV Pr.

In vivo transcription of KSHV AP and Pr/AP mRNAs during the viral life cycle

To examine the transcription of the KSHV Pr/AP and AP genes in lytic infection, the KSHV-infected B-cell line, BCBL-1, was employed. This line harbors the viral genome in latent form, and treatment of these cells with TPA induces lytic replication (Renne *et al.*, 1996). Equivalent amounts of Poly(A)-enriched RNA from uninduced or induced BCBL-1 cells in the presence or absence of PFA were separated on a formaldehyde/agarose gel, transferred to a membrane, and hybridized to a probe made from the 1.5 kb fragment containing the Pr/AP ORF of KSHV (Figure 2-4A). A band migrating at approximately 950 bases, the expected size of the AP transcript, hybridizes weakly to the probe in lane 1, which contains RNA from uninduced cells; production of this species is strongly inhibited by PFA, an inhibitor of herpesviral DNA replication, as noted by its absence in lane 2, which contains RNA isolated from uninduced, PFA-treated cells. The band in lane 1 is presumably due to the small amount of spontaneous lytic reactivation in BCBL-1 cells (Renne *et al.*, 1996). This RNA species is not present when a single-stranded antisense probe specific to the Pr domain (i.e. that does not contain the AP transcript) is hybridized to RNA from either induced or uninduced BCBL-1 cells (Figure 2-4C, lanes 1 and 2), but hybridizes strongly to the 1.5 kb single stranded

U.S. LIBRARY

antisense probe for Pr/AP (Figure 2-4C, lanes 3 and 4). Expression of the AP transcript is strongly upregulated upon lytic induction of KSHV (Figure 2-4A lane 3); after induction it is also possible to see a band migrating around 1.8 kb, a size consistent with what would be expected from the transcript encoding the Pr/AP ORF. This species hybridizes to a single-stranded probe specific for the Pr domain (Figure 2-4C, lane 2), indicating that this RNA species is the Pr-containing transcript. There are also slower migrating species (roughly 3 and 4 kb) that have the same temporal induction pattern as the Pr transcript; the origin of these RNAs is unclear, but they may emanate from read-through into flanking viral sequences. Indeed, there is a canonical poly(A) signal approximately 2 kb downstream from the predicted Pr/AP poly(A) site. The second band at approximately 3 kb is presumable read-through of the AP transcript, since it does not hybridize to the Pr-specific single-stranded probe. The roughly 4 kb, weaker signal may represent the read-through of the Pr/AP transcript. Both the 950 bp and 1.8 kb bands are inhibited in the presence of PFA upon TPA induction, as are the slower migrating bands, indicating that they are late transcripts made primarily after viral DNA replication.

WEST LIBRARY

DISCUSSION

In this report we present the sequence of the Pr/AP coding region of KSHV, and demonstrate that the translated Pr domain is catalytically active. The similarity of the genomic coding organization of the KSHV Pr/AP region to those of other herpesviruses strongly suggests that the functional role of the KSHV Pr in lytic replication mirrors that described for its cognates in the related viruses. We also identify the abundant AP transcript and the low-abundance Pr transcript as late genes, strongly upregulated by TPA and inhibited in the presence of PFA, a viral replication inhibitor.

Comparison of the sequence of KSHV Pr with those of other herpesviral Pr's allows instructive inferences to be made about the KSHV enzyme. With HCMV, affinity labeling experiments using diisopropyl fluorophosphate identified Ser132 as the putative active site nucleophile of its protease (DiIanni *et al.*, 1994). Replacing Ser132 with an alanine abolished proteolytic activity, supporting this identification. His63 was shown to be the second member of the catalytic triad by mutagenesis studies. The three-dimensional structure of HCMV Pr confirmed the identity of Ser132 and His63 as catalytic residues, and suggested His157 as the third member of the triad (Chen *et al.*, 1996; Qiu *et al.*, 1996; Shieh *et al.*, 1996; Tong *et al.*, 1996). KSHV protease has a serine at position 114 in CD3, a histidine at position 46 in CD2, and a histidine at position 134 in CD1; these are presumably the corresponding catalytic residues (Figure 2-2). The assignment of Ser114 as the active-site nucleophile is supported by our kinetic analysis of the S114A-substituted KSHV Pr.

WEST LIBRARY

The high sequence identity, 45%, between the KSHV and HCMV proteases suggests that the two enzymes have similar three-dimensional structures. The unique fold of proteases of the herpesvirus family creates a Ser-His-His catalytic triad in contrast to the Ser-His -Asp active site of other serine proteases such as trypsin, subtilisin and yeast carboxypeptidase (Perona & Craik, 1995) . The latter, digestive enzymes are significantly more active, exhibiting peptide hydrolysis rates three to five orders of magnitude greater than the viral proteases. A trypsin variant in which the active site aspartic acid has been replaced with an asparagine, trypsin D102N, exhibits an activity on a peptide substrate that is similar to that of the KSHV Pr (Table 2-1). Trypsin D102H, not yet expressed or characterized, would perhaps present a more accurate comparison but is not necessary to draw conclusions regarding the loss of Asp within the catalytic triad. The instructive value of D102H versus D102N is likely to be subtle, although it is an issue which may deserve further experimental consideration.

A less active protease can be understood in the context of the more selective processing activity associated with the herpesvirus life cycle. Indeed, the slightly higher k_{cat}/K_m value for KSHV Pr directed toward the HCMV substrate may be indicative of this. Perhaps it is favorable for the KSHV M-site to be processed slightly more slowly than other sites. It is also possible that the difference in M-site composition between the two synthetic substrates (P5-P6' for KSHV and P6-P5' for HCMV) is responsible for this difference, a fact that has been observed with HSV-1 Pr, for which peptide substrates containing positions P9-P8' were required for optimal hydrolytic activity (DiIanni *et al.*, 1993). In addition, the different fluorophore moieties could contribute to altered subsite binding properties; indeed, trypsin and trypsin D102N appear to discriminate between the

LIBRARY

two substrates, as well. The absence of the aspartic acid in the active site of the viral protease, while reducing the enzyme's velocity, also results in less sensitivity to standard serine protease inhibitors such as phenylmethylsulfonyl fluoride and tosyl lysyl chloromethyl ketone (Burck *et al.*, 1994; Cox *et al.*, 1995; Liu & Roizman, 1992; Stevens, *et al.*, 1994; Welch *et al.*, 1993). This was similarly observed for trypsin D102N (Craik *et al.*, 1987). Hence, subsequent inhibitor design for this new class of serine proteases must take into account the highly reduced nucleophilicity of the active site serine, and may, in fact, be aided by parallel investigations of this issue with trypsin D102N.

The prospect for specific inhibitor design is now enhanced by the availability of KSHV Pr. The bacterially-expressed, His₆-tagged Pr molecule is capable of catalyzing peptide bond hydrolysis of related viral processing sites. Preliminary analysis of the KSHV Pr reaction products by mass spectrometric methods (data not shown) indicates that three sites within the 11 amino acid KSHV M-site peptide are cleaved by KSHV Pr (Ser6-Ser7, Ala5-Ser6, and Arg8-Ser9) and that two sites within the HCMV M-site peptide (Ala6-Ser7 and Ser7-Ser8) are hydrolyzed by the enzyme. The expected Ala*Ser bond is cleaved in both cases. The basis for the relaxed substrate specificity of KSHV Pr toward these substrates is currently under investigation, as is a more complete kinetic characterization of the enzyme. This will allow direct comparison of the kinetic behavior of the herpesvirus family of maturational proteases with that of the now-identified KSHV enzyme. Results of this ongoing study will aid in the understanding of the molecular recognition properties of KSHV Pr.

LIBRARY
UNIVERSITY OF
TORONTO

Although the various protease members of the herpesvirus family are highly similar in their primary structure, there are several differences, especially with regard to their individual substrate specificities. This can be seen in the kinetic analysis of various synthetic substrates (Tigue *et al.*, 1996), as well as differences in the amino acid sequences of the release sites of the viral proteases. In particular, amino acid differences can be seen in the P3, P2, P2', P3' and P4' sites of KSHV Pr when compared with the R-sites of other members of the family (Figure 2-2). These differences may permit the design of more specific inhibitors of the KSHV protease. Furthermore, the prospect of achieving antiviral specificity with limited host cell toxicity may be enhanced by the fact that herpesvirus proteases have no known cellular homologs.

Finally, the three-dimensional structure of the HCMV protease reveals a dimeric assembly stoichiometry, consistent with both sedimentation studies (Cole *et al.*, 1996) and the concentration-dependence profile of its enzymatic activity (Darke *et al.*, 1996). Not unexpectedly, this assembly requires an extensive interface between its constituent protomers. A major component of this interface is an α -helix composed of residues 217 to 230, as well as residues from CD7. This region is conserved in its entirety in KSHV Pr, and strongly suggests a linkage between dimerization and enzymatic activity for this newly identified enzyme as well. This likely feature of the KSHV protease provides the opportunity to develop KSHV-specific or more broadly active anti-herpesviral agents, through disruption of Pr or Pr/AP homodimer formation. This strategy, using small molecule or dominant-negative inhibitors of dimerization, has proven to be effective in inhibiting the HIV protease (Babe *et al.*, 1992; Junker *et al.*, 1996; McPhee *et al.*, 1996). Such inhibitors can be used to dissect the role of the protease in the KSHV viral life

USC LIBRARY

cycle, and to examine the impact of antiviral therapy on the natural history of KSHV infection.

Acknowledgments

T.R.P. and A.U. contributed equally to the preparation of this manuscript. This work was supported by NIH grant GM39552 to C.S.C, the Biotechnology Research and Education Program and Center for AIDS Research Program to A.U., and the Howard Hughes Medical Institute (D.G.). We thank Dr. Toshi Takeuchi for providing trypsin and trypsin D102N for this study, and Dr. Christine Debouck and Dr. Stephen Todd for helpful discussions.

During the preparation of this manuscript the genomic sequence of KSHV was published (51) . Comparison of KSHV Pr DNA sequences showed a difference at codon 217, resulting in a Thr in the sequence presented in this manuscript and an Arg in the above mentioned publication. This difference could be due to strain differences, cloning artifacts, or sequencing errors.

MS
LIB
10
10

FIGURES

Figure 2-1

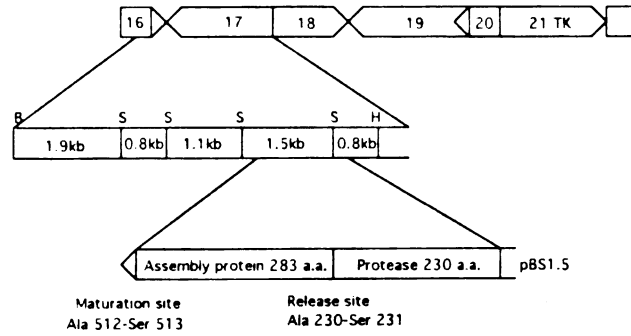


FIG. 1. Schematic of partial genome of KSHV and location of ORF 17. Arrowheads denote the directions of transcription. Abbreviations: B, *Bam*HI; S, *Sac*I; H, *Hind*III; a.a., amino acids.

LIBRARY

Figure 2-3

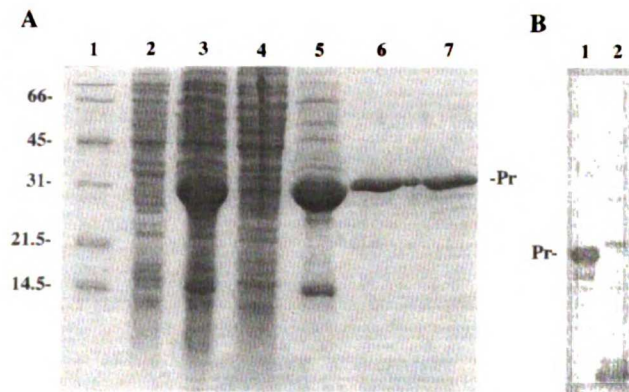


FIG. 3. SDS-polyacrylamide gel electrophoresis and immunoblot analysis of KSHV Pr expression and purification. (A) Coomassie blue-stained, 12.5% polyacrylamide-SDS gel. Lane 1 contains molecular size standards, with their masses (in kilodaltons) annotated to the left. Lane 2 contains a bacterial lysate harvested prior to IPTG induction. Lane 3 contains a lysate collected at the time of protein harvest. Lane 4 contains the soluble fraction after sonication of the lysate. Lane 5 contains urea-solubilized inclusion bodies. Lane 6 contains purified KSHV His₆-Pr(S114A). Lane 7 contains KSHV His₆-Pr. (B) Immunoblot of purified KSHV His₆-Pr (lane 1) and pQE30-transformed, IPTG-induced bacterial lysate (lane 2). The migration of Pr, noted between the two panels, differs due to different electrophoresis conditions.

Figure 2-4

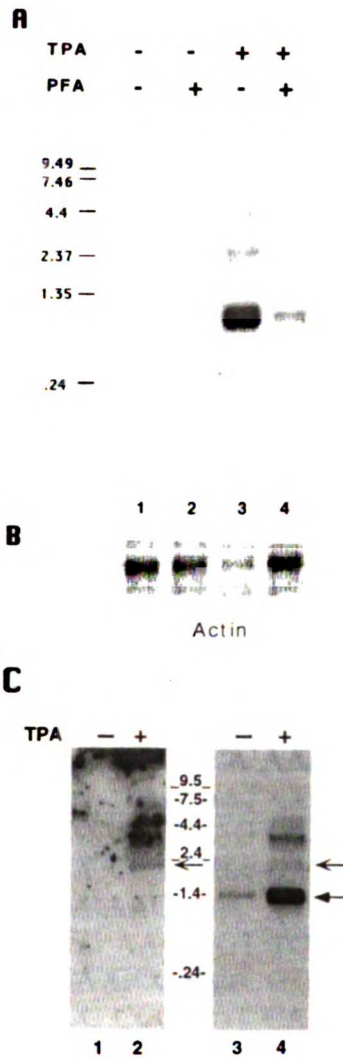


FIG. 4. Northern blots of BCBL-1 RNA hybridized to probes from Pr or Pr/AP. (A) Total RNA (300 μ g) from BCBL-1 cells that were uninduced (lane 1), uninduced in the presence of PFA (lane 2), induced with TPA (lane 3), or induced with TPA in the presence of PFA, was poly(A) enriched, separated on a 1% agarose-formaldehyde gel, and transferred to a nylon membrane. The membrane was hybridized to a probe made from sequences in Pr/AP (see Materials and Methods) and exposed to Kodak XAR5 film. (B) Same blot as shown in panel A, but hybridized to an actin probe. (C) Poly(A)-enriched RNA from uninduced BCBL-1 cells (lanes 1 and 3) and TPA-induced BCBL-1 cells (lanes 2 and 4) was hybridized to single-stranded antisense probes to the Pr domain alone (lanes 1 and 2, probe from the 0.8 kb *Sac*I fragment described earlier) and exposed to film for 2 days or was hybridized to the Pr/AP probe and exposed for 5 h (lanes 3 and 4). The bottom arrow indicates a transcript corresponding to the predicted size of the AP transcript, and the top arrows indicate RNA species corresponding to the predicted size of the Pr/AP transcript. Values adjacent to the gels are molecular sizes (in kilobases).

Figure 2-5: DNA sequence of KSHV Pr/AP.

ATG GCA CAG GGC CTG TAC GTC GGA GGG TTT GTA GAT GTT GTG TCC
TGC CCC AAG CTG GAG CAA GAG CTC TAT CTC GAT CCG GAT CAG GTG
ACG GAT TAT CTC CCA GTC ACA GAA CCC CTT CCA ATA ACA ATC GAA
CAC CTA CCA GAG ACA GAA GTG GGC TGG ACA CTG GGT CTA TTT CAA
GTG TCC CAC GGT ATT TTC TGC ACC GGA GCC ATC ACG TCG CCA GCC
TTC CTA GAG CTG GCA TCC AGG CTG GCG GAC ACC TCC CAC GTG GCC
AGA GCC CCC GTG AAA AAT CTC CCT AAG GAA CCA CTG TTG GAG ATA
CTC CAC ACG TGG CTC CCG GGG CTG TCT TTA TCG TCC ATA CAT CCC CGC
GAG TTA TCC CAG ACT CCC AGC GGT CCC GTG TTT CAA CAC GTA TCA
CTA TGC GCC CTG GGG CGC CGA CGC GGC ACA GTG GCC GTG TAC GGA
CAC GAC GCC GAG TGG GTG GTT TCC AGA TTC TCA TCA GTA TCT AAG
TCG GAG CGC GCC CAC ATC CTC CAG CAC GTA AGT AGC TGC AGG CTG
GAG GAC CTT TCC ACA CCA AAT TTC GTC AGT CCC CTG GAG ACC TTA
ATG GCA AAA GCT ATA GAT GCC AGC TTC ATA CGG GAC CGC CTC GAC
CTA TTG AAA ACT GAC AGA GGT GTG GCC AGC ATA TTG AGC CCG GTG
TAT TTA AAG GCC AGC CAA TTC CCG GCC GGC ATC CAA GCC GTC ACA
CCA CCC AGA CCA GCC ATG AAC AGC TCT GGT CAA GAG GAT ATC ATA
TCC ATC CCC AAA TCC GCC TTC CTG AGC ATG CTA CAA AGC AGC ATC
GAT GGA ATG AAG ACC ACA GCG GCA AAA ATG TCA CAT ACA CTT TCA
GGG CCA GGC CTA ATG GGG TGT GGG GGC CAG ATG TTC CCC ACC GAC
CAT CAC CTA CCT TCG TAT GTT TCA AAC CCA GCG CCA CCA TAC GGC
TAC GCT TAC AAG AAC CCA TAC GAT CCA TGG TAT TAC TCG CCA CAG
CTG CCT GGA TAT AGG ACG GGG AAG CGC AAG CGC GGC GCA GAG GAC
GAC GAA GGA CAC CTC TTT CCA GGA GAG GAG CCG GCG TAT CAC AAG
GAT ATC TTG TCC ATG TCA AAG AAC ATA GCG GAA ATA CAG TCT GAA
CTC AAA GAG ATG AAA CTG AAC GGT TGG CAC GCA GGG CCA CCG CCG
TCC TCC TCT GCA GCA GCA GCC GCA GTA GAT CCA CAC TAC AGG CCC
CAC GCC AAT TCA GCG GCC CCG TGT CAA TTC CCG ACA ATG AAG GAG
CAC GGA GGA ACC TAC GTA CAC CCA CCC ATT TAC GTG CAG GCG CCA
CAC GGT CAG TTC CAG CAA GCG GCG CCC ATC CTT TTT GCT CAG CCA
CAT GTG AGC CAC CCG CCA GTC TCT ACA GGA CTC GCG GTA GTT GGC
GCA CCA CCC GCT GAA CCC ACC CCC GCC TCC AGC ACG CAG AGC ATC
CAA CAA CAG GCA CCG GAG ACC ACG CAT ACA CCA TGC GCG GCG GTG
GAG AAA GAC GCT CCT ACG CCG AAC CCT ACA TCG AAC CGC CTT GAA
GCC AGC AGT CGC TCT AGT CCA AAA TCT AAA ATT CGC AAG ATG TTC
TGC GAG GAG CTC CAG CTT TTG GTT CCC TTT AGT GAG GGT TAA TTT
CGA GCT TGG CGT TAT CAT GGT CAT AGC TGT TTC CTG TGT GAA AAT GTT
ATC CGC TCC CCA ATT CCC CCC AAC ATT CGA

Table 2-1

TABLE 1. k_{cat} / K_m values for herpesviral Pr's and trypsins

Enzyme	k_{cat}/K_m ($M^{-1} min^{-1}$)		
	KSHV M-site	HCMV M-site	Related herpesvirus processing site(s) ^f
KSHV Pr ^a	165	590	
KSHV Pr S114A	ND ^b	ND	
Trypsin D102N ^c	457	2,162	
Trypsin ^d	3.7×10^6	2.3×10^6	
HSV-1 Pr			<100–2,200; ^e 27–27,000 ^f
HCMV Pr ^e			110–4,000
HHV-6 Pr ^e			3,000–17,000

^a Values determined in this study.

^b ND, not detectable in this assay.

^c Values from reference 18.

^d Values from reference 29.

^e Values from reference 64.

^f See individual references for exact substrates used.

Chapter 3

Auto-inactivation by Cleavage within the Dimer Interface of Kaposi's Sarcoma-associated Herpesvirus Protease

Todd R. Pray¹, Anson M. Nomura², Michael W. Pennington⁴, and Charles S. Craik^{2,3*}

¹Graduate Group in Biophysics, ²Dept. of Pharmaceutical Chemistry, and ³Depts.
of Biochemistry and Biophysics and of Cellular and Molecular Pharmacology,
University of California, San Francisco, California 94143-0446

⁴BACHEM Biosciences, Inc., King of Prussia, Pennsylvania 19406

This chapter is reprinted with the permission of the Journal of Molecular Biology

J. Mol. Biol. (1999). **289**, 197-203.

SUMMARY

An autolysis site of functional and structural significance has been mapped within the dimer interface of Kaposi's sarcoma-associated herpesvirus protease. Cleavage 27 residues from the C-terminus of the 230 amino acid, 25 kD protein was observed to cause a loss of dimerization and proteolytic activity, even though no active site moieties were lost. Gel-filtration chromatography and analytical ultracentrifugation were used to analyze the changes in oligomerization upon autolysis. The selective auto-disruption of this essential protein-protein interface by proteolytic cleavage resulted in a 60% loss in mean residue ellipticity by circular dichroism as well as a 20% weaker, 10 nm red-shifted intrinsic protein fluorescence emission spectrum. These apparent conformational changes induced a strict inhibition of enzymatic activity. An engineered substitution at the P1' position of this cleavage site attenuated autolysis by the enzyme and restored wild-type dimerization. In addition to retaining full proteolytic activity in a continuous fluorescence-based enzyme assay, this protease variant allowed the determination of the enzyme's dimerization dissociation constant of $1.7 \pm 0.9 \mu\text{M}$. The structural perturbations observed in this enzyme may play a role in viral maturation, and offer general insight into the allosteric relationship between the dimer interface and active site of herpesviral proteases. The functional coupling between oligomerization and activity presented in this study may allow for a better understanding of such phenomena, and the design of an enzyme variant stabilized to autolysis should further the structural and mechanistic characterization of this viral protease.

Kaposi's sarcoma, the most common neoplasm affecting patients with acquired immunodeficiency syndrome, is linked to the presence of the recently identified Kaposi's sarcoma-associated herpesvirus (KSHV) (reviewed in Ganem, 1997). As is the case for herpes simplex virus type 1 (HSV-1) and human cytomegalovirus (hCMV), KSHV most likely requires a serine protease, KSHV Pr, encoded in its own genome for capsid assembly. The development of mature capsids by cleavage at the maturation site (M-site) and release site (R-site) of the virally encoded protease-assembly protein precursor molecule is contingent upon protease activity (reviewed in Gibson, 1996; Roizman & Sears, 1996). KSHV Pr was sequenced, cloned, expressed and characterized preliminarily by our laboratory (Ünal *et al.*, 1997).

Significant biochemical and structural evidence suggests that dimerization is linked to enzymatic activity for HSV-1 and hCMV Pr. K_d s ranging from 0.55 to 50 μ M have been determined through the use of light-scattering and chemical crosslinking (Margosiak *et al.*, 1996), centrifugation (Cole, 1996), and gel-filtration (Darke *et al.*, 1996; Schmidt & Darke, 1997). The three-dimensional structures of the proteases encoded by hCMV (Chen *et al.*, 1996; Qiu *et al.*, 1996; Shieh *et al.*, 1996; Tong *et al.*, 1996), HSV-1 and -2 (Hoog *et al.*, 1997), and varicella-zoster virus (VZV) (Qiu *et al.*, 1997) reveal a novel fold, a Ser-His-His catalytic triad, and indicate that these proteins homodimerize through the association of α -helices near their C-termini.

Although it is believed that dimerization is required for activity in this class of enzymes, neither the structural nor functional consequences of a loss of dimerization have been documented. In this study we find a direct correlation between loss of dimerization through autolysis at a naturally occurring site within KSHV Pr's dimer

interface α -helix, and the subsequent loss of its proteolytic activity. Perturbation of the enzyme's secondary and tertiary structures, detected spectroscopically, accompanies this auto-inactivation and provides information regarding the possible regulatory role of dimerization for this protease.

Identification of an Auto-inactivation Site within KSHV Protease

To facilitate the structural characterization of KSHV Pr, an expression system was developed to produce the enzyme in a soluble form. The KSHV Pr ORF was amplified by PCR from the plasmid pBS λ 21-5.8 (Ünal *et al.*, 1997), inserting a stop codon after Ala230 of the R-site, corresponding to Ala256 of hCMV Pr, and was ligated into the *Nco* I and *Hind* III sites of the vector pQE60 (Qiagen, Inc.) such that no His-tag was incorporated into the coding sequence of the enzyme. Initial studies demonstrated high expression levels in *Escherichia coli*, but indicated that a significant fraction of the protein was present as a lower molecular weight species (Figure 3-1a). Preliminary characterization indicated that the protease displayed hydrolytic activity against synthetic substrates. However, the loss of such activity within 60 minutes at high protease concentrations, and during the purification itself, was accompanied by further production of the lower molecular weight proteolytic fragment (not shown). KSHV Pr S114A lacking the active-site serine (hCMV Pr residue 132), created by PCR-mediated site-directed mutagenesis, did not exhibit the same proteolytic pattern when expressed and harvested under identical conditions (Figure 3-1a). Thus, the cleavage of KSHV Pr most likely proceeded in an autolytic fashion and was not due to digestion by bacterial enzymes.

The size difference between KSHV Pr and its truncation product, Pr Δ , was 3 kD as judged by SDS-PAGE/immunoblot analysis (Figure 3-1a). Sequence analysis identified a possible cleavage site 27 amino acid residues from the enzyme's C-terminus; the loss of these 27 residues would convert the 25.2 kD protein to a 23.3 kD fragment. This region contained a preferred Ala-Ser bond at positions 203 and 204, which aligns with the Ala228-Leu229 dipeptide of hCMV Pr (Figure 3-1b), but was not previously identified as an internal site (I-site) due to its location relative to those of hCMV. While hCMV Pr's two I-sites are present within loops (Chen *et al.*, 1996; Qiu *et al.*, 1996; Shieh *et al.*, 1996; Tong *et al.*, 1996) and do not significantly perturb proteolytic activity (Holwerda *et al.*, 1994; O'Boyle *et al.*, 1995), the I-site of KSHV Pr is predicted to be present within the conserved α -helix of the protease's dimer interface based on an homology model of the enzyme (Figure 3-2a). Due to this autolysis site's position and function within KSHV Pr, and to differentiate it from those of the hCMV enzyme, in this report it is referred to as the dimer disruption site (D-site).

Stabilization of KSHV Protease to Autolysis

In an attempt to reduce autolysis while maintaining an intact dimer interface, a conservative substitution was sought for the D-site of KSHV Pr. After examination of a multiple sequence alignment of this region of herpesviral proteases, a Ser \rightarrow Gly (S204G) substitution at the P1' position was suggested (Figure 3-1b). The only other protease of this class with an Ala-Ser dipeptide at this position is that of murine herpesvirus-68 (MHV68), which has not been characterized. The more closely related herpesvirus saimiri (HVS) enzyme differs, as does that of Epstein-Barr virus (EBV), at the P1'

position with Gly. While EBV Pr has activity in the range of other characterized enzymes of this class, it does not inactivate with an Ala-Gly bond at this site, even though the remaining residues are similar (Donaghy & Jupp, 1995). The similarity between KSHV and hCMV Pr within this region is quite high, which is why hCMV Pr, rather than HSV or VZV Pr, was used as the basis for the model in Figure 3-2a. HSV and VZV Pr differ significantly from the sequence of both KSHV and hCMV enzymes near the KSHV D-site, and demonstrate a different dimer interface contact pattern from hCMV Pr (Hoog *et al.*, 1997; Qiu *et al.*, 1997).

Construction of KSHV Pr S204G by PCR-mediated site-directed mutagenesis resulted in the reduction of autoproteolysis during bacterial expression (Figure 3-1a), and the purified variant retained full activity in a continuous fluorescence-based enzyme assay (Table 1). The migration of this enzyme by SDS-PAGE is identical to full-length wild-type KSHV Pr and the S114A variant, and little or no visible truncation product was present by immunoblotting in repeated expression trials. In addition, the k_{cat}/K_m value for wild-type KSHV Pr prior to autolysis is the same as that of the S204G variant, $1.1 (\pm 0.4) \times 10^3 \text{ M}^{-1} \text{ min}^{-1}$, for the hCMV M-site substrate used previously (Holskin *et al.*, 1995; Ünal *et al.*, 1997). KSHV Pr S204G was also tested for reactivity against a newly synthesized fluorogenic KSHV R-site substrate, and was found to hydrolyze this molecule at roughly half the rate, $0.52 (\pm 0.1) \times 10^3 \text{ M}^{-1} \text{ min}^{-1}$ (Table 1). This compound exhibited 5-fold greater solubility and fluorescence enhancement than a previously utilized KSHV M-site substrate (Ünal *et al.*, 1997). Purified KSHV Pr Δ did not exhibit detectable peptidolytic turnover, consistent with the loss of proper active site geometry

and/or substrate binding upon truncation; as expected, the active site variant S114A was also incapable of hydrolysis (Table 1).

Loss of dimerization upon KSHV Protease D-site Cleavage

Due to the D-site's presence within the predicted dimer interface of KSHV Pr (Figure 3-2a), the oligomerization properties of the enzyme were examined. At concentrations above 5 μM , purified full-length KSHV Pr was present predominantly as a dimer, eluting from a gel-filtration column with an estimated molecular weight of 50.1 kD (Figure 3-2b). However, upon reduction of the total protein concentration to 1.8 μM , a nearly 1:1 ratio of dimer to monomer was present, indicative of the sample being at a concentration near its K_d . On the other hand, isolated KSHV Pr Δ displayed no dimerization, either at concentrations in the 10 μM range as assayed by gel-filtration where it eluted with an M_r of 23.6 kD (Figure 3-2b), or at nearly 0.1 mM levels as examined by analytical equilibrium ultracentrifugation (not shown). From these experiments it became apparent that KSHV Pr D-site cleavage disrupted not only enzymatic activity but also dimerization.

The dimerization of the D-site S204G variant was analyzed using conditions identical to those for the wild-type enzyme. In the same gel-filtration assay KSHV Pr S204G dimers eluted at an M_r of 50.8 kD, essentially identical to that of the non-truncated wild-type enzyme which eluted at 50.1 kD (Figure 3-2b). Since KSHV Pr S204G was stabilized to autolysis, it was assayed by sedimentation equilibrium to further evaluate its dimerization properties. Simultaneous analysis of data collected at loading concentrations of 1 and 5 μM , and at three rotor speeds from 10,000 to 20,000 rpm,

resulted in a K_d for S204G dimerization of $1.7 \pm 0.9 \mu\text{M}$ (Figure 3-2c,d). This value agreed with a previous analysis of hCMV Pr dimerization by similar means (Cole, 1996), and also coincided with the 1:1 dimer:monomer ratio of KSHV Pr at low micromolar concentrations (Figure 3-2b).

Conformational Changes during Autolytic Inactivation of KSHV Protease

In order to further understand the structural significance of proteolytic inactivation of KSHV Pr at its dimer interface, a spectroscopic characterization was performed. While the three intact, dimeric molecules exhibited nearly indistinguishable circular dichroism (CD) spectra, qualitatively similar to that of hCMV Pr (Liang *et al.*, 1998), KSHV Pr Δ suffered a greater than 60% loss in ellipticity (Figure 3-3a). A computational analysis of the spectral properties of KSHV Pr Δ was performed, yielding an apparent reduction in helical content relative to the full length protease molecules (Table 1). While this finding is consistent with the cleavage site's presence within the dimer interface α -helix, firm conclusions regarding the exact nature of the secondary structural loss are difficult to resolve from such analyses. In particular, because of the novel α/β fold of the dimeric herpesvirus type serine proteases, the established reference sets of protein CD spectra may not adequately represent the conformational changes taking place upon KSHV Pr D-site cleavage.

While the helical packing interactions contributing to KSHV Pr dimerization are lost upon D-site cleavage, it appears that the effects of truncation are not limited to the secondary structure within this protein-protein interface. An apparent loss of tertiary structure is evident in the 20% weaker, 10 nm red-shifted fluorescence emission spectrum

of KSHV Pr Δ relative to full-length KSHV Pr (Figure 3-3*b*). Truncation of KSHV Pr at its D-site is not predicted to remove any Trp residues, although the P2' Phe of the D-site is lost, as well as the Tyr residue four positions from the C-terminus of the enzyme. Neither of these amino acid residues likely contribute much to the overall fluorescence emission of KSHV Pr. Their low experimental fluorescence sensitivities relative to Trp preclude this (Tyr, 2.0×10^{-2} ; Phe, 0.08×10^{-2} ; Trp, $11.0 \times 10^{-2} \text{ M}^{-1} \text{ cm}^{-1}$) (Cantor & Schimmel, 1980), especially since all three Trp residues and the remaining seven Phe and four Tyr side-chains are retained in KSHV Pr Δ . Rather, in the homology model of the enzyme, it appears that two of the three Trp residues within each KSHV Pr monomer become more solvent-exposed upon truncation. Trp109, corresponding to hCMV Pr Ser127, is directly behind the dimer interface α -helix of its own monomer, and KSHV Pr Trp156, conserved in hCMV Pr at position 179, contacts residues near the C-terminus of the protease which are lost upon autolysis (Figure 3-2*a*). On the other hand KSHV Pr Trp54, which aligns with hCMV Pr His71, is near neither the dimer interface nor residues lost upon truncation. This may indicate that the red-shift of the entire emission spectrum is due to partial relaxation of the hydrophobic core of the protein. However, the likely maintenance of apparent secondary structure within KSHV Pr Δ (Figure 3-3*a*, Table 1), coupled with its cooperative unfolding at relatively high temperature (A. Nomura, V. Dötsch & C. Craik, unpublished observations), seems to preclude the wholesale loss of tertiary packing of the remaining α -helical and β -sheet elements.

Possible Role of D-site Cleavage in Regulation of KSHV Maturation

The inactivation of KSHV Pr by disruption of its dimer interface, and the resultant structural transitions which give rise to the altered spectroscopic signature of the enzyme, provide an interesting and novel mechanism for the regulation of viral protease activity (Babe & Craik, 1997). By selectively perturbing essential protein-protein contacts distal from its active site, KSHV Pr transmits structural information to its catalytic residues and/or substrate binding determinants (Bonneau *et al.*, 1997; Tong *et al.*, 1998). The precise role of the inactivation event in the viral life cycle is yet to be determined, although recent evidence suggests the presence of KSHV Pr Δ in viral particles produced in culture (T. Pray, M. Lagunoff, D. Ganem & C. Craik, unpublished observations).

Perhaps KSHV Pr activity is subject to different regulatory mechanisms than related enzymes due to unknown requirements of KSHV maturation. The only other herpesviral proteases with known I-sites are those of the cytomegalovirus lineage. hCMV Pr contains two I-sites whose cleavage has no apparent biochemical consequence in terms of regulating enzyme activity, although autolysis at one of these sites does perturb crystallization of the enzyme (Chen *et al.*, 1996; Holwerda *et al.*, 1994; O'Boyle *et al.*, 1995; Qiu *et al.*, 1996; Shieh *et al.*, 1996; Tong *et al.*, 1996). While KSHV Pr is most closely related to HVS Pr, the latter enzyme does not contain the Ser preferred for cleavage at P1' of the KSHV D-site (Figure 3-1*b*). The fact that MHV68 Pr does contain this site, even though this virus is more distantly related to KSHV, may indicate selective pressure governing such a cleavage event. The role of D-site cleavage will be further addressed in subsequent cell culture and high-resolution structural studies of KSHV Pr and Pr Δ , as will the linkage between dimerization and activity. The functional coupling

between KSHV Pr's dimer interface and catalytic machinery, as probed in this study using the autolysis site as an experimental tool, provides strong evidence for the positive regulatory role of oligomerization in this class of enzymes.

ABBREVIATIONS

KSHV (Pr), Kaposi's sarcoma-associated herpesvirus (protease); HSV, Herpes simplex virus; hCMV, human cytomegalovirus; VZV, varicella zoster virus; MHV68, murine herpesvirus 68; EBV, Epstein-Barr virus; HVS, herpesvirus saimiri; EHV, equine herpesvirus; AHV, avian herpesvirus; sCMV, simian cytomegalovirus; HHV-6, human herpesvirus 6; M-site, maturation site; R-site, release site; I-site, internal site; D-site, dimer disruption site; CD, circular dichroism; ESI-MS, electrospray ionization mass spectrometry; DTT, dithiothreitol; EDTA, ethylenediamine tetraacetic acid.

ACKNOWLEDGEMENTS

The authors thank Volker Dötsch, Michelle Lamb, Kinkead Reiling, and Steven Todd for helpful suggestions regarding this manuscript, and the David Agard laboratory for use of the CD spectrometer. This work was supported by the NIH (C.S.C. – GM56531, A.M.N. – GM08388, T.R.P. – GM08204) and by the ARCS Foundation (T.R.P.).

FIGURES

Figure 3-1

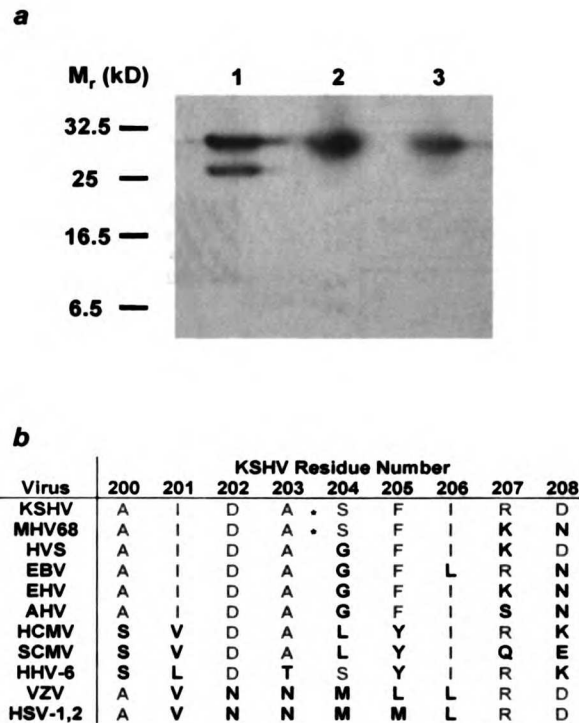


Figure 1 Identification of an autolysis site within KSHV Pr.

Panel a: Immunoblot of KSHV Pr autolysis product during bacterial expression. Lane 1 contains wild-type KSHV Pr. Lane 2 contains the active site mutant S114A. Lane 3 contains the D-site mutant S204G. Relative molecular weights are indicated to the left of lane 1. Samples were harvested following five hours of protein expression after induction with 100 μ g/ml IPTG. All samples contain 2 μ l from a 200 μ l boiling lysis in Laemmli buffer of the transformed X-90 *E. coli* pellet from 1 ml of identically treated and harvested cultures. Samples were run on a 12.5% polyacrylamide-SDS gel (Laemmli, 1970) and electrophoretically transferred to BA-85 nitrocellulose (Schleicher & Schuell). Anti-KSHV Pr serum was incubated with the membrane at a dilution of 1:2000 and detected using enhanced chemiluminescence (Amersham).

Panel b: Identification of KSHV Pr D-site by sequence analysis. Only residues spanning KSHV Pr positions 200-208 and hCMV residues 225-233 are depicted. Residues identical to the KSHV sequence are in red, indicating high sequence similarity with all of the proteases except those of the α -herpesviruses VZV and HSV-1 and -2 in this region. The cleavage site is indicated by an asterisk between KSHV Pr Ala203 and Ser204. EHV: equine herpesvirus. AHV: avian herpesvirus. SCMV: simian cytomegalovirus. HHV-6: human herpesvirus-6.

Figure 3-2

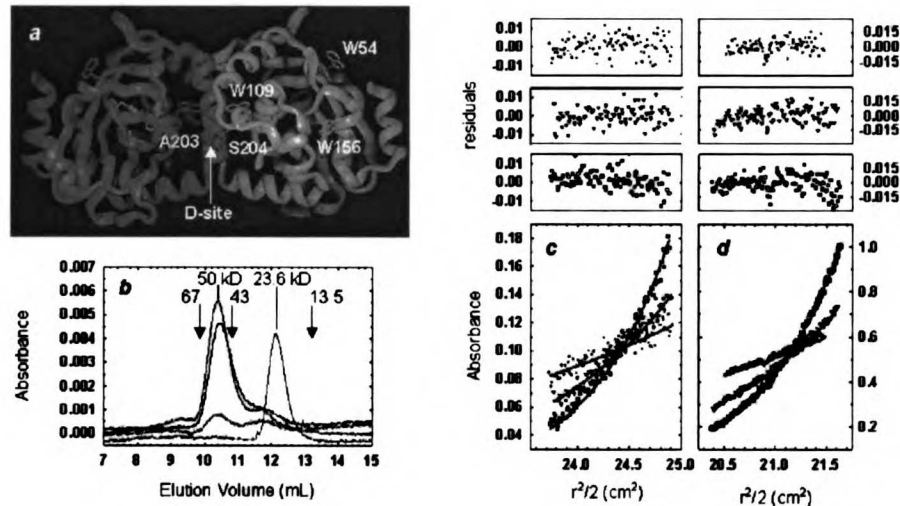


Figure 2 Effect of D-site cleavage on KSHV Pr dimerization.

Panel a: Homology model of KSHV Pr dimer. Monomers are presented in gray and blue. The 27 amino acid fragment cleaved from one monomer upon D-site autolysis is depicted in red. Active site residues from this monomer are in yellow. Disordered loop regions from the hCMV structure were omitted from the model. The Ala203-Ser204 D-site junction is labeled, as are the three Trp residues of one monomer. The KSHV Pr homology model was based upon hCMV Pr (PDB accession code CMV1). Following a sequence alignment using pileup (GCG, Madison, WI) provided through the Computer Graphics Laboratory at UCSF, the residues of hCMV Pr differing from KSHV Pr were replaced using the Biopolymer module of the Insight software package (Molecular Simulations, Inc.). Insertions in hCMV Pr relative to KSHV Pr are present in disordered loop regions of the CMV1 structure: nine residues at the N-terminus (within an 11 residue disordered region), 44-51 (within a 13 residue disordered region), 147-151 (within a 19 residue disordered region), and 203-204 (within an 11 residue disordered region).

Panel b: Loss of dimerization upon D-site cleavage. Size-exclusion chromatography was performed with a Superdex-75 HR 1 cm x 30 cm column (Pharmacia). 100 μ l samples were loaded in assay buffer at a flow rate of 0.5 ml min⁻¹ at room temperature. Full-length KSHV Pr at 5 μ M (black) and S204G at 7.5 μ M (green) exhibit dimerization. At 1.8 μ M, KSHV Pr is roughly 1:1 dimer:monomer (red). 12 μ M KSHV Pr Δ exhibits no detectable dimerization, eluting at a monomeric molecular weight (blue). The column was calibrated with sizing standards, indicated by downward arrows.

Panels c-d: Sedimentation Equilibrium Analysis of KSHV Pr S204G dimerization. Panels c and d contain absorbance data (230 nm) collected at two total protein concentrations, 1 and 5 μ M, respectively, and at three rotor speeds, 10,000 (circles); 15,000 (triangles); and 20,000 rpm (squares). The red curves represent simulated data derived from the best fit parameters of a monomer molecular weight of 20.5 kD and a K_d of 1.7 ± 0.9 μ M. Residuals are plotted in separate panels above c and d. The monomer mass was resolved as 20.5 kD, lower than the prediction of 25 kD, but similar to the value observed for hCMV Pr in analogous experiments. Attempts to fix the mass at the predicted value resulted in larger, significant deviations in the residuals of the fit (not shown), and a 20-fold higher K_d . KSHV Pr S204G was dialyzed extensively against assay buffer, placed in a 6 chamber centerpiece with dialysis buffer serving as reference, and spun in a Beckman Optima XL-A. Equilibrium was verified after 20 hours at each rotor speed by overlaying 4-hour-spaced radial absorbance scans. The data set was simultaneously analyzed by non-linear least squares fitting using the Beckman-supplied package for Origin 4.1 software (Microcal Software, Inc.) using an ideal monomer-dimer assembly model. Sednterp 1.01 software was used to estimate the protein's partial specific volume and the solvent density.

Figure 3-3

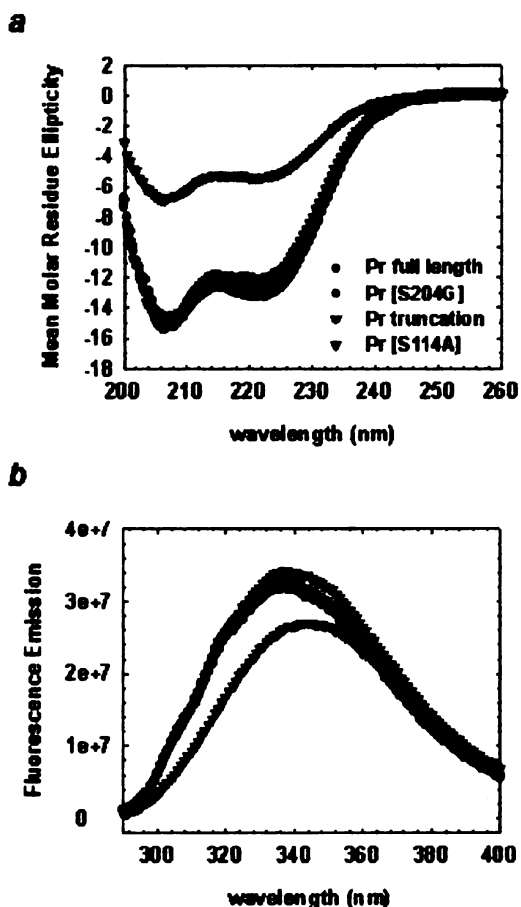


Figure 3 Spectroscopic detection of structural changes within KSHV Pr upon D-site cleavage.

Panel a: Secondary structure loss detected by CD spectroscopy. All full-length protease molecules exhibit nearly identical CD spectra and secondary structures at 0.5 to 1.5 μM concentrations in assay buffer (Table 1). At the same concentration, KSHV Pr Δ has an altered spectrum, with a much reduced mean molar residue ellipticity ($\text{mdeg cm}^2 \text{ dmol}^{-1} \text{ g}^{-1}$). CD scans were acquired on a Jasco 710 Spectropolarimeter; the samples held in 0.2 cm pathlength cuvettes at 20 $^{\circ}\text{C}$, and were obtained by 10-fold signal averaging and solvent correction.

Panel b: Tertiary structural changes or more highly solvent-exposed hydrophobic core of KSHV Pr Δ detected by intrinsic protein fluorescence. Protein samples were at 1 μM concentration in assay buffer at 20 $^{\circ}\text{C}$. All full-length protease molecules have coincident spectra, while KSHV Pr Δ differs significantly in magnitude and the wavelength of peak emission intensity. Fluorescence excitation was at 275 nm, and emission ($\text{cps}/\mu\text{Amp}$) monitored by 5-fold averaged, solvent- and lamp intensity-corrected scans.

Table 3-1

Table 1. Summary of kinetic data and apparent secondary structure

Protein	k_{cat}/K_M ($10^3 \text{ M}^{-1} \text{ min}^{-1}$)		Apparent secondary structure content (%) ^c		
	HCMV M-site ^a	KSHV R-site ^b	α -Helix	β -Strand	Other
KSHV Pr	1.1 (± 0.4)	ND ^d	45	23	31
Pr S204G	1.1 (± 0.4)	0.52 (± 0.1)	45	23	31
Pr S114A	<0.01	ND ^d	45	23	31
KSHV Pr Δ	<0.01	ND ^d	24	24	53

The KSHV R-site was chemically synthesized: N-Fmoc-L-Glu-(EDANS)-OH was prepared similarly to methods previously described (Maggiora *et al.*, 1992). Synthesis was initiated with Boc-Gly-Merrifield resin, DABCYL was incorporated using orthogonally protected Boc-N²-Lys(N²Fmoc)-OH, and Fmoc was removed. DABCYL was activated in the presence of HOBt and coupled (Konig & Geiger, 1992), and the remainder of the peptide assembled using standard solid-phase methodology. N-Fmoc-L-Glu-(EDANS)-OH was coupled in the last step and Fmoc removed. The peptide was then cleaved and deprotected (Pennington, 1994). After purification by RP-HPLC in an aqueous TFA/MeCN gradient, the product was lyophilized and verified by amino acid analysis and ESI-MS. ESI-MS ($M + H$)_{theory} 2107.48, ($M + H$)_{exp} 2108.

Protein samples were purified after expression in *E. coli* strain X-90 grown in LB medium after five hours induction with 100 $\mu\text{g}/\text{ml}$ IPTG at 30 °C. Following sonication and centrifugation in 50 mM potassium phosphate (pH 7.8), 25 mM NaCl, 1 mM DTT, 1 mM EDTA, streptomycin sulfate was added to a concentration of 1%. $(\text{NH}_4)_2\text{SO}_4$ was added to 25% saturation following centrifugation, the sample cleared, and protein precipitated by 45% saturation with $(\text{NH}_4)_2\text{SO}_4$. After resuspension, protease was eluted from butyl sepharose FF resin (Pharmacia) using a 0.5 \rightarrow 0 M $(\text{NH}_4)_2\text{SO}_4$ gradient in 50 mM potassium phosphate (pH 8), 25 mM NaCl, 1 mM DTT, 0.1 mM EDTA. Protease-containing fractions were dialyzed into 50 mM Tris (pH 8.0), 1 mM DTT, 0.1 mM EDTA, and eluted from a Mono-Q HR column (Pharmacia) in a 0 \rightarrow 0.5 M NaCl gradient. Protease-containing fractions were dialyzed into assay buffer (25 mM potassium phosphate (pH 7.0), 25% (v/v) glycerol, 150 mM KCl, 0.1 mM EDTA, 1 mM DTT or 2-mercaptoethanol), concentrated using YM-10 membranes (Amicon, Inc.), and fractionated over a Superdex-75 HiLoad 26/60 prep grade column (Pharmacia). Approximately 2-5 mg per liter culture of >99% pure KSHV Pr were obtained for all variants as judged by Coomassie Brilliant Blue staining of SDS-PAGE gels. Protein concentrations were determined using a calculated $\epsilon_{280} = 0.9 \text{ ml mg}^{-1} \text{ cm}^{-1}$ for full-length molecules, and $\epsilon_{280} = 1.0 \text{ ml mg}^{-1} \text{ cm}^{-1}$ for KSHV Pr Δ .

Enzyme assays were performed at 20 °C in 0.5 ml assay buffer using a Fluorolog-3 fluorometer (ISA-SPEX). Product formation was monitored as described (Holskin *et al.*, 1995; Matayoshi *et al.*, 1990; Ünal *et al.*, 1997). The k_{cat}/K_M values were determined by a linear fit of [product]/time versus [substrate] in range of 1-25 μM with an enzyme concentration of 1 μM .

^a HCMV M-site: (DABCYL)-Arg-Gly-Val-Val-Asn-Ala(Ser-Ser-Arg-Leu-Ala-(EDANS)).

^b KSHV R-Site: Glu-(EDANS)-Val-Tyr-Leu-Lys-Ala(Ser-Gln-Phe-Pro-Ala-Gly-Ile-Lys-(DABCYL)-Gly-OH).

^c Secondary structure estimated using *k2d* software (Andrade *et al.*, 1993; Merelo *et al.*, 1994).

^d ND, not determined.

Chapter 4

Functional Consequences of the Kaposi's Sarcoma-Associated Herpesvirus Protease Structure: Regulation of Activity and Dimerization by Conserved Structural Elements[⊥]

K. Kinkead Reiling[‡], Todd R. Pray[‡], Charles S. Craik[§] & Robert M. Stroud^{§*}

[§]Departments of Biochemistry & Biophysics and Pharmaceutical Chemistry, and

[‡]Graduate Group in Biophysics, University of California in San Francisco,

San Francisco, CA 94143

[†] Research was supported by the NIH (R.M.S. & C.S.C., GM56531). K.K.R & T.R.P. were partially supported by a graduate training grant NIH GM08204 and by the ARCS Foundation (T.R.P.)

[⊥]The coordinates have been deposited in the Brookhaven Protein Databank; accession code 1FL1.

This chapter is reprinted with the permission of the American Chemical Society

Biochemistry (2000). **39**: 12976-12803.

Abbreviations and textual footnotes

¹**Abbreviations:** rmsd, root mean squared deviation; KSHV Pr, Kaposi's sarcoma-associated herpesviral protease; KS, Kaposi's sarcoma; HIV, human immunodeficiency virus; HSV, herpes simplex virus; VZV, Varicella-zoster virus; hCMV, human cytomegalovirus; HHV-6 & HHV-7, human herpesviruses 6 and 7; EBV, Epstein-Barr virus; AP, assembly protein; NCS, non-crystallographic symmetry; CD, Circular dichroism;

²hCMV Pr numbering (as in ref (1-4)) is used, with the number in {} reflecting the residue number in the protease being addressed (e.g. KSHV Pr, VZV Pr, etc.). Non-conserved positions in sequence have both residue types listed.

³Error estimates used to report and evaluate conformational differences between groups of residues are calculated as rms. deviations between equivalent residues in monomer A to monomer B that are then averaged over all three herpesviral proteases (hCMV, HSV-2, KSHV).

Abstract

The structure of Kaposi's sarcoma-associated herpesvirus protease (KSHV Pr), at 2.2Å resolution, reveals the active site geometry and defines multiple possible target sites for drug design against a human cancer-producing virus. The catalytic triad of KSHV Pr, (Ser114, His46, and His157) and transition state stabilization site are arranged as in other structurally characterized herpesviral proteases. The distal histidine-histidine hydrogen bond is solvent accessible, unlike the situation in other classes of serine proteases. As in all herpesviral proteases, the enzyme is active only as a weakly associated dimer ($K_d \sim 2\mu\text{M}$), and inactive as a monomer. Therefore, both the active site and dimer interface are potential targets for antiviral drug design. The dimer interface in KSHV Pr is compared with the interface of other herpesviral proteases. Two conserved arginines (Arg209), one from each monomer, are buried within the same region of the dimer interface. We propose that this conserved arginine may provide a destabilizing element contributing to the tuned micromolar dissociation of herpesviral protease dimers.

Introduction

Kaposi's sarcoma (KS) has emerged as a debilitating and disfiguring disease among the human immunodeficiency virus (HIV) infected population (Ganem, 1997). HIV infected men are at least 10,000 times more likely to develop aggressive KS lesions, such as peripheral effusion lymphomas (PEL) or body cavity-based lymphomas (BCBL) than the population at large (Biggar & Rabkin, 1996). While HIV appears to be a cofactor for the development of KS, an epidemiological link relating KS to the sexual history of HIV positive patients suggested a separate transmissible etiological agent (Reitz *et al.*, 1999). A human herpesvirus (Kaposi's Sarcoma-associated herpesvirus, KSHV), found in PEL and BCBL neoplastic tissues, is thought to be this transmissible agent (Chang *et al.*, 1994). Treatment of KS is hampered by a dearth of therapeutic agents specific for KSHV, and is currently limited to compounds directed at related viruses such as herpes simplex virus (HSV) or at HIV itself (Jacobsen *et al.*, 1999).

Herpesviruses are double-stranded DNA viruses with a common viral particle architecture. They are divided into three sub-families based on clinical characteristics, which include host cell types and natural history of infection (Roizman *et al.*, 1992). These sub-families are the α -herpesviruses, which include herpes simplex virus-1 and -2 (HSV-1 & -2) and Varicella-zoster virus (VZV), the β -herpesviruses, which include human cytomegalovirus (hCMV) and human herpesviruses 6 and 7 (HHV-6, HHV-7), and the γ -herpesviruses, represented in humans by KSHV and Epstein-Barr virus (EBV). Sequence comparison of herpesviral proteases yields an average amino acid identity of 27% between subfamilies and 51% within each subfamily. Despite the clinical nature of

the sub-families, similarity among the herpesviral protease structures is consistent with these classifications.

KSHV, like other herpesviruses, requires a maturational protease to generate infectious virions (Gibson, 1996; Roizman & Sears, 1996). Formation of viral capsids is initiated by the viral assembly protein (AP), which forms a scaffold on which spherical procapsids assemble. The virally encoded serine protease KSHV Pr is expressed as an N-terminal fusion attached to roughly 10% of KSHV AP molecules (Ünal *et al.*, 1997). Maturation of the viral procapsid into a structure receptive to DNA packaging requires the cleavage of AP at a maturation site (M-site) near its C-terminus. In addition to processing AP at its M-site, KSHV Pr cleaves itself away from the precursor fusion protein (Pr/AP) at the release site (R-site), which separates all herpesviral protease domains from their AP constituents. The M and R sites exhibit consensus cleavage sequences of (V/L)-(N/Q/E)-A*S and Y-(V/L/I)-(K/Q)-A*S (Gibson *et al.*, 1994). A third proteolytic event, unique to KSHV, acts as an auto-regulatory mechanism, whereby the protease inactivates itself upon cleavage at a dimer-disruption site (D-site) (Pray *et al.*, 1999). By analogy to HSV-1, inhibition of KSHV Pr will prevent maturation of virions and the subsequent dissemination of infectious viral particles (Gao *et al.*, 1994; Preston *et al.*, 1983; Matusick-Kumar *et al.*, 1995).

The herpesviral protease family shares a common tertiary fold and a dependence on dimerization for proteolytic activity, despite the stability of the inactive monomer (Darke *et al.*, 1996). The relatively weak micromolar dimerization affinity of herpesviral proteases (Pray *et al.*, 1999; Darke *et al.*, 1996; Cole, 1996; Schmidt & Darke, 1997) is thought to act as a regulatory mechanism that can limit protease activity to the interior of

the maturing viral particle where the concentration is sufficient to support dimerization. Herpesviral proteases hydrolyze peptide bonds using a Ser-His-His catalytic triad in which the position of the aspartic acid residue seen in other classes of serine protease is occupied by a histidine. The catalytic efficiency of herpesviral proteases is lower by 100 to 1000-fold (in k_{cat}/K_m) relative to the trypsin family (Ünal *et al.*, 1997). The crystal structures of the hCMV Pr (Qiu *et al.*, 1996; Tong *et al.*, 1996; Shieh *et al.*, 1996; Chen *et al.*, 1996), HSV-1 and HSV-2 Pr (Hoog *et al.*, 1997), and VZV Pr (Qiu *et al.*, 1997) characterize the overall fold and allow the structural evaluation of the α - and β -herpesviral protease families.

We report the crystal structure of KSHV Pr at 2.2Å resolution. This is the first structure of a γ -herpesviral protease to be determined. The KSHV Pr catalytic triad and oxyanion hole geometry are congruent with those of other herpesviral proteases. The hydrogen bonds, between side chains of the catalytic triad of KSHV Pr and all other herpesviral proteases, are found to be more solvent exposed than those in other classes of serine proteases. The structural divergence of the dimer interface helices among herpesviral proteases is evaluated in the context of the transition that generates the active dimer from inactive monomers. Burial of two conserved arginines (Arg234{209}²), one from each monomer, close to each other and within the interface of KSHV Pr is discussed in reference to the regulation of dimerization and thus activity of herpesviral proteases.

Experimental Procedures

Protein Purification and Crystallization

KSHV Pr used for crystallization was prepared as described previously (Pray *et al.*, 1999), and contained the mutation S204G, which blocks autolysis. After purification, protein was concentrated to 3.0 mg/ml using Amicon YM-10 membranes. Crystals of KSHV Pr were grown by hanging drop vapor diffusion. KSHV Pr crystallized from a mixture of 1 microliter of 1mM *t*-Boc-YLKA-chloromethyl ketone (obtained from Z. Zhang and P. Ortiz de Montellano) in 10% acetonitrile, 2 microliters of well buffer, and 2 microliters of 3-mg/ml protease solution. The protease solution used in crystallization contained 25-mM potassium phosphate (pH 7.0), 10% glycerol and 1 mM dithiothreitol. Crystallization well buffer contained 22% PEG-2K, 100 mM Tris-HCl (pH 7.5), 10% glycerol and 190 mM LiSO₄. Crystals of KSHV Pr grew at 25 C over the course of one to two months as small trapezoidal or hexagonal plates measuring 0.2 mm x 0.075 mm x 0.050 mm and belonging to space group P3₁21 with unit cell dimensions a=b=53.58Å and c=323.06Å. The asymmetric unit contained a dimer, yielding a crystal solvent content of 53.7%.

Data Collection, Refinement Tools

The structure was refined against a 2.2Å data set collected at SSRL beam line 9-1 using a crystal frozen in 20% glycerol as the cryoprotectant. Diffraction data was integrated, scaled and merged using the HKL package (Otwinowski, 1993). The structure was solved by molecular replacement methods utilizing AMoRe (Navaza, 1994) from the CCP4 suite (Collaborative Computational Project, 1994). Non-crystallographic

symmetry (NCS) averaging was performed using the program dm (Cowtan, 1994). Manual cycles of model rebuilding were performed using the MOLOC (Muller *et al.*, 1988) graphical interface. The automated refinement of the model, including rigid body, positional, and temperature factor refinement and simulated annealing, utilized the CNS package (Brunger *et al.*, 1998).

Refinement Protocol

Molecular replacement was performed with a polyserine search model composed of residues 12-21, 56-109, 119-134, 154-186 and 218-256 from the structure of hCMV Pr (1CMV- (Qiu *et al.*, 1996)). Data from 10Å to between 4.5 and 3.0Å resolution yielded a post-rigid body R factor of 48.4%(3.0 Å). Three initial cycles of non-crystallographic symmetry (NCS) averaging of electron density maps generated using the polyserine model allowed assignment of 75% of the sequence. The model ($R_{\text{cryst}} = 37.6\%$, $R_{\text{free}} = 39.4\%$) was then subjected to multiple rounds of torsional simulated annealing, and positional and group B-factor minimization. NCS restraints were maintained for backbone atoms throughout refinement and for side chains until R_{free} dropped below 30%. Attention was paid throughout refinement to the possible presence of the tetrapeptide chloromethyl ketone, which was not observed in the crystal structure but was present during crystallization. Iterative rounds of manual rebuilding and automated refinement have brought the current model to crystallographic R-factors of 25.97% free and 22.53% cryst. The current model of KSHV Pr contains 86% (399/460 residues) of the sequence, with two loops (16-37, 117-131 in monomer A; 15-27, 121-129 in

monomer B) disordered in each monomer. The model exhibits good geometry with rmsd for bond lengths and angles of 0.561Å and 3.8° respectively (Table 4-1).

Structure and Sequence Alignments and Solvent Accessibility Measurements:

Structure alignments were carried out by the method of least-squares superposition as implemented in lsqman of the O suite (Kleywegt, 1994). In all structural alignments, the β -barrel of the herpesviral protease structures was defined as follows: KSHV Pr β 1 5-9, β 2 41-43, β 3 51-60, β 4 65-71, β 5 113-115, β 6 134-137, β 7 147-150; hCMV Pr (PDB accession codes: apo-1CMV & inhibited-2WPO) 14-18, 58-60, 68-77, 82-88, 131-133, 157-160, 170-173; HSV2 Pr (PDB accession code:1AT3) 21-25, 56-58, 66-75, 80-86, 128-130, 148-151, 161-164; VZV Pr (PDB accession code: 1VZV) 13-17, 47-49, 57-66, 71-77, 119-121, 139-141, 152-155. Helices were defined as follows: KSHV Pr α 1 74-84, α 2 100-110, α 3 154-159, α 4 167-179, α 5 193-203, α 6 209-220; hCMV Pr 91-101, 118-128, 177-182, 190-202, 218-229, 234-245; HSV2 Pr 89-99, 115-125, 168-173, 181-193, 210-221, 226-237; VZV Pr 80-90, 106-116, 159-164, 172-184, 199-210, 215-226. Multiple sequence alignments were carried out using ClustalW (Thompson *et al.*, 1994). Active site solvent accessibility was determined by the double cubic lattice method as implemented in ASC (Eisenhaber *et al.*, 1995). The helical packing analysis for each protease was carried out using PROMOTIF (Hutchinson & Thornton, 1996).

RESULTS

KSHV Pr Monomer: Fold

Each monomer of KSHV Pr is composed of a seven-stranded, predominantly anti-parallel β -barrel, one end of which is surrounded by a hemispherically packed set of six α -helices (Fig. 4-1). Residues 1 to 87{70} form a four-stranded, twisted β -sheet, which constitutes half of the β -barrel, and the loop that presents His63{46} of the catalytic triad. Residues 90{74}-128{110} contain the first of three helical pairs (α 1 and α 2), which exhibit a crossing angle of 95° and pack against the end of the β -barrel proximal to the dimer interface. Loop 4 (LP4: residues 101{84}-118{100}) is in a closed conformation resulting in a 60° rotation hinged at the base of the loop, or in a 12\AA shift at the end of the loop when compared to the open conformation of HSV-2 Pr and VZV Pr (Qiu *et al.*, 1997). A second twisted sheet, formed by residues 129{111} to 175{152}, constitutes the three remaining strands of the β -barrel. Residues 176{153} to the C-terminal Ala256{230} form four helices. The first two helices (α 3 and α 4) pack anti-parallel to each other with a crossing angle of 150° , and contact the first sheet of the β -barrel (residues 1 to 87{70}). Helices α 5 and α 6 pack against the loops containing the central active site His63{46} and the oxyanion hole loop, respectively. In total, these six helices sequester 50% of the β -barrel from solvent. Helices α 1 and α 5 are the central features of the dimer interface, contributing 86% of the surface area buried by each monomer upon dimerization.

KSHV Pr Monomer: Structural Conservation of the Core β -barrel with Divergence in Helical Packing.

The structural similarity among herpesviral proteases is strongest within the core β -barrel, and diverges in the surrounding helices and loops (Fig. 4-2a). The core β -barrel is conserved among the four herpesviral protease structures (KSHV, hCMV, HSV2, VZV) with an average C_{α} rmsd of 0.5Å. Lesser conservation in the helical packing against the β -barrel results in an average overall C_{α} rmsd for the aligned secondary structures of 1.4Å. However, the degree of structural divergence in helical packing is not uniform, and ranges from 0.88Å rmsd for helix α_6 to 2.68Å rmsd for helix α_5 (Fig. 4-2b).

Positioned at the convergence of helices α_3 , α_4 and α_6 is a conserved aromatic bundle formed by residues Phe19{10}, Phe83{66}, and Phe184{161}. Phe19{10} and Phe83{66} emanate from β -barrel strands β_1 and β_4 , while Phe184{161} lies within the loop connecting helices α_3 and α_4 (Fig. 4-3). Structural alignment of this motif across the herpesviral proteases reveals conserved side chain packing with an average rmsd of 0.24Å for atoms through C_{β} and 1.4Å for all atoms. This conserved hydrophobic bundle may serve as an anchor point on the surface of the β -barrel stabilizing the packing of helices α_3 , α_4 and α_6 . In contrast, the packing of helices α_1 and α_5 is predominantly defined by interactions within the dimer interface. Stabilization of helices α_3 , α_4 , and α_6 by the conserved Phe-bundle as opposed to the dimerization dependent stabilization of helices α_1 and α_5 may contribute to the differing magnitudes of structural divergence seen in the helices of herpesviral proteases (Fig. 4-2b).

Active Site: Environment of Catalytic Machinery and Substrate Binding Groove

KSHV Pr's catalytic triad (Ser132{114}, His63{46} and His157{134}) is located on the solvent exposed surface of strands $\beta 5$ and $\beta 6$ within a shallow active site depression bracketed by helices $\alpha 5$ and $\alpha 6$ from one monomer and $\alpha 1$ from the other monomer. Across the active site and distal to the dimer interface, two loops (LP1 & LP0) and a helix ($\alpha 0$) define the extended substrate binding site (P3, P4) in the structure of inhibited hCMV Pr (Tong *et al.*, 1998). In KSHV Pr, a crystal contact near loop 1 (LP1: residues 43{34}-58{41}), helix $\alpha 0$ (residues 37{28}-42{33}) and loop 0 (LP0: residues 23{14}-37{28}) appears to disrupt the conformation of these structures. LP1 of KSHV Pr parallels strand $\beta 3$, unlike in other herpesviral protease structures where it follows strand $\beta 6$, resulting in a backbone C_{α} difference for KSHV Pr LP1 of up to 7Å. In KSHV Pr, helix $\alpha 0$ is present as a distorted helix in one monomer, while LP0 is disordered in both. The absence of LP0 and $\alpha 0$ does not disturb the conformation of either the catalytic residues or the oxyanion hole, nor does it preclude the definition of the S1 binding pocket in the current KSHV Pr structure.

Active Site: Catalytic Triad, S1 Binding Site and Oxyanion Hole are Preformed

Structural alignment of KSHV Pr with inhibited and uninhibited herpesviral proteases characterizes the catalytic triad, S1 binding pocket and oxyanion stabilizing loop as being competent for binding and processing of substrate. KSHV Pr's catalytic triad aligns with the catalytic triads of hCMV, HSV-2 and VZV proteases with a rmsd of 0.21, 1.04 and 0.73Å (± 0.15 Å)³. By analogy to other herpesviral proteases, the backbone

amide of Arg165{142}, within the oxyanion-binding loop (residues 164{141}-169{146}), forms the oxyanion-binding site of KSHV Pr (Hoog *et al.*, 1997; Tong *et al.*, 1998) (Fig. 4-4). This oxyanion-binding loop contains the highest concentration of conserved residues in the enzyme family (Gly164{141}, Arg165{142}, Arg166{143}, Gly168{145} and Thr169{146}). Aligning uninhibited hCMV and VZV proteases onto the conserved β -barrel of KSHV Pr, the oxyanion loop of KSHV Pr overlays with that of the other structures with an average rmsd of 0.72 Å for main chain atoms. This structural agreement is comparable to the 0.8Å rmsd seen for the active site residues in the same alignment. Thus, the conformation of the catalytic triad and oxyanion-binding site in KSHV Pr agrees with those of all other herpesviral protease structures.

Mapping the inhibited hCMV Pr S1 binding pocket onto KSHV Pr reveals a shallow binding groove complementary to the herpesviral consensus P1 alanine (Tong *et al.*, 1998) (Fig. 4-4). Contributors to the binding pocket include the active site nucleophile Ser132{114}, the oxyanion loop Arg165{142} and the conserved Leu133{115}. On substrate binding, the carbonyl oxygen and the conserved side chain of Leu133{115} become an acceptor for the backbone amide of the substrate P1 residue and an hydrophobic contact for the P1 side chain (Tong *et al.*, 1998). Leu133{115} and its neighbor, the conserved Val158{135}, adjacent in sequence to the active site residues Ser132{114} and His157{134}, are packed against each other in the core of the β -barrel, such that alignment of the catalytic triad of all herpesviral protease structures brings these side chains into register with an average rmsd of 1.04Å. Together, these conserved non-catalytic residues connect the positions of the substrate-binding pocket and the catalytic residues using both Val158{135} and Leu133{115} (Fig. 4-4).

Dimer Interface: Unique Tertiary Array of Conserved Secondary Structural Elements.

In contrast to the similarity in catalytic architecture among herpesviral proteases, the dimer interface of KSHV Pr differs from that of proteases of the other subfamilies. Like other herpesviral proteases, greater than 80% of the dimer interface of KSHV Pr is formed by helices $\alpha 1$ and $\alpha 5$ (Fig. 4-1). The dimer interface $\alpha 5$ - $\alpha 5$ crossing angle of 18.3° in KSHV Pr is similar to the 19.2° in hCMV, while it is different from the 50° -crossing angle exhibited by the α -herpesviral proteases (VZV and HSV-2). The orientation of the β -barrels between monomers of KSHV Pr resembles that of HSV-2 and VZV, which all differ in orientation from that of hCMV by a 20° rotation about an axis roughly perpendicular to the dimer two-fold symmetry axis. To allow for both the inter- β -barrel orientation of the α -herpesviral proteases (HSV-2 & VZV) and the $\alpha 5$ - $\alpha 5$ interface helical packing of the β -herpesviral protease (hCMV), the dimer interface $\alpha 5$ helices in KSHV Pr are rotated 30° away from each as compared to the homologous $\alpha 5$ helices of hCMV Pr (Fig. 4-5b). This 30° rotation of helix $\alpha 5$ distances it from helix $\alpha 1$, expanding and deepening the KSHV Pr dimer interface groove defined by the two helices. The dimer interface of KSHV Pr presents the conserved dimer interface secondary structural elements of this class of enzymes in a novel tertiary array and demonstrates yet a third mode of dimer interface packing for herpesviral proteases.

Dimer Interface: Disruptive Conservation

Despite the crucial role of the dimer interface as a regulator of catalysis for herpesviral proteases (Pray *et al.*, 1999; Darke *et al.*, 1996; Schmidt & Darke, 1997),

sequence conservation within the interface is limited to residues Leu221{196} and Arg234{209}. The first of these, Leu221{196}, is located in the N-terminal turn of helix $\alpha 5$ and interacts with the catalytic triad through hydrophobic contacts to the side chain of Asp64{Leu47} in KSHV Pr, adjacent in sequence to the active site residue His63{46}. The side chains of the two conserved Arg234{209} are sequestered together, away from solvent in a hydrophobic portion of the dimer interface. The side chains are located in the groove that accepts helix $\alpha 5$ from the other monomer (Fig. 4-1). Each is surrounded by two sets of clustered hydrophobic side chains from within the same monomer, and residues from helices $\alpha 5$ and $\alpha 6$ of the other monomer. Residues Ser162{Ala139}, Val163{Leu140}, and Ile231{206} comprise the first cluster and connect this region to the base of the oxyanion loop (Fig. 4-3). Leu238{213}, Leu235{210} and Tyr230{Phe205} form the second cluster. The size of these clusters and the environment they create for Arg234{209} are conserved with an average side chain volume across the enzyme family for clusters one and two of 309\AA^3 (± 16.51) and 388\AA^3 (± 8.53), respectively. Together, these clusters orient the guanidinium groups of Arg234{209} either parallel to one another, 10\AA apart and separated by waters as in KSHV Pr (Fig. 4-6b) or by a cavity as in HSV-2 Pr, or to interact with each other as seen in hCMV Pr ($\sim 4\text{\AA}$ apart - Fig. 4-6c) and VZV Pr (stacking). Dimerization buries two guanidinium cations within the same region of the dimer interface in all herpesviral proteases.

Discussion

KSHV Pr is the first γ -herpesviral protease to be characterized at atomic resolution. Representative structures from each branch of herpesviridae now allow for a comparison between members of the three herpesviral protease sub-families.

Active Site: Catalytic Efficiency and Active Site Solvent Accessibility

The catalytic triad H-bonding geometry of KSHV Pr and other herpesviral proteases is similar to that of other classes of serine proteases. However, the catalytic triads of herpesviral proteases are more solvent accessible than the catalytic triads of other serine proteases. This exposure may contribute to a tuned catalytic efficiency of herpesviral proteases, which is 100 to 1000-fold lower in k_{cat}/K_m than that seen in the trypsin family (Ünal *et al.*, 1997). Alignment of the catalytic residues Ser132{114}, His63{46}, and His157{134} of KSHV Pr with the catalytic triad Ser195, His57 and Asp102 of trypsin (PDB code 1BTW) overlays the C_α of the three residues with a rmsd of 1.1Å. The His157{134}-N^{ε2} to His63{46}-N^{δ1} H-bond distance in KSHV Pr is 2.66Å, close to the Asp102-O^{δ2} to His 57-N^{δ1} distance of 2.71Å seen in trypsin. O^{δ1} and O^{δ2} of Asp102 are multiply hydrogen bonded within trypsin, and these bonds, in particular the hydrogen bond to His57-N^{δ1}, are completely shielded from solvent. This is in contrast to the hydrogen bonded atoms of His157{134}-N^{ε2} and His63{46}-N^{δ1}, which retain 75% of their exposure to solvent in the context of the whole protein (Fig. 4-7). The initial proteolytic events within the capsid are catalyzed with the protease covalently attached to the assembly protein and thus may occur in a different structural and environmental context than the isolated catalytic domains. Nevertheless, the *in vivo* catalytic activity of

the polyprotein of HSV-1, hCMV and SCMV (Welch *et al.*, 1995) is comparable to that of the isolated protease suggesting that the catalytic parameters may be similar.

Dimer Interface: Structural Variability within a Conserved Regulator of Activity.

Herpesviral proteases dimerize via helices $\alpha 5$ and $\alpha 1$ in a non-conserved fashion, as is evident from the multiple modes of helical packing seen at the dimer interface of herpesviral proteases (Fig. 4-2a & 4-2b). The KSHV Pr structure reveals a third dimerization mode combining topological elements from both the α - and β - herpesviral protease structures, while exhibiting a 30° rotation of helix $\alpha 5$ not seen in other structurally characterized herpesviral proteases. Within a single enzyme small shifts and rotations can be seen at the dimer interface, with hCMV exhibiting changes at the interface on substrate binding (6.5°) or variation in solvent conditions (Tong *et al.*, 1998). Proteins structures with contact interfaces greater than 2000\AA^2 exhibit a tendency for structural reorganization upon oligomerization (Conte *et al.*, 1999). The disproportionately large structural divergence of the dimer interface helices (Fig. 4-2b) among the herpesviral proteases suggests a conservation not of position, but possibly of structural mutability. As has been previously suggested (Qiu *et al.*, 1996; Chen *et al.*, 1996), a structural transition of helix $\alpha 5$ could act as a switch activating the dimeric species of herpesviral proteases.

The use of the interface helices as a route of regulation is uniquely realized in KSHV Pr through the presence of an autolytic site within helix $\alpha 5$. Cleavage at this D-site, between residues 228{203} and 229{204}, removes the 27 C-terminal residues, including one turn of helix $\alpha 5$ and all of helix $\alpha 6$. KSHV Pr Δ , the product of this

cleavage, exhibits no detectable dimerization or activity (Pray *et al.*, 1999). Circular dichroism (CD) studies on KSHV Pr Δ indicate a 47% decrease in helical content compared to dimers of full-length enzyme (Pray *et al.*, 1999). While removal of residues C-terminal to the D-site would reduce helical content by only 17%, the loss of helix $\alpha 6$ combined with the unwinding of the dimer interface helices $\alpha 1$ and $\alpha 5$ would reduce the overall helical content by 52%, in agreement with the CD studies. Recent detection of KSHV Pr Δ in maturing capsids implicates D-site cleavage in committed *in vivo* self-deactivation (Pray, Ganem, Craik, unpublished observations).

Similar spectral changes are seen during the monomer to dimer transition in full-length KSHV Pr (Pray, Craik, manuscript in preparation) as are seen with KSHV Pr Δ . Although CD is an inexact measure of secondary structure, it communicates the degree of structural change that occurs upon D-site cleavage and during the structural transition from monomer to dimer. The most structurally conserved of the herpesviral protease helices (0.88 Å C_{α} rmsd - Fig. 4-2b), helix $\alpha 6$ buttresses the oxyanion hole loop, burying 20% of the loop's surface. Alterations in the structure of helix $\alpha 5$ may affect the conformation of the loop harboring the active site His63{46}, which it contacts, or of helix $\alpha 6$, which it is adjacent to in sequence. Cleavage at the autolytic D-site and monomerization of full-length KSHV Pr may affect activity through the loss of crucial secondary structural elements proximal to the dimer interface ($\alpha 5$ & $\alpha 6$), and the contacts these motifs stabilize near the active site and oxyanion hole.

Dimer Interface: Burial of Two Conserved Arginines and Dimerization Affinity

Despite the burial of a hydrophobic surface area averaging 2000 \AA^2 upon dimerization, herpesviral protease dimers exhibit micromolar dissociation constants. Based on an approximation of 20 cal of binding energy per \AA^2 of hydrophobic area buried, herpesviral proteases would be expected to exhibit binding energies on the order of 40kcal/mol, in stark contrast to the ≈ 10 kcal/mol seen for herpesviral proteases (Pray *et al.*, 1999; Schmidt & Darke, 1997; Margosiak *et al.*, 1996; Cole, 1996; Darke *et al.*, 1996). Comparison of the electrostatic potential of the dimer interface of KSHV Pr in the context of both a monomer and a dimer indicates a large increase in positive potential around Arg234{209} upon dimerization (Fig. 4-6a). The low dimerization affinity of herpesviral proteases may be due, in part, to the charge (Arg234{209}) buried by each monomers within the interface, just as substitution of an unsatisfied charge into the hydrophobic core of some proteins has been shown to be destabilizing by 2 to 9 kcal per mole (Dao-Pin *et al.*, 1991; Stites *et al.*, 1991; Ladbury *et al.*, 1995). The energetic penalty due to reorganization of the dimer interface helices as indicated by CD studies combined with the cost of burying two arginine residues within the dimer interface may reduce the monomer-monomer affinity of KSHV Pr and all herpesviral proteases.

Conclusion

The structure of KSHV Pr, the first determined of a γ -herpesviral protease, defines the active site, the S1 substrate binding pockets, and the dimer interface of this potential antiviral target. The herpesviral protease fold, as initially elucidated by the structures of hCMV Pr, can now be discussed in the context of a comparative analysis incorporating all three branches of herpesviridae. Sequence and structural alignments of KSHV Pr with other herpesviral proteases suggest a structural basis for the weak micromolar dimerization affinities of herpesviral proteases. Burial of a conserved arginine residue (Arg234{209}) provides a structural rationale for the weak dimerization affinity of herpesviral proteases despite their large dimer interface (2500 – 2700 Å²). The observation of yet a third dimer interface conformation for a herpesviral protease, in the KSHV Pr structure, coupled with the relatively large structural divergence of the dimer interface helices supports a model in which these helices undergo an activating structural transition upon dimerization. The information distilled from the structural analysis of the three herpesviral protease sub-families aids in understanding of the dimerization and mechanism of hydrolysis in this family of serine proteases. Structure-based development of inhibitory compounds targeted to the active site or the dimer interface may aid in the clinical treatment of KS, a common AIDS-associated neoplasm, or serve as probes useful in the study of the mechanism and regulation of herpesviral proteases.

Acknowledgement

We thank Richard Morse, Scott Pegg, Andrew Bogan and Janet Finer-Moore for valuable discussions and suggestions for the manuscript. We thank Jolanta Krucinski for advice in the development of crystallization conditions. This work is based upon research conducted at the Stanford Synchrotron Radiation Laboratory (SSRL), which is funded by the Department of Energy (BES, BER) and the National Institutes of Health (NCRR, NIGMS).

Table 4-1. Crystallographic Statistics

Data reduction resolution range (Å)	30-2.2
Unique structure factors	28220
Rmerge (%) ^a	6.2
Average I/σ(I):	17.5
Completeness (%)	99.4
Mosaicity (°)	0.40
Refinement Resolution Range (Å)	30-2.2
Number of Protein Atoms	2994
Number of Water Molecules	195
R _{free} (%) (3σ)	26.0(25.0)
R _{cryst} (%) (3σ) ^b	22.5(21.5)
Average protein B (Å ²)	49.38
Average water B (Å ²)	58.35

^a $R_{\text{merge}} = \frac{\sum |I - \langle I \rangle|}{\sum \langle I \rangle}$

^b $R_{\text{cryst}} = \frac{\sum |F_{\text{obs}} - |F_{\text{calc}}||}{\sum |F_{\text{obs}}|}$

Figures

Figure 4-1: a) Shown here is a schematic representation of the KSHV Pr dimer viewed along the dimer two-fold axis. Secondary structure is represented with helices as cylinders in red, sheets in yellow and loops in blue. Active site residues His157{134}, His63{46}, and Ser132{114} along with dimer interface Arg234{209} are rendered as ball and stick. b) Monomer A is visualized as a stereo diagram with every twentieth residue numbered to indicate chain progression. As above, the active site residues and Arg234{209} are represented as ball and stick.

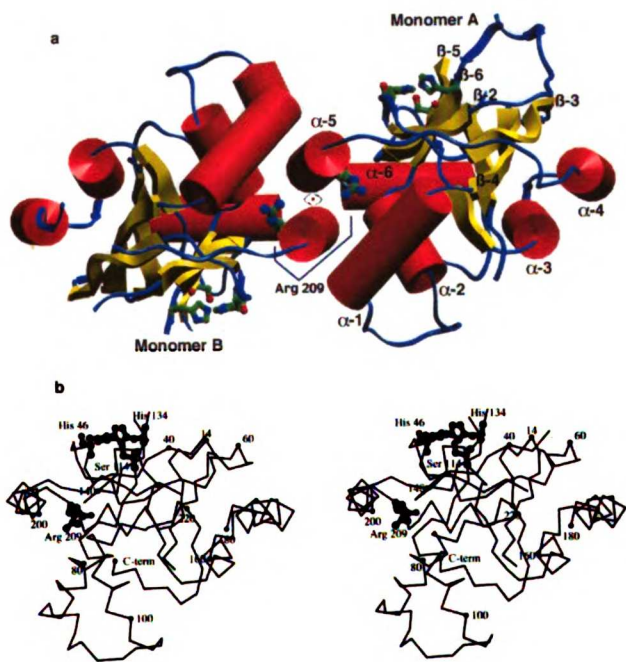


Figure 4-2: It has been suggested that the dimer interface helices may act as a structural switch in the transition from inactive monomer to active dimer (1, 4). The degree of structural divergence of the dimer interface helices of herpesviral proteases suggested a conservation of mutability as a structural switch and not position. a) The four herpesviral proteases were aligned onto the β -barrel of one monomer. RMSD values were then calculated for the β -barrel alone and the β -barrel plus the six conserved helices. 2b) KSHV Pr monomer B was aligned onto the β -barrel of one monomer from hCMV, HSV2 and VZV . Based on this alignment, the rmsd values were calculated for each of the six-conserved α -helices. Included, as error bars, are the average error values for each helix³. The two most variable helices, the dimer interface helices, and the most spatially conserved helix, α_6 , are labeled.

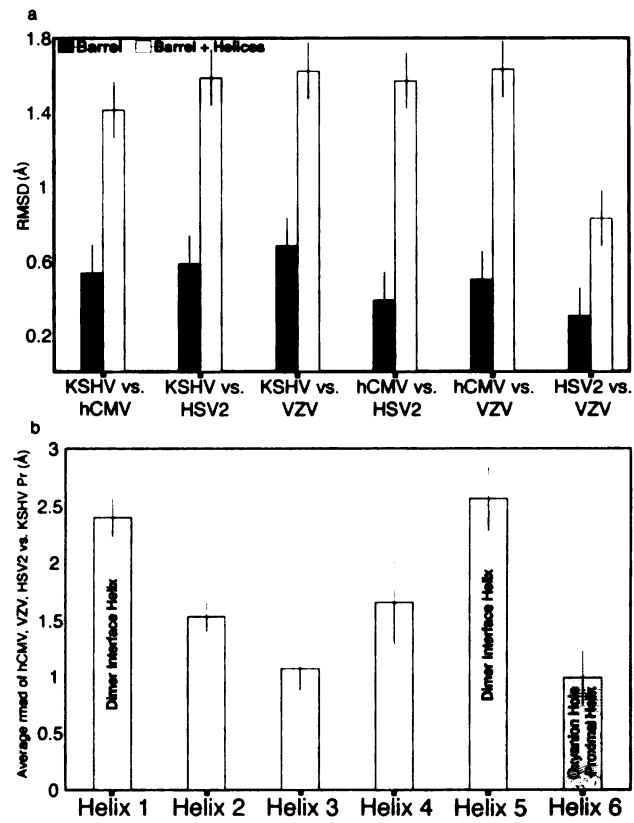
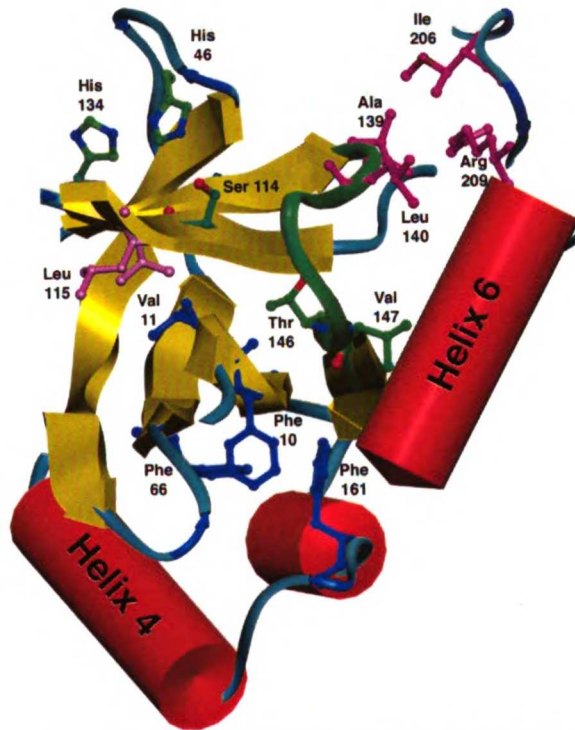


Figure 4-3: Mapping sequence conservation to the structure reveals clusters of residues conserved in both primary sequence and tertiary fold. Residues are colored identically in the multi-sequence alignment and in the structure of KSHV Pr. Active site residues His157{134}, His63{46}, and Ser132{114} reside on the core β -barrel of the enzyme. Colored green in the figure and boxed in blue on the alignment, the oxyanion hole loop contains the highest concentration of conserved residues in the herpesviral protease family. Residues Leu163{140} and Ala162{139}, the N-terminal residues of the oxyanion hole loop, constitute two-thirds of a volumetrically conserved hydrophobic cluster packing against the putative dimer-destabilizing Arg234{209}. In purple, the hydrophobic bundle consisting of Phe83{66}, Phe19{10}, and Phe184{161} lies at the convergence of helices α 3, α 4, and α 6.



	KSHV	GG	D	GI	CT	LD	SS	FO	VS	IC	NG	RR	RC	GA	R	S	F	R	D	L
γ	EBV	CG	E	GL	SA	LD	AS	FD	VS	IC	NG	RR	RC	GA	H	S	F	R	N	V
	Alcelaphine	AG	D	GL	CT	LD	SS	FR	IS	LC	NG	RR	RC	GA	R	Q	F	S	N	I
	Ateline-HV3	AG	D	GV	CV	LD	SS	FO	VS	LC	NG	RR	RC	GA	Q	Y	F	K	D	L
	CMV	GG	A	GL	CL	LD	SS	FR	VS	LC	NG	RR	RC	GA	R	P	Y	R	E	L
	HSV-6	GG	C	GL	CV	LD	SS	FR	VS	VC	NG	RR	RC	GA	R	S	Y	R	K	F
	HSV-7	AG	C	TV	FV	LD	SN	FR	VS	IC	NG	RR	RC	GA	R	S	Y	R	K	F
β	Equine	GG	D	GL	CV	LD	SS	FO	VS	LC	NG	RR	RC	GA	K	T	F	R	N	L
	Marine	GG	T	GL	CL	LD	SS	FR	VS	LC	NG	RR	RC	GA	R	A	Y	A	E	L
	Simian	GG	V	GL	CL	LD	SS	FR	VS	LC	NG	RR	RC	GA	R	P	Y	R	E	L
	HSV-1	AG	A	GP	FV	VH	ST	FA	VS	LC	NG	RR	RC	GA	P	R	M	R	D	W
	HSV-2	AG	A	GP	FV	VH	ST	FA	VS	LC	NG	RR	RC	GA	P	R	M	R	D	W
α	VZV	AG	A	GP	FL	VH	SS	FT	VS	LC	NG	RR	RC	GA	P	R	L	R	D	W
	Bovine	GG	A	GL	FV	VH	SS	FA	VS	LC	NG	RR	RC	GA	P	R	L	R	D	W
				22	3	11	13	22	22	22	22	22	22	22	22	22	22	22	22	22

Figure 4-4: The catalytic triad and oxyanion loop are shown with a model substrate based on the inhibitor-bound hCMV Pr structure. The distances between hydrogen bonding atoms of the catalytic triad, and oxyanion hole reveal the proximity of the oxyanion loop to the catalytic residues and substrate upon binding. The model includes the P1' to P3 residues with the P1 position darkened. A surface of the binding pocket of KSHV Pr is shown superimposed on the active site and colored yellow in regions within 3.0Å of the modeled substrate to indicate the S1 pocket. Regions colored in blue fall between 3.0Å and 4.0Å from the substrate.

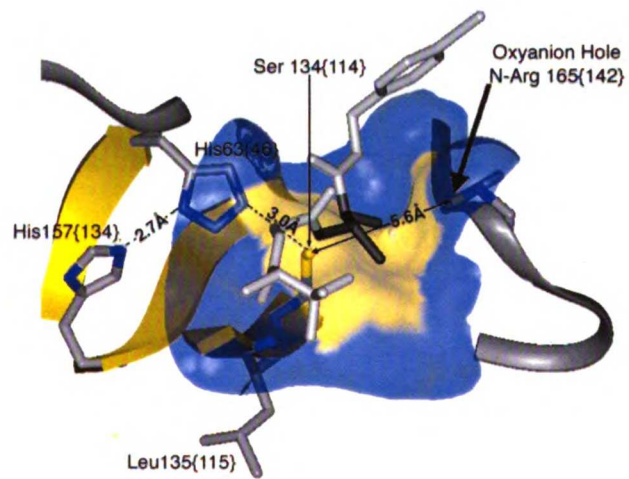


Figure 4-5: The dimer interface of KSHV Pr reveals a third mode of helical packing for a herpesviral protease further characterizing the variability in dimerization of herpesviral proteases. a) Shown here is a view of the van der Waals surface of the KSHV Pr dimer interface in which the dimer two fold is oriented vertically. The surfaces of helices $\alpha 1$ and $\alpha 5$ are colored green. Pictured as ribbons in front of the surface of monomer A (mon A), the monomer B (mon B) β -barrels of KSHV Pr and hCMV Pr are represented in blue and in yellow, respectively. When the β -barrels of both KSHV Pr and hCMV Pr mon A are aligned, the position of hCMV Pr's mon B β -barrel is rotated 20° about an axis roughly perpendicular to the dimer two fold as compared to KSHV Pr mon B. b) Rotated 90° about the vertical with respect to fig. 5a and now looking down the dimer 2-fold axis, fig. 5b further illustrates the 20° difference of the β -barrel of hCMV mon B and shows the 30° rotation of KSHV Pr helix α -5 within the interface.

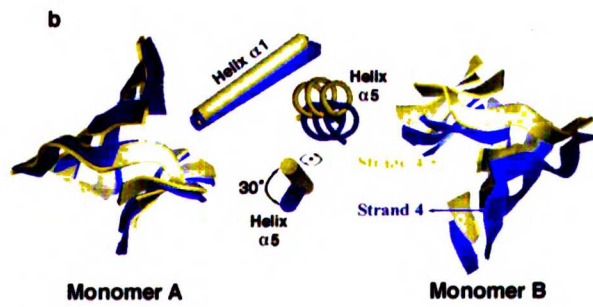
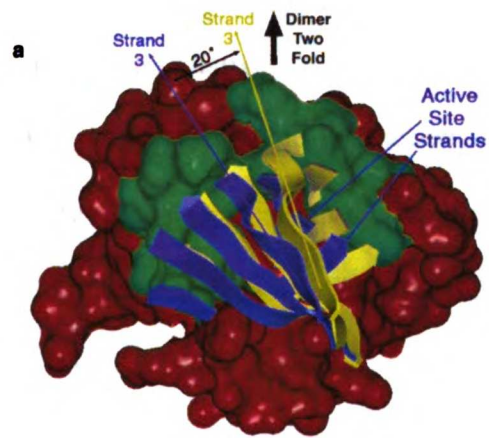


Figure 4-6: Pictured are the unfavorable electrostatic consequences of burying Arg234{209} within the $\approx 2500 \text{ \AA}^2$ dimer interface and the environment of Arg234{209} within the interface. a) A GRASP generated surface of the KSHV Pr mon A dimer interface is shown in which the electrostatic potential is calculated in the context of either the monomer (left) or the dimer (right). Positive potential is represented in blue and negative is shown in red with the two surfaces colored on a common scale. In the left image, the position of Arg234{209} in the dimer interface is highlighted. b) Rotated 90 about the dimer two-fold axis relative to figure 5a, this image shows KSHV Pr Arg234{209} and its few non-hydrophobic interactions within the hydrophobic dimer interface. Electron density ($2F_o - F_c$ contoured at 1σ) is shown for Arg234{209} of one monomer. c) Similar to the presentation in VZV, Arg234{209} of hCMV Pr interacts with its dimer two-fold related arginine (5b and 5c produced using MOLSCRIPT).

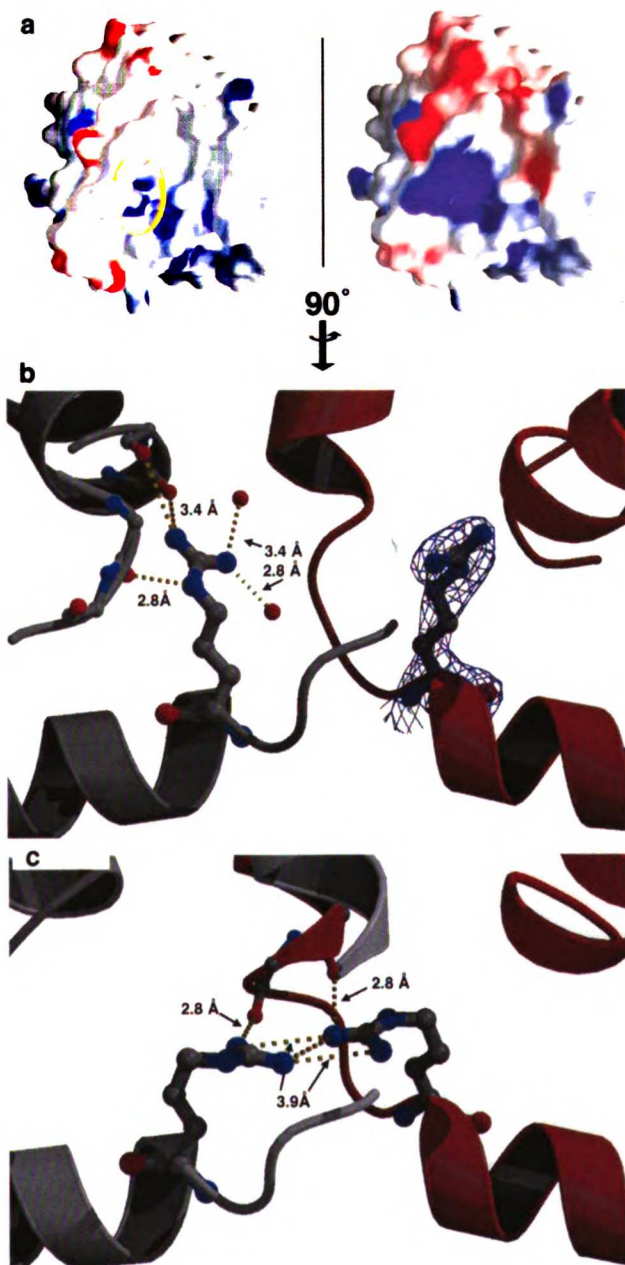
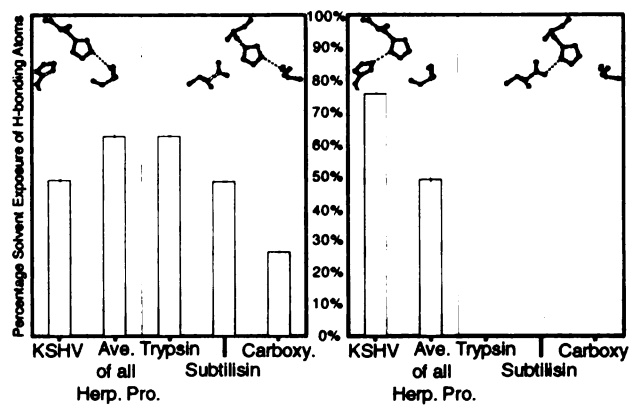


Figure 4-7: KSHV Pr and other herpesviral proteases exhibit similar percent surface area burial of the Ser-His bond, but greater percent solvent accessible surface area for the His-His bond(His-Asp in trypsin) as compared to other serine protease folds. The susceptibility of the His63 {46}-His157 {134} bond to the influences of bulk solvent may be a contributing factor in the reduced catalytic efficiency of herpesviral proteases (100 to 1000-fold as compared to mammalian trypsins). The solvent accessible surface area of the active site hydrogen bonding atoms was calculated in both the context of the entire protein and of only the catalytic triad residues. Represented here is the percentage of surface area still accessible to solvent when the catalytic triad is placed into the active site environment provided by each protease.



Chapter 5

Conformational Change Coupling the Dimerization and Activation of KSHV Protease

Todd R. Pray¹, Kinkead K. Reiling¹, Berj G. Demirjian²,
Robert M. Stroud^{2,3} & Charles S. Craik^{2,3,*}

¹Graduate Group in Biophysics, ²Depts. of Pharmaceutical Chemistry and of
³Biochemistry and Biophysics.

The University of California, San Francisco,
CA 94143

This chapter is in preparation for submission to *Biochemistry*.

ABSTRACT

The mechanism of herpesviral protease activation upon dimerization is poorly understood. In this study, apparently subtle, perhaps global conformational changes have been observed during dimerization of Kaposi's sarcoma-associated herpesvirus protease (KSHV Pr). KSHV Pr dimerization, which has a K_d of 320 nM at 37 °C under optimized buffer conditions, was detected by a greater than 50-fold increase in the enzyme's specific activity. This enzyme appears to acquire enhanced hydrophobic packing within its dimer interface and/or core, as well as altered or shifted secondary structural elements, detected by fluorescence and circular dichroism spectroscopies, respectively. The spectral changes observed are sensitive probes of this enzyme's activation process, as well as of its oligomerization, regardless of the precise structural changes which may occur. KSHV Pr molecules engineered to remain monomeric by site-directed mutagenesis of selected residues within the dimer interface, L196 and M197, are completely inactive, exhibiting the spectroscopic signature and high thermal stability of wild-type, dissociated monomers, denaturing with an apparent T_M of 75 °C. This provides further evidence of the role of oligomerization and possible conformational change in the allosteric activation of herpesviral proteases. In addition, the autoproteolytic inactivation of KSHV Pr at its dimer disruption site (Pray *et al.*, 1999, *J. Mol. Biol.* **289**, 197-203) was detected in capsid particles produced in a tissue culture model of KSHV infection, corroborating the importance of oligomerization and conformational change for this enzyme *in vivo*. Insight into the extent of conformational change possible for this protein fold, which is subject to strict regulatory requirements *in vivo*, may provide a rational basis for understanding the function of dimerization for this class of enzymes essential for herpesvirus pathogenicity.

INTRODUCTION

The recently identified and sequenced human herpesvirus 8 (HHV-8) (Russo *et al.*, 1996), also known as Kaposi's sarcoma-associated herpesvirus (KSHV), is the sexually transmitted, etiological agent for Kaposi's sarcoma (KS), one of the most common AIDS-associated malignancies (reviewed in Ganem, 1997). An enzyme essential to the propagation of all herpesviruses, expressed as a late gene product during lytic viral replication, is each virus' self-encoded protease (reviewed in Roizmann & Sears, 1996 and in Gibson, 1996). These serine proteases, involved in capsid maturation, specifically process the capsid's scaffolding, composed of roughly 10^3 assembly protein (AP) molecules, liberating them from the interior of the viral precursor to allow for the packaging of genomic DNA. The crystal structures of the proteases from KSHV (Reiling *et al.*, 2000), human cytomegalovirus (hCMV) (Qiu *et al.*, 1996; Tong *et al.*, 1996; Shieh *et al.*, 1996; Chen *et al.*, 1996), Varicella Zoster virus (VZV) (Qiu *et al.*, 1997), and herpes simplex virus-1 and -2 (HSV-1 and -2) (Hoog *et al.*, 1997) demonstrate this class of enzymes' novel fold, Ser-His-His active site, and ability to dimerize, which has been implicated in their activation (Darke *et al.*, 1996, Schmidt & Darke, 1997; Margosiak *et al.*, 1996; Cole, 1996; Pray *et al.*, 1999).

Oligomerization for a variety of proteases has been observed, and a structural understanding of the relationship between quaternary assembly and enzymatic activity is beginning to emerge for a number of these enzymes. Perhaps the best-understood case is that of the retroviral proteases, such as that of HIV, which construct a single, shared active site at their dimer interface (Navia *et al.*, 1989; Wlodawer *et al.*, 1989). The protease calpain's catalytic and regulatory subunits heterodimerize and undergo

conformational rearrangement upon Ca^{2+} binding (Hosfield *et al.*, 1999). Other proteases exhibit a wide range of oligomeric properties. For instance: bleomycin hydrolase exhibits dimer and hexamer formation (Joshua-Tor *et al.*, 1995), trypsin - a heparin-stabilized tetramer - has been shown to undergo conformational changes during association/dissociation (reviewed in Sommerhoff *et al.*, 2000), and tricorn protease (Tamura *et al.*, 1996) and the proteasome function as supermolecular assemblies, wherein, at least for the case of the proteasome, oligomerization induces autocatalytic activation of a partial set of the constituent protomers (Chen & Hochstrasser, 1996).

Recently, the ability of herpesviral proteases to undergo structural changes related to oligomerization and/or activation has also become apparent. Structural differences, namely the loss of a large degree of α -helical content, have been observed between active KSHV Pr dimers and truncated KSHV Pr Δ monomers upon autolytic cleavage within a buried position at its dimer interface (Pray *et al.*, 1999). Cleavage at this dimer disruption site (D-site), which *in-activates* KSHV Pr, can be abrogated by point substitution of its P1' Ser204 residue to Gly. KSHV Pr S204G exhibits full wild-type enzyme activity and dimerization (Pray *et al.*, 1999), and has allowed for the structural characterization of this protease (Reiling *et al.*, 2000). The related protease from HCMV has also recently been shown to undergo slight conformational rearrangement upon inhibitor binding using both spectroscopic techniques (Bonneau *et al.*, 1997) and X-ray crystallography (Tong *et al.*, 1998). The finding that herpesviral proteases undergo conformational changes during autolysis and inhibitor binding led to the hypothesis that dimerization may also be an effector of the structural plasticity of these enzymes. In effect, oligomerization of these molecules, and the concomitant ordering of their active

sites, could in this way serve as a zymogen → enzyme switch, distinct from, but analogous to, the regulatory strategies utilized by other classes of proteases (reviewed in Khan & James, 1998).

In this study, utilizing various biophysical analyses, evidence is provided to support the hypothesis that herpesviral proteases require subtle activating conformational changes, which occur only upon oligomerization, in order to be properly regulated. In addition, the observation of autolysis at the dimer interface of KSHV Pr during lytic viral replication indicates that the enzyme undergoes inactivation *in vivo*. The detection of both the full-length and truncated KSHV Pr Δ in viral capsid particles suggests that the enzyme proceeds through different secondary, tertiary and quaternary structural states during the KSHV life cycle.

EXPERIMENTAL PROCEDURES

Protein Purification

KSHV Pr variants were expressed in *Eschericia coli* and purified as described previously (Pray et al, 1999). The total protein concentration of purified samples was determined by measuring their absorbance at 280 nm using a calculated ϵ_{280} of $0.9 \text{ ml mg}^{-1} \text{ cm}^{-1}$, after dilution into 8 M GuHCl to avoid any differences in absorbance between monomeric and dimeric protease molecules.

Virus/Capsid Isolation

BCBL-1 cells were cultured essentially as described (Renne *et al.*, 1994). Late gene expression and lytic replication were induced by the addition of TPA to a concentration of 20 ng/ml. The cultures were then grown for an additional 6 days. To harvest the media supernatant, containing virus particles as well as any nucleocapsids released upon cell lysis, cells were pelleted by centrifugation at 1500 rpm for 10 min at 4 °C. The supernatant was decanted and spun again at 2500 rpm for 10 min at 4 °C. In order to isolate viral and capsid particles, this cleared media was spun in an SW-28 rotor at 15,000 rpm for 2 hr at 4 °C. Following centrifugation, the media was gently aspirated and the pellets from all tubes resuspended in a total volume of 200 μl 1X SDS-PAGE loading buffer and frozen at $-75 \text{ }^\circ\text{C}$ until further analysis could be performed.

Kinetic Assays

KSHV Pr activity assays were performed using a synthetic oligopeptide substrate containing a fluorescence donor-quencher pair flanking the native KSHV M-site

sequence (Pray *et al.*, 1999). The assay buffer contained 0.7 M potassium phosphate (pH 8), 150 mM KCl, 25% (vol/vol) glycerol, 0.1 mM EDTA, 1 mM β -mercaptoethanol. Assays were performed as described (Pray *et al.*, 1999), at the conditions indicated in the text and figure legends. The substrate was stored as a 2.5 mM stock in DMF, and the concentration of DMF kept constant in all assays at 0.8% (vol/vol). The total concentration of substrate in all assays was kept at or below 20 μ M in order to avoid the inner-filter effect (Holskin *et al.*, 1995).

Site-directed Mutagenesis

Mutations encoding for the amino acid substitutions L196A, M197D and M197K were introduced into the KSHV Pr gene by PCR-mediated overlap extension as described previously for S204G and S114A mutations of this protease (Pray *et al.*, 1999). The mutant codons were flanked upstream and downstream by 4 wild-type codons. The integrity of the KSHV Pr ORF and the mutations were verified by DNA sequencing.

Spectroscopy

CD and fluorescence emission spectroscopy were performed essentially as described (Pray *et al.*, 1999). CD scans were performed on a Jasco 710 instrument in 1 cm or 0.2 cm temperature-controlled quartz cuvettes. Mean molar residue ellipticities were obtained after solvent spectrum subtraction and 15-fold signal averaging. Fluorescence emission scans were performed on a JY-SPEX Fluorolog-3 instrument. The excitation wavelength was 275 nm, and scans were solvent corrected and ten-fold

averaged. Emission intensity was normalized to lamp strength (which varied no more than 1%) to yield fluorescence units of cps/ μ A.

RESULTS AND DISCUSSION

Stimulated activity of KSHV Pr upon oligomerization

To examine the possible functional role of dimerization for KSHV Pr, a study was undertaken of the concentration dependence of the enzyme's specific activity. In order to do this, however, an attempt was first made to optimize the KSHV Pr assay conditions to maximize their sensitivity. The k_{cat}/K_M value for KSHV Pr in cleaving its R-site sequence was markedly enhanced to roughly $50,000 \text{ M}^{-1} \text{ min}^{-1}$, with a K_M of $5 \mu\text{M}$ and a k_{cat} of 0.25 min^{-1} . This increase is greater than 50-fold higher than found previously for this enzyme, and was accomplished by increasing the phosphate buffer's concentration from 50 mM to 700 mM and the pH of the buffer medium from 7.0 to 8.0 (Ünal *et al.*, 1997; Pray *et al.*, 1999). This was similar to previous observations made with the proteases from hCMV and HSV-1 (Hall & Darke, 1995; Darke *et al.*, 1996). Using these optimized conditions, KSHV Pr exhibits a striking enhancement of specific activity with increasing total protein concentration at physiological temperature (Figure 5-1). At low concentrations, in the $20 - 50 \text{ nM}$ range, KSHV Pr has very low, but detectable, specific activity on the order of $0.005 - 0.01 \mu\text{M product/min/} \mu\text{M enzyme}$. As the transition from monomer to dimer KSHV Pr is crossed a large stimulation of product turnover, here under nearly saturating substrate concentrations ($20 \mu\text{M}$), is observed. This data was analyzed with a model assuming that the specific activity of KSHV Pr scales directly with the concentration of free dimers in solution, as described previously (Darke *et al.*, 1996; Schmidt & Darke, 1997). This analysis yielded a best-fit K_d of $320 \pm 150 \text{ nM}$ for two independent but simultaneously analyzed data sets. This value, lower than the $1.7 \pm 0.9 \mu\text{M}$ K_d previously observed under less activating conditions (Pray *et al.*, 1999),

agreed with the stimulation of dimerization affinity for HSV-1 and hCMV Pr molecules upon alteration of their solution conditions (reviewed in Waxman & Darke, 2000).

The greater than 50-fold enhancement of the enzyme's specific activity was higher than that detected for HSV-1 and HCMV proteases (Darke *et al.*, 1996; Schmidt & Darke, 1997), while following the same general pattern for these previously characterized enzymes. The greater stimulation of specific activity in this study (50-fold vs. roughly 10-fold) was likely due to heightened assay sensitivity, resulting from the optimized buffer conditions and the use of a cooled photomultiplier tube as a fluorescence emission detector. In order to verify a lack of proteolytic activity of the monomeric form of KSHV Pr, the enzyme's concentration was lowered as far as possible to the limits of detection of the optimized assay. Below protein concentrations of 20 nM, the detection of proteolytic activity for KSHV Pr was not possible. Any activity at these low enzyme levels was masked by the intrinsic noise of the assay conditions. As noted previously for this class of enzymes (reviewed in Waxman & Darke, 2000), the non-detectable activity of KSHV Pr when dimers are not present limits the threshold for high-throughput screening of submicromolar inhibitory compounds against this protease.

Destabilization of KSHV Pr structure and activity upon dimer dissociation

While the enhancement of catalytic activity upon dimerization for herpesviral proteases has been confirmed here for KSHV Pr, the molecular basis for this stimulation has not been addressed experimentally for this class of enzymes. To further understand what possible structural factors effected KSHV Pr activity, the temperature dependence of observed spectral and activity changes was used (Figure 5-2). In panel A, it can be

seen that at 2.5 μM , the activity of the protease increased with temperature from 20 $^{\circ}\text{C}$ to 40 $^{\circ}\text{C}$, then declined rapidly above 40 $^{\circ}\text{C}$ (Figure 5-2A). In stark contrast, the activity of 250 nM KSHV Pr increased only to 30 $^{\circ}\text{C}$, then decreased rapidly to the nearly undetectable levels seen for the 2.5 μM protease sample at only higher temperatures (Figure 5-2A). The increase in activity between 20 $^{\circ}\text{C}$ and 30 $^{\circ}\text{C}$ for both the 250 nM and 2.5 μM KSHV Pr samples agreed with transition state theory, which predicts a 3-fold rate enhancement for every 10 $^{\circ}\text{C}$ temperature rise (Fersht, 1985). The concentration-dependent inactivation as a function of temperature suggested that the loss of activity was due to the disruption of monomer-monomer association and perhaps an associated conformational change, and not due to a structural perturbation of the dimer alone.

This hypothesis is supported by two spectroscopic assays of protein structure. First, using CD spectroscopy, it was seen that the concentration-dependence of the temperature-induced loss in ellipticity at 222 nm was synchronous with that of the enzyme's activity (Figure 5-2B, C). For both the 250 nM (panel C) and 2.5 μM (panel B) protease samples, the loss of ellipticity at intermediate temperatures, possibly due to changes in secondary structure of the dimer interface α -helices or elsewhere in the protein, paralleled very closely the loss of activity of these enzymes. In addition, it was observed that the high temperature loss in CD signal was due to the global unfolding of dissociated monomers. This interpretation was implied since this transition was the same at both KSHV Pr concentrations with apparent T_M values of 75 $^{\circ}\text{C}$. The transition, however, was irreversible, and the protein samples visibly precipitated upon cooling.

The second, independent, spectroscopic assay monitored the intrinsic fluorescence emission of the enzyme as a function of temperature, and revealed that it also correlated

with the loss of activity in the intermediate temperature regime (Figure 5-3). The decrease in intensity of fluorescence, at least in part, was likely to be dependent on the effect of elevated temperature upon fluorophore emission (Cantor & Schimmel, 1980). However, the change in spectral definition, seen in the loss of the shoulders below 320 nm, and the shift in peak emission wavelength from 335 to 339 nm, both pointed to the possibility that the hydrophobic packing of emitting moieties within the protein overall was somewhat relaxed and more solvent-accessible in the inactive conformation of KSHV Pr. Trp109 is located at the dimer interface of KSHV Pr in the crystal structure of the active, dimeric form of the molecule (Figure 5-4A). This residue likely undergoes a change in environment upon dimer dissociation and interface remodeling. Trp54 and Trp156 are both partially buried near the surface of the enzyme's hydrophobic core in the crystal structure, and do exhibit a slight amount of solvent exposure (Figure 5-4A). The overall change in the emission spectrum of the protein indicates that there may have been a global conformational rearrangement, at least at parts of the protein's surface, upon dimer dissociation, and that the spectral change was not due to a single emitting moiety changing its environment (Figure 5-3). The formal possibility does exist, however, that the change in spectral shape of fluorescence emission was simply due to dimer dissociation and changes at Trp 109, without a global change in the solvent accessibility of the enzyme at regions distal from the dimer interface. In any case, the observed fluorescence change upon KSHV Pr inactivation and dimer dissociation served as a probe of these processes, and suggested, in combination with the CD data and temperature-activity-concentration profile of the enzyme, that KSHV Pr may have undergone both secondary and tertiary structural changes. Such subtle conformational plasticity, possibly

global in its extent within protease monomers, could transmit the activating structural signal from the dimer interface to the active site catalytic residues and/or substrate binding determinants.

Selective perturbation of oligomerization and activity by dimer interface mutagenesis

To further aid in the spectroscopic examination of conformational changes upon dimerization and their role in the positive regulation of KSHV Pr activity, the enzyme was selectively perturbed by site-directed mutagenesis. Two positions, L196 and M197, were chosen within the dimer interface of KSHV Pr to undergo substitution. L196 is conserved across the herpesviral protease family, as previously noted (Reiling *et al.*, 2000), but appears to adopt different packing arrangements in the different structurally characterized enzymes of this fold. In KSHV Pr, L196 contacts both the dimer interface and the loop containing the active site histidine proximal to the nucleophilic Ser (Fig. 5-4B). In HCMV and HSV-1 Pr, on the other hand, this conserved Leu residue displays varied packing orientations. This residue was substituted with an alanine side chain in the context of the autolysis stabilizing S204G mutation (Pray *et al.*, 1999) to create KSHV Pr L196A/S204G. The L196A substitution was proposed to perturb dimerization and/or activity, due to its contacts with both the active site and dimer interface of the protease, if its hydrophobic character was required for the stabilization of either region of the molecule.

The second position chosen for substitution was M197. This residue is not as highly conserved across the herpesviral protease family, but in KSHV Pr this side-chain makes intimate inter-monomer contacts with the 2-fold related M197 across the interface

(Fig. 5-4B). In order to maximally perturb this position it was substituted with either an Asp or Lys residue, once again in the context of the S204G mutation, to create M197D/S204G and M197K/S204G. These substitutions were introduced in an attempt to abrogate the enzyme's ability to homo-dimerize due to the introduction of the repulsive like charges.

Initial expression and purification trials for these dimer interface variants gave an early indication of phenotypic differences between the variant proteins and the dimeric, active KSHV Pr S204G. While both the L196A- and M197D-substituted proteases expressed well in the *E. coli* system developed for KSHV Pr S204G, the M197K variant protease was more rapidly degraded in the bacteria (not shown). The M197D- and L196A-substituted proteases were purified by the protocol developed for KSHV Pr S204G. After the first two chromatographic enrichment steps - butyl sepharose hydrophobic interaction and Mono-Q anion exchange, it appeared that the M197D and L196A substitutions did not perturb the bulk hydrophobic or ionic characteristics of the enzyme (not shown). The only minor difference occurred with the elution of KSHV Pr M197D/S204G from the Mono-Q resin, where it eluted slightly earlier in the NaCl gradient. In contrast to these similar purification profiles, both L196A and M197D substitutions induced a marked loss in dimerization of KSHV Pr during the third chromatographic step. Size-exclusion of these samples over a Superdex-75 preparatory column, at loading concentrations in the range of 2 – 3 mg/ml (~100 μ M), indicated a total loss of detectable oligomerization when compared with the dimerizing wild-type and KSHV Pr S204G molecules (Fig. 5-5). The monomers induced by these mutations eluted slightly earlier than the 22 kD autolytic truncation product, KSHV Pr Δ (Pray *et*

al., 1999), due to the full-length molecules' higher molecular weight of 25 kD. These results were further confirmed by analytical gel-filtration (not shown) in the newly optimized assay buffer used for the kinetic and spectroscopic experiments. Monomers of KSHV Pr S204G were not detected even down to micromolar concentrations at room temperature, consistent with the newly obtained kinetic data where the enzyme's K_d is in the high nanomolar range, and dimers of the mutants were not detected even at up to 10 μ M monomer concentration.

The inability of these engineered KSHV Pr monomers to oligomerize correlated with a complete loss in detectable peptidolytic activity. Using the same synthetic oligopeptide KSHV Pr R-site substrate that was used to characterize the enhanced activity of KSHV Pr S204G under the optimized assay conditions, no product formation was observed even at enzyme concentrations as high as 5 - 10 μ M for the M197D and L196A variants.

Dimer interface KSHV Pr mutants retain near-native monomer structural properties

While the inactivity of these monomeric dimer interface variants was consistent with the same lack of activity for KSHV Pr S204G monomers at low concentrations, it could also have been due to alterations in the overall structure of the mutant monomers. To verify that the M197D and L196A substitutions did not perturb properties other than the dimer interface of KSHV Pr, the same spectroscopic assays were used to examine these monomers as were used to characterize the monomer-dimer transition which occurs at the activation threshold of KSHV Pr S204G. First, the temperature dependencies of the CD spectra for the variant proteases were recorded. Both KSHV Pr M197D/S204G

and L196A/S204G molecules, lacking any concentration dependent loss in ellipticity at intermediate temperatures, exhibited only a single temperature-dependent transition (Figure 5-6A). This behavior corresponded nearly exactly with that observed at high temperature for the active KSHV Pr S204G, which exhibited an apparent T_M of 75 °C (Fig. 5-6A). This indicated that the global thermodynamic stability of dissociated monomers of both active, dimerization-competent S204G molecules, and the inactive dimer-interface mutants, were identical. Thus, the mutations did not perturb detectably the global structure or stability properties of the KSHV Pr monomer.

Wavelength scans, from 200 to 250 nm, of these protease samples at 20 °C indicated that the monomeric, inactive KSHV Pr variants had similar CD spectra (Figure 5-6B). The active, dimeric KSHV Pr S204G, on the other hand, had a much more pronounced spectral minimum at 222 nm (Figure 5-6B), indicating the presence of a different degree of secondary structure content in this quaternary, dimeric state. At 55 °C, where KSHV Pr S204G exhibited minimal activity, its CD spectrum overlaid very closely with those of the inactive dimer interface protease variants M197D/S204G and L196A/S204G at lower temperature (Figure 5-6B inset). These data taken together indicated that the secondary structures of KSHV Pr S204G monomers and the dimer interface variants may be similar, and that the α -helices at the dimer interface were in similar conformations in the different proteins.

While these spectral data demonstrate that there are differences in the CD signal of monomers vs. dimers, the amount of secondary structural change was not able to be resolved computationally. This is in contrast to previous studies of the KSHV Pr \rightarrow KSHV Pr Δ autolytic conversion, where a nearly 50% loss in helical content was

predicted (Pray *et al.*, 1999; Andrade *et al.*, 1993; Merelo *et al.*, 1994). The helical content resolved in this previous study is consistent with the dimeric, active enzyme's crystal structure (Reiling *et al.*, 2000). Numerous software packages were used to try to resolve the secondary structural differences between the dimeric and monomeric full length KSHV Pr species in this current study, but none were able to resolve any difference (not shown). This inability to parse secondary structural content differences between the distinct spectral profiles of KSHV Pr monomers and dimers was likely due to two facts. First, herpesviral protease dimers have a novel fold and the monomers are completely uncharacterized; thus, the tertiary packing of secondary structural elements within these subunits may not be represented adequately in the sets of basis spectra used by currently available structure content prediction software packages. Second, it was not possible to obtain spectral data below 200 nm at 20 °C (or 205 nm at 55 °C) due to aberrant signal intensity (likely due to the large amount of buffer additives in the optimized assay conditions) and the subsequent nonlinear response of the photomultiplier tube on the CD instrument. The inability to collect these data, which are critical in the comparison of secondary structure predictions in current algorithms, hampered this effort.

As an independent spectroscopic probe of possible protein conformational changes, the intrinsic fluorescence emission spectra of KSHV Pr S204G and the two inactive dimer interface variants were collected and compared (Figure 5-7). The spectrum of KSHV Pr S204G at 55 °C, the temperature at which it is inactivated and monomeric (as seen in Figure 5-3), overlaid quite well with the coincident spectra of the constitutively monomeric protease variants at 20 °C (Figure 5-7). This indicates that the overall tertiary fold of the dimer interface variants may resemble that of dissociated

monomers from the active KSHV Pr S204G dimer species. The spectral probes of secondary and tertiary structure thus indicated that the monomeric dimer interface-substituted proteases mimicked the overall stability and conformational state of the native monomers of KSHV Pr, which are competent to dimerize and thus become activated.

Modulation of KSHV Pr dimerization and activity by autolysis during virus replication

As a final check on the importance of the regulation of KSHV Pr dimer interface interactions, a more *in vivo* setting was sought to test the hypothesis that the modulation of oligomerization is significant during viral replication. Although the conformational changes which occur upon monomer → dimer assembly and KSHV Pr D-site cleavage have been documented here and previously (Pray *et al.*, 1999), the linkage between these *in vitro* biophysical studies and the *in vivo* milieu in a KSHV-infected cell has remained uncertain. In particular, the occurrence of KSHV Pr D-site cleavage during viral replication, and the concomitant conversion of KSHV Pr dimers to inactive KSHV Pr Δ monomers, could provide insight into the role of herpesviral protease activation and/or deactivation.

In order to analyze the presence of KSHV Pr and/or KSHV Pr Δ during the viral life cycle in infected cells, an attempt was made to determine whether these molecules could be detected during the replication of KSHV in a tissue culture model. For this purpose the latently infected BCBL-1 cell line was used (Renne *et al.*, 1996). KSHV undergoes lytic reactivation in these cells upon treatment with the phorbol ester TPA, which induces viral late gene expression, including those encoding the protease-assembly protein (Pr/AP) precursor molecule and the separately transcribed AP (Renne

et al., 1996; Ünal *et al.*, 1997). Due to the expression of catalytic amounts of the enzyme, as well as the localization of the protease to viral capsid and/or procapsid structures, KSHV Pr could not be detected by Western immunoblotting in whole lysates of induced BCBL-1 cells (data not shown).

To test the possibility that KSHV Pr was present in released capsid and/or viral particles, these species were isolated from the media fraction of an induced BCBL-1 culture to determine their protease content. Not only was the presence of KSHV Pr confirmed, the occurrence of D-site cleavage was evident (Fig 5-8A). *In vitro* studies have demonstrated that the 203 residue KSHV Pr cleavage product, KSHV Pr Δ (modeled in Fig. 5-8B), neither binds nor inhibits the full-length, 230 residue KSHV Pr molecule (not shown), so it is not likely that this occurs *in vivo*. This is a formal possibility, however, given the uncertain milieu of the capsid interior.

CONCLUSIONS

In this study experimental data are presented supporting a possible mechanism for the stimulation of herpesviral protease activity upon dimerization, wherein the ordering of interface α -helices transmits a structural signal to the molecule's two otherwise independent active sites. Upon this ordering of the catalytic residues and/or substrate binding determinants, there also appears to be a global decrease in solvent exposure of aromatic residues of each KSHV Pr monomer, implying that the hydrophobic core of the enzyme is more tightly ordered. While the positive regulatory role of dimerization has been observed previously *in vitro* for both HSV-1 and HCMV Pr molecules (Darke *et al.*, 1996; Schmidt & Darke, 1997), the presumed and necessary structural coupling has not been elucidated. X-ray crystallographic analyses have allowed for speculation regarding such allostery based on the structure of herpesviral proteases from KSHV, HCMV, HSV-1 and -2 and VZV (Reiling *et al.*, 2000; Qiu *et al.*, 1996; Shieh *et al.*, 1997, Tong *et al.*, 1996; Chen *et al.*, 1996; Qiu *et al.*, 1997; Hoog *et al.*, 1997; Tong *et al.*, 1998). These structural arguments, however, rely upon a static picture of the dimeric, active protease molecules, and cannot directly account for the possible conformational plasticity of this unique class of molecules. These enzymes, which have no detectable significant homology to other proteins in the sequence or structure databases, provide an interesting case study for the allosteric transitions which order active site and/or substrate binding determinants upon monomer-monomer association of proteases. In addition, the data in this study further establish that proteases are capable of the subtle conformational transitions which govern the binding and/or enzymatic activity of a wide range of other molecules such as the globins, kinases, lipases and polymerases.

This study, however, is not the first to note the apparent structural plasticity of a herpesviral protease. HCMV Pr has been observed to undergo changes in the intrinsic tryptophan fluorescence and the aromatic component of HCMV Pr's CD spectrum upon binding of a peptidomimetic inhibitor spanning the S4 to S1' binding pockets (Bonneau et al, 1997). The subtle changes in dimer structure implied by these results were borne out by the crystallographic detection of a slight tertiary reorganization of the molecule when compared to the free enzyme (Tong *et al.*, 1998). The even more pronounced spectroscopic differences seen in this study upon dimerization of KSHV Pr indicate that perhaps even larger conformational changes take place during this event than during inhibitor binding to HCMV Pr. In the crystal structure of inhibitor-bound HCMV Pr, changes within the dimer interface upon inhibitor binding hints at the possible linkage here between the active site and oligomerization, although cooperative substrate binding and/or hydrolysis has not been reported in the literature for any herpesviral protease, or seen by us with KSHV Pr (unpublished observations). The related enzyme from HSV-2, which has been crystallized in the presence and absence of the smaller inhibitor diisopropyl fluorophosphate, did not exhibit the dimer interface rearrangements seen in HCMV Pr, perhaps due to the lack of extended recognition determinants. As of yet, however, there has been no demonstration of substrate-induced dimerization for this class of enzymes.

It thus appears that herpesviral proteases may keep their catalytic residues intrinsically disordered prior to dimerization. Evidence for this is provided by the spectroscopic observation of apparent global conformational changes upon protease dimerization in this study. One important caveat is that the current and past structural

studies on herpesviral proteases have been performed in the absence of its co-translationally expressed substrate, the viral scaffold AP molecule. As in HIV PR, perhaps certain sequences or domains of KSHV AP act in cis (or in trans during oligomeric assembly) to auto-regulate the release of the protease catalytic domain. Then, the allosteric properties (during dimerization and D-site cleavage) of KSHV Pr would become the relevant control mechanism during and after capsid maturation. Proteases characterized to date undergo a controlled activation process (Khan & James, 1998). This process, normally performed utilizing an N-terminal propeptide release mechanism, generally induces order in, and/or releases a blocking motif from, the enzyme's active site. Herpesviral proteases, on the other hand, do not have such zymogen activation sequences, but rather are expressed with C-terminal scaffold molecule fusions, and thus must use a different mechanism of activation. Although the high-resolution molecular details of the structural changes detected here remain to be elucidated, a picture emerges of possible global conformational changes among the herpesviral protease family in order to regulate their activity.

It has been recently demonstrated that HSV-1 Pr is selectively maintained in mature virus particles even though its substrate molecule, the viral scaffolding protein, is removed in order to package viral genomic DNA (Sheaffer *et al.*, 2000). It is possible that KSHV Pr may function in an analogous manner in KSHV, and that D-site cleavage may play some structural and/or functional role in the virion, especially given the conformational changes which have been detected spectroscopically upon D-site cleavage (Pray *et al.*, 1999). These results, combined with the observation in this study of the modulation of KSHV Pr's dimer interface by autolysis during lytic viral

replication in a latently infected human B-lymphocyte cell line from a KS tumor, provide a striking correlation between the *in vitro* regulation and *in vivo* function of herpesviral proteases.

ACKNOWLEDGEMENTS

The authors would like to thank Profs. Don Ganem and Michael Lagunoff for resources and advice regarding KSHV culture and purification. This work was supported by the NIH (C.S.C. & R.M.S., GM56531; T.R.P. and K.K.R., GM08204), by the ARCS Foundation (T.R.P.), and by the UCSF Summer Research Training Program (B.G.D.).

FIGURES

Figure 5-1: Stimulation of KSHV Pr specific activity upon dimerization. Plot of specific activity ([product] formed per minute per μM total enzyme monomer) vs. total enzyme monomer concentration (circles). Assays were performed at $37\text{ }^{\circ}\text{C}$ in $500\text{ }\mu\text{l}$ quartz cuvettes with $20\text{ }\mu\text{M}$ total KSHV Pr M-site substrate and between 20 nM and $10\text{ }\mu\text{M}$ total enzyme. The best fit K_d of $320 \pm 150\text{ nM}$, shown by the solid line, was obtained by simultaneously fitting two independent data sets.

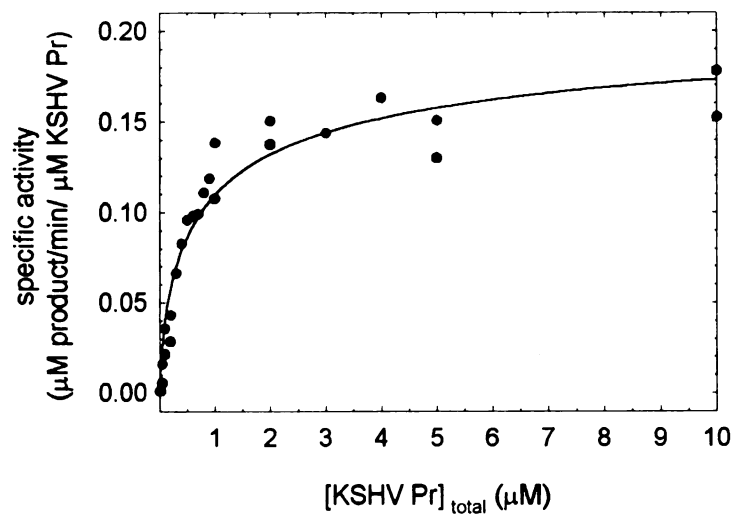


Figure 5-2: Linkage between structural changes and KSHV Pr's dimerization-enhanced activity. Panel A: Overlay of specific activity of 250 nM (filled circles) and 2.5 μ M (open circles) KSHV Pr against cleavage of 20 μ M KSHV Pr M-site substrate. Panel B: 2.5 μ M KSHV Pr temperature-activity profile from panel A (solid circles), overlaid with the enzyme's temperature-dependent change in secondary structure detected by circular dichroism spectroscopy (line). Panel C: The same experiment done with 250 nM KSHV Pr (data from panel A), demonstrating the concentration-dependent increase in activity and stability of the enzyme.

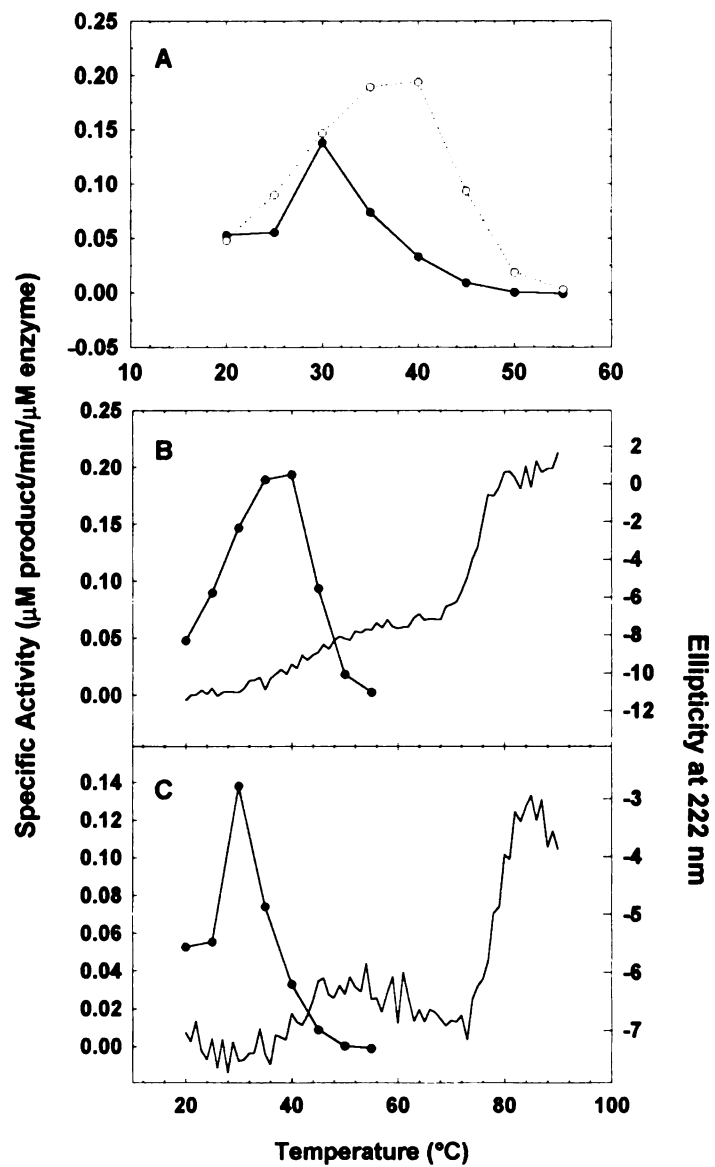


Figure 5-3: Temperature dependence of the fluorescence emission spectrum of KSHV Pr. 2.5 μM KSHV Pr was incubated in assay buffer at the indicated temperatures, and the intrinsic fluorescence emission was excited at a wavelength of 275 nm (20 $^{\circ}\text{C}$, solid; 37 $^{\circ}\text{C}$, dotted; 55 $^{\circ}\text{C}$, dashed). The change in shape and peak emission wavelength of the spectrum indicate possible tertiary structural changes and/or an overall increase in the solvent exposure of the partially buried aromatic residues within the enzyme upon dimer dissociation (see Figure 5-4A for a presentation of the crystal structure of KSHV Pr).

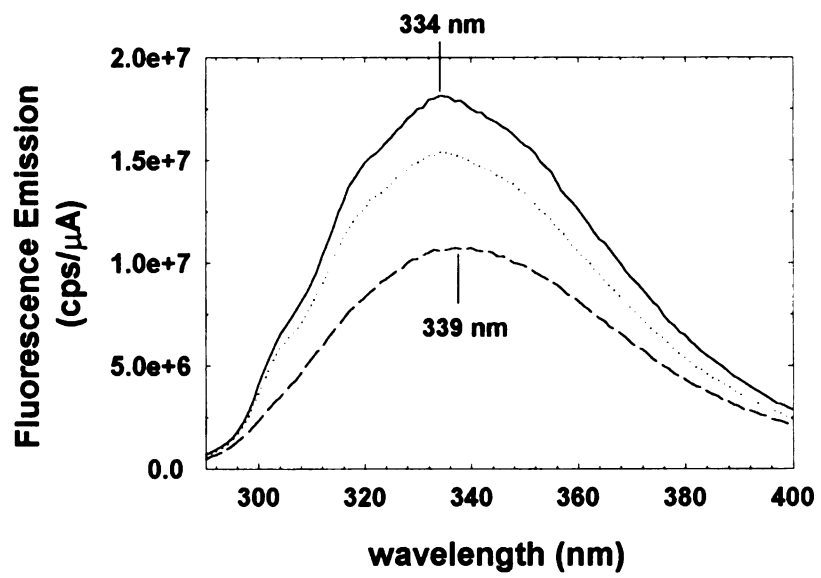


Figure 5-4: A) Structure of KSHV Pr dimer (Reiling *et al.*, 2000). The two active sites are labeled, as are the positions of the three Trp residues present near the surface of each monomer. B) Dimer interface residues chosen for substitution to test the role of oligomerization and structural changes for KSHV Pr are presented. The residue L196, which is absolutely conserved among herpesviral proteases, was substituted with an Ala. The residue M197, which makes intimate dimer-mate contacts, was substituted with the charged residues Lys or Asp.

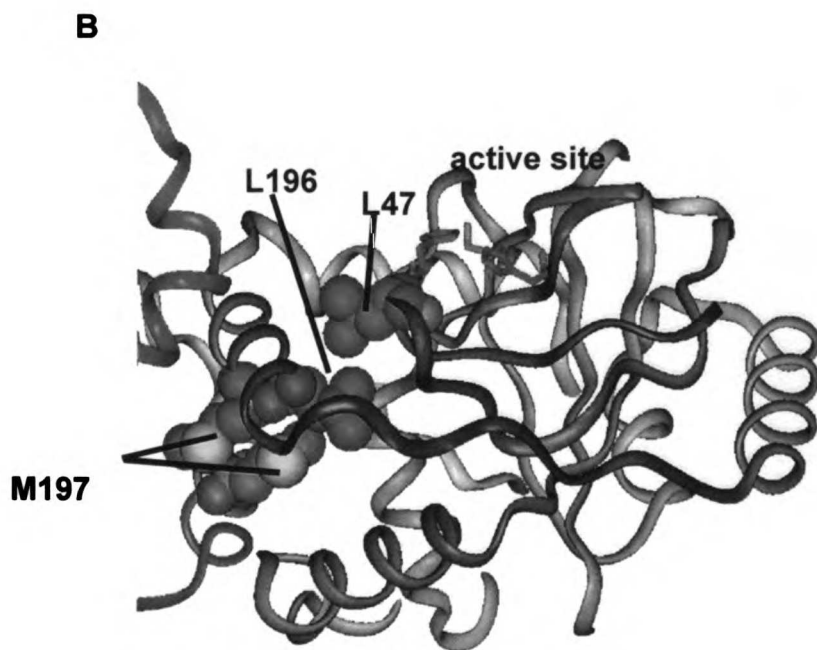
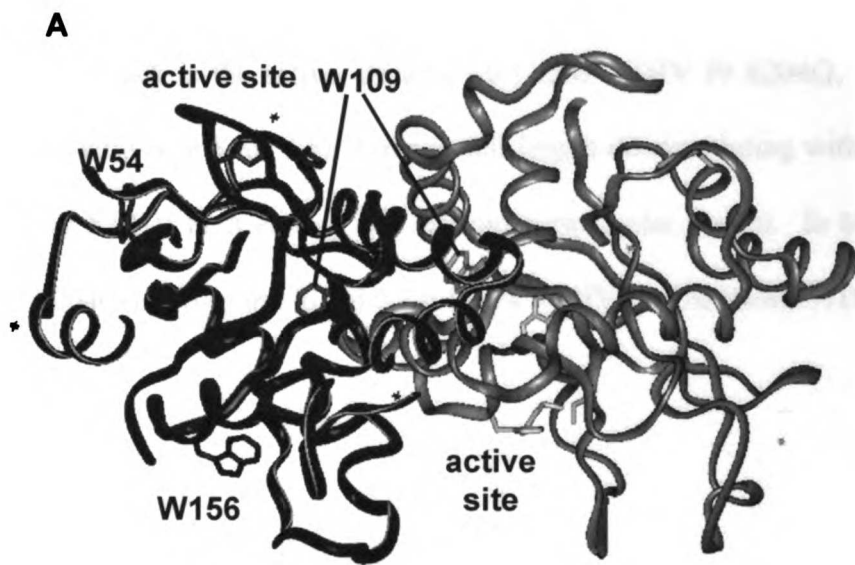


Figure 5-5: Perturbation of dimerization and activity of KSHV Pr by point mutations within its dimer interface. Gel-filtration chromatography shows the loss of detectable dimerization at 0.1 mM of KSHV Pr upon introduction of the point mutations L196A or M197D. In solid black is the active, dimeric ~0.1 mM KSHV Pr S204G. In dashed black is ~0.2 mM wild-type KSHV Pr showing full-length dimers eluting with KSHV Pr S204G, as well as KSHV Pr Δ eluting at a monomer molecular weight. In blue is ~0.1 mM KSHV Pr S204G/L196A, and in red is ~0.1 mM KSHV Pr S204G/M197D.

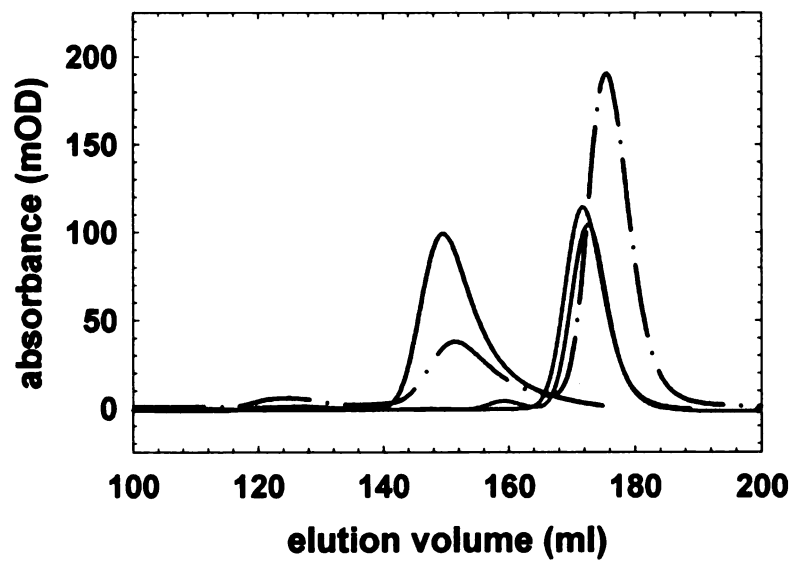


Figure 5-6: Putative alterations in the secondary structure of KSHV Pr upon point mutation within the dimer interface correlate with the monomer-dimer transition of the active enzyme. Panel A: Temperature dependence of ellipticity at 222 nm for these forms of KSHV Pr. Only the dimer form of KSHV Pr S204G (solid) has a low temperature transition, while the mutants, M197D (dotted) and L196A (dashed), appear to exhibit wild-type global stability, denaturing at 75 °C, indicating that the global structural properties of the monomer form of KSHV Pr are unaffected by substitution at the dimer interface. Panel B: CD spectra of 2.5 μ M KSHV Pr S204G, M197D/SG and L196A/SG at 20 °C and 55 °C (inset). (Note: at 55 °C the signal below 205 nm was out of the linear range of the spectrophotometer's detector, so only data from 205 – 250 nm is plotted). The large difference in spectral shape between monomeric and dimeric KSHV Pr at the lower temperature is dramatically reduced upon temperature elevation.

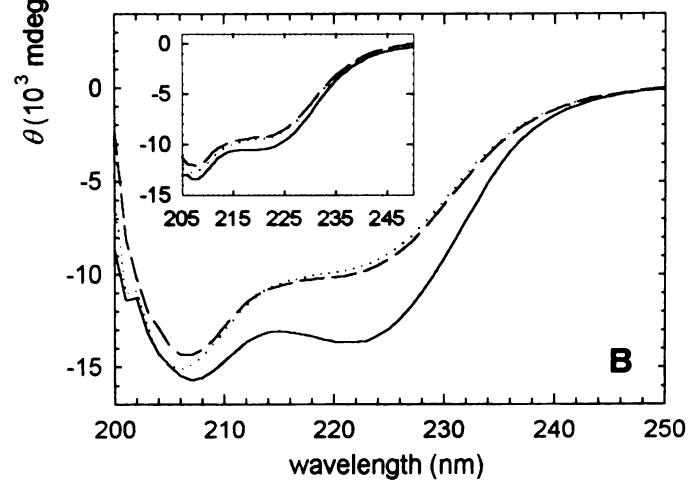
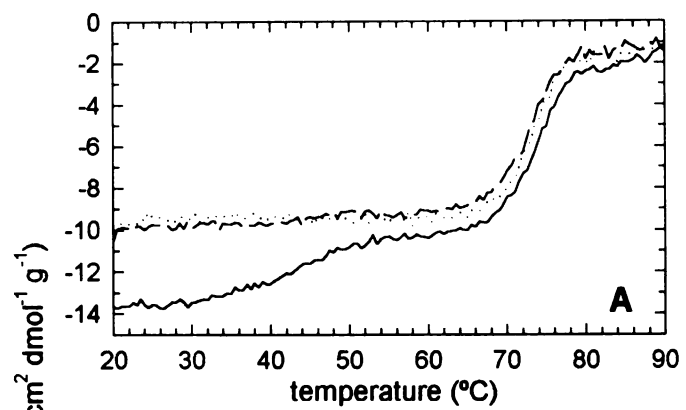


Figure 5-7: Deactivating dimer interface substitutions within KSHV Pr mimic the fluorescence emission spectrum of heat-inactivated monomers of the active enzyme. Fluorescence emission spectra were collected as in Figure 5-3. At 20 °C the emission spectra of KSHV Pr S204G/L196A (blue) and S204G/M197D (red) overlay with the spectrum of KSHV Pr S204G (black) at 55 °C. The wavelength of peak emission for all of the 2.5 μM samples was 339 nm. The emission intensity was lower for the KSHV Pr S204G sample due to the higher temperature, therefore it has been scaled to offer better comparison with the spectral shapes of the monomeric proteins' profiles.

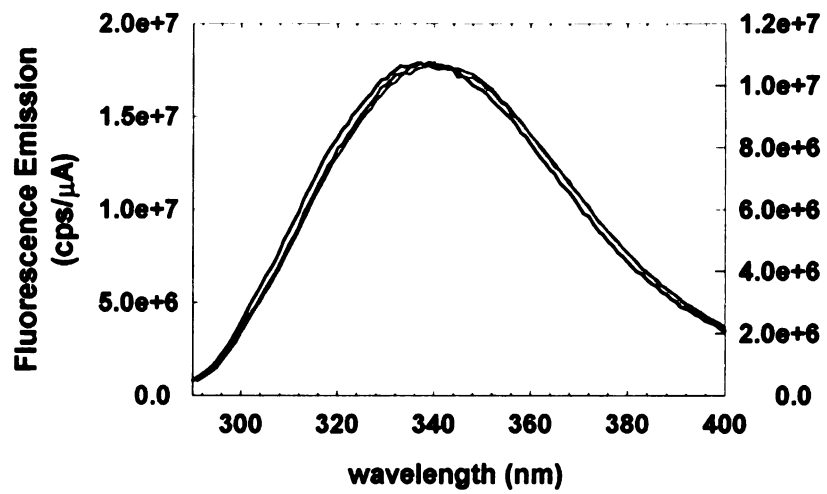
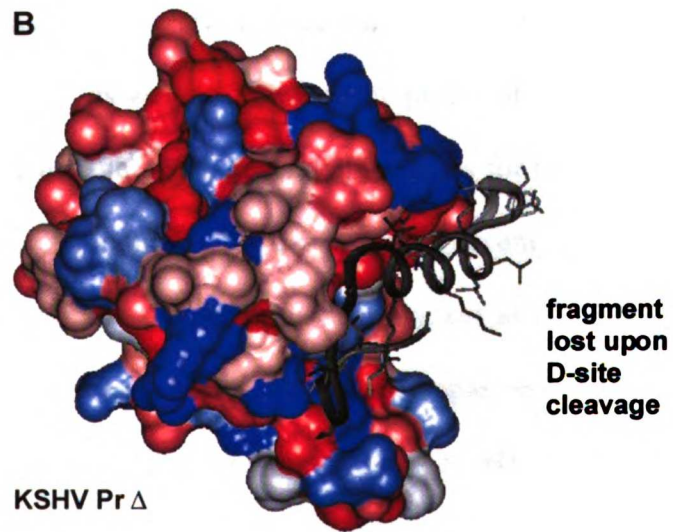
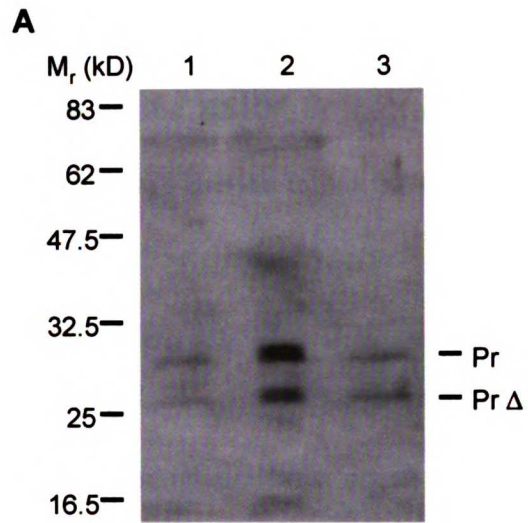


Figure 5-8: Autolysis of KSHV Pr within its dimer interface during viral replication.

Panel A: Detection of KSHV Pr D-site cleavage by western immunoblotting of partially purified viral particles/capsids from the media fraction of TPA-induced BCBL-1 cells.

Panel B) Depiction of the altered molecular surface which may be displayed upon KSHV Pr D-site cleavage. The structure shows a monomer from the dimer structure (Reiling *et al.*, 2000). The surface Connolly rendering, colored according to a hydrophobicity scale, depicts KSHV Pr Δ , and the ribbon represents the peptide released upon autolysis.



Chapter 6

Future Directions

As a final chapter in this thesis, it seemed appropriate to leave a few possible ideas for future exploration of the KSHV Pr system. This, hopefully, will serve to provide new or current members of the lab either novel projects or ideas which they can use to their benefit.

Examination of the Substrate Specificity and Kinetic Mechanism of KSHV Pr

One of the major remaining questions about KSHV Pr surrounds its substrate specificity. A better understanding of what amino acid residues of the enzyme interact with which substrate moieties will have a large impact upon studies of the biological role and regulation of KSHV Pr, as well as on the development of specific inhibitors targeted against the protease's active site. Two general approaches for the optimization of KSHV Pr substrate molecules come to mind. The use of the non-primed side positional scanning combinatorial substrate libraries might be useful (Backes *et al.*, 2000 & Harris *et al.*, 2000) – but perhaps a FRET-pair based assay able to span to the primed side positions (St. Hillaire *et al.*, 1999), would be more applicable to KSHV Pr. Also, substrate phage display, as was done preliminarily (and perhaps not very well) for HSV-1 Pr (O'Boyle *et al.*, 1997), could prove useful for KSHV Pr. These proposed experiments will aid in a number of endeavors including the definition of extended substrate binding pockets for application to inhibitor development and the identification of possible novel protein substrates by database scanning of optimal sequences.

Another fundamental issue surrounding herpesviral proteases and KSHV Pr are these enzymes' kinetic mechanism. Information regarding substrate on- and off-rates, as well as rates of chemical conversion (acylation and deacylation) and product release, should be accessible using stopped-flow assay methodologies as well the examination of different substrate leaving group properties. The results from these studies will also aid in the characterization of putative inhibitor molecules, as well as in the understanding of how the less nucleophilic KSHV Pr serine and the entire active site catalytic triad are able to carry out the enhancement of peptide bond hydrolysis, especially in the more solvent-exposed milieu of the herpesviral protease active site (Reiling *et al.*, 2000). The issues of catalytic mechanism are also intimately related to those of substrate specificity; a study of these two aspects of KSHV Pr activity would form a rigorous and thorough project, especially when performed in the context of the development of specific inhibitors of this enzyme.

Continuation of the Structure-Function Analysis of the Dimer Interface of KSHV Pr

While it has become clear in our studies of KSHV Pr that dimerization is necessary for proteolytic activity, there is a lack of understanding as to the molecular basis of this. It seems that there is some sort of subtle conformational change which occurs upon dimerization and activation, but as of yet we have absolutely no concrete idea of the amino acid residues involved in the allosteric communication between the dimer interface and active sites of KSHV Pr. The experiments presented briefly below are designed to tease such information from this interesting enzyme system.

The obvious first step, and one that is ongoing, is the elucidation of the high-resolution structure of a monomer of KSHV Pr. Anson Nomura is making headway in this regard using NMR spectroscopy, in particular studying the D-site cleavage product, KSHV Pr Δ . Any differences in active site residue configuration and/or overall protein conformation, when compared to the crystal structure of the active dimer (Reiling *et al.*, 2000), will shed light on the mechanism of proteolytic inactivation upon autolysis and monomerization of KSHV Pr. An additional proposal, which has been discussed by Anson, Kinkead Reiling and myself, is attempting to solve the crystal structure of KSHV Pr Δ and/or one of the dimer interface mutants (such as M197D or L196A) which remain monomeric. The NMR structure of one of these full-length mutant monomers might also be attainable, and would be a promising tool in the determination of what residues or regions of the protein undergo changes during the monomer \rightarrow dimer transition. Such information would, of course, not prove any mechanism of allostery for KSHV Pr, but would provide a fascinating picture of what changes do occur as this enzyme is activated.

While the structural information gained in the above-proposed studies would be invaluable, a set of experiments directed at functional aspects of KSHV Pr would complement these efforts. For instance, alanine scanning of the dimer interface helices α -1 and α -5 (Reiling *et al.*, 2000), in addition to residues in what may be considered the "80s loop" of KSHV Pr, may identify a set of residues important in either dimerization or proteolytic activity. Following the purification of these mutant enzymes, our already established dimerization and activity assays, gel-filtration, sedimentation equilibrium and cleavage of the fluorogenic KSHV R-site substrate, would provide energetic and kinetic parameters for each of the alanine-substituted proteins. The results of these studies

would be important and publishable in their own right, as a contribution to understanding the protein binding interface of herpesviral proteases (by changes in the dimerization constant of KSHV Pr). They could also elucidate the molecular role of dimerization in activity by analyzing the relative change of the activity of KSHV Pr with respect to its dimerization parameters for each mutant enzyme.

In addition to being a significant study on its own, the alanine scanning effort would be useful and perhaps even necessary for the development of a functional screen for activators and/or inhibitors of dimerization. Such agents could take the form of a small molecule, an oligopeptide-based structure, or a macromolecule such as a dominant-negative KSHV Pr monomer or another protein altogether. Not only will an alanine scan direct structure-based efforts towards possibly critical regions of the dimerization interface, it will also allow for a more rational approach to designing a genetic screen or selection for effectors of KSHV Pr activity which interact with the monomer form of its dimer interface surface. One possible strategy to develop such a selection would be to engineer a KSHV Pr site, such as its D-site, within an heterologous protein, such as within the linker region of the bacteriophage λ *cI* repressor. This has been performed with HIV protease (Sices & Kristie, 1998), carried out as a screen for bacteria susceptible to lysis due to HIV protease-mediated cleavage of *cI*, and the subsequent loss of immunity to phage infection. A selection for colonies expressing inactive, dimer interface-randomized (at residues other than alanine scan "hotspots") mutant KSHV Pr monomers in the context of wt KSHV Pr which retain immunity, thus surviving lysis, would be one way to develop a dominant negative inhibitor. This strategy could also be modified to exploit the *cI*-mediated repression of phage regulatory sequences upstream of

a drug resistance gene, allowing for the selection of surviving colonies with the mutant KSHV Pr gene of interest. Also, the repression of a toxic gene by *cI* could be used to monitor the attainment or activation of protease activity. Such a strategy could be useful, perhaps, in attempting to identify an active monomer of the enzyme, or in screening putative KSHV Pr activators or inhibitors (such as might be found in a library of expressed cDNA clones).

Other interesting, biochemical assays could also be applied to understanding the energetics of dimerization, protein stability and enzymatic activity of KSHV Pr. Such assays could be used in understanding the activity of the native enzyme, as well as the dimer interface mutants which have already been generated or candidates identified in some of the genetic screening efforts outlined above. For instance, differential scanning calorimetry could be used to measure the enthalpy and heat capacity change of dimerization directly, and the temperature dependence of the K_d of KSHV Pr (measured by the stimulation of its activity), would give the van't Hoff enthalpy associated with this dimerization and activation. The calorimetric parameters thus obtained could be used to speculate regarding possible conformational changes of the enzyme (Spolar & Record, 1994), as well as to understand the forces differentially stabilizing the KSHV Pr dimer and monomer species. Another interesting twist to studying the dimerization of KSHV Pr would be to develop a high-throughput *in vitro* dimerization assay. For instance, the individual members of a FRET pair could be placed on separate preparations of KSHV Pr, and dimerization assayed by following the loss of donor emission or the increase in acceptor emission upon heterodimerization of the two samples. This could be used to test the effect of combinatorial libraries or pools of possible dimer disrupters, and could be

coupled directly to the microplate assay format currently in use in the lab by Alan Marnett to screen active site-directed inhibitors.

Studies of KSHV AP and its Interaction with the Viral Protease

One of the larger questions left in the field of herpesviral proteases in general is if and how their structure and function are modulated by their macromolecular substrate AP molecules. This topic actually formed the basis for my orals proposal, but I was not able to address it experimentally due to having to focus on more protease-centric issues. In addition, from my experience and from anecdotal evidence, it is clear that KSHV AP and its homologs in other herpesviruses are very difficult to work with in a biochemical sense. These molecules' purpose is to form extremely high molecular weight aggregates (on the order of the size of the viral capsid itself); such assemblies are thus not amenable to straightforward solution studies.

This fact was borne out in some preliminary *in vitro* assays performed in our lab. The mature form of AP (mAP), spanning residues between the R-site and M-site, was expressed in *E. coli* as a His-tag fusion in the same vector as our initial protease studies (pQE30) and purified from inclusion bodies. Following purification and resolubilization (see Nealon *et al.*, 2000) of this protein, a number of attempts were made to examine its oligomeric state in solution. Its insolubility and propensity to aggregate, properties likely related to one another, precluded a rigorous study of the protein, but some interesting information was arrived at. While nearly all of the protein in solution was not filterable, the small fraction that was assayed by gel-filtration chromatography on a Superdex 200 analytical column (Figure 6-1). Of this soluble filtrate, the great majority was present as

a large aggregate of apparent molecular mass greater than 600,000 Daltons. However, a significant fraction was also present at what appeared to be the molecular weight of a trimer. This is consistent with the prediction, using the MultiCoil algorithm (Wolf *et al.*, 1997), that all herpesviral AP coiled-coil domains will form trimers rather than dimers, and is also consistent with some preliminary data from tissue culture studies of HSV-1 AP aggregates isolated from capsid assemblies (Newcomb *et al.*, 1999).

Purified KSHV mAP has also allowed for the production of a highly specific and reactive polyclonal antiserum (Figure 6-2), which has been used effectively in tissue culture assays of KSHV Pr substrate processing. Our own studies clearly show the conversion of Pr/AP to AP and mAP in viral capsid assemblies isolated from induced BCBL-1 cells (Figure 6-3). In addition, this antiserum has been used by Dean Kedes' lab (Dean is a recently departed post-doc from Don Ganem's group) at the University of Virginia to characterize the localization and behavior of KSHV AP, and is included in a recently completed manuscript (Nealon *et al.*, 2000).

The above studies could certainly be continued in the Craik lab, in particular in relationship to how AP sequences and structures interact with the catalytic KSHV Pr domain itself. For instance, how does AP trimerization facilitate Pr dimerization? Is a species such as a Pr/AP-AP-AP heterotrimer an inactive protease precursor reservoir, with the Pr domain only becoming activated upon association with another Pr domain from a second heterotrimer? How do the initial R-site cleavage events take place to release Pr from Pr/AP, allowing for it to process the ten-fold molar excess of AP present in the procapsid? Much work is left to be done, and the KSHV Pr project could take on many interesting aspects not yet dealt with in the Craik lab. These structure-function

questions pertaining to the activation of KSHV Pr in the context of AP and in the virus itself will get to the heart of the role of the protease in viral replication. In addition, they may provide a definitive link between the biophysical studies performed so far, and the actual biology of the protease. This connection is what will be needed if the field is to advance to a more realistic picture of herpesviral proteases, their *in vivo* role, and their inhibition to effect desired therapeutic outcomes.

Figure 6-1: Gel filtration of AP showing apparent trimerization. The symbols represent the peak elution volume of sizing standards and KSHV His₆-mAP run on a Superdex 200 HR 10/30 column. The solid line and regression coefficients represent the theoretical relationship between elution volume and molecular weight. The KSHV AP molecule appears to elute as a trimer of 93 kD. Of note is the fact that the majority of AP eluted in the void volume of the column, indicating its ability to form large macromolecular assemblies.

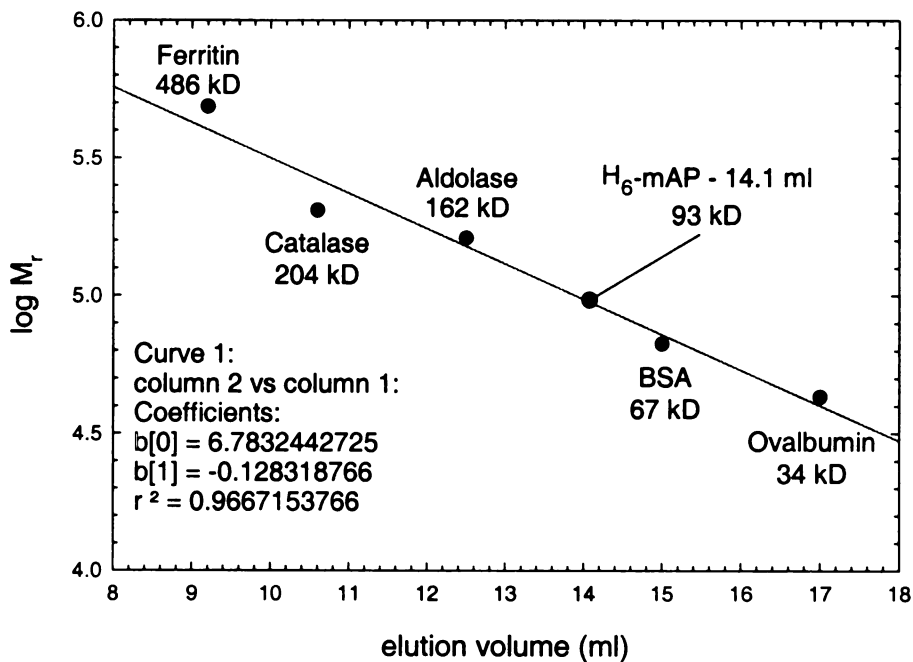


Figure 6-2: Specific immunoreactivity of anti-KSHV mAP antiserum against recombinant and virally produced AP. Lane 1: purified recombinant mAP. Lane 2: pelleted media fraction from induced BCBL-1 cells. Lane 3: induced BCBL-1 whole cell lysate. Lane 4: uninduced BCBL-1 whole cell lysate

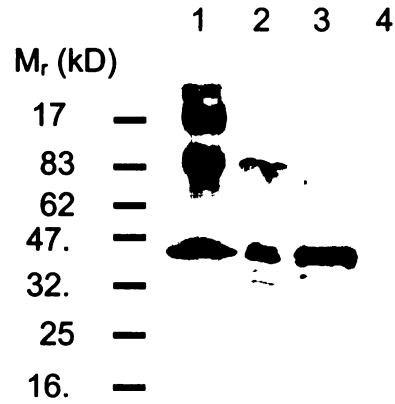
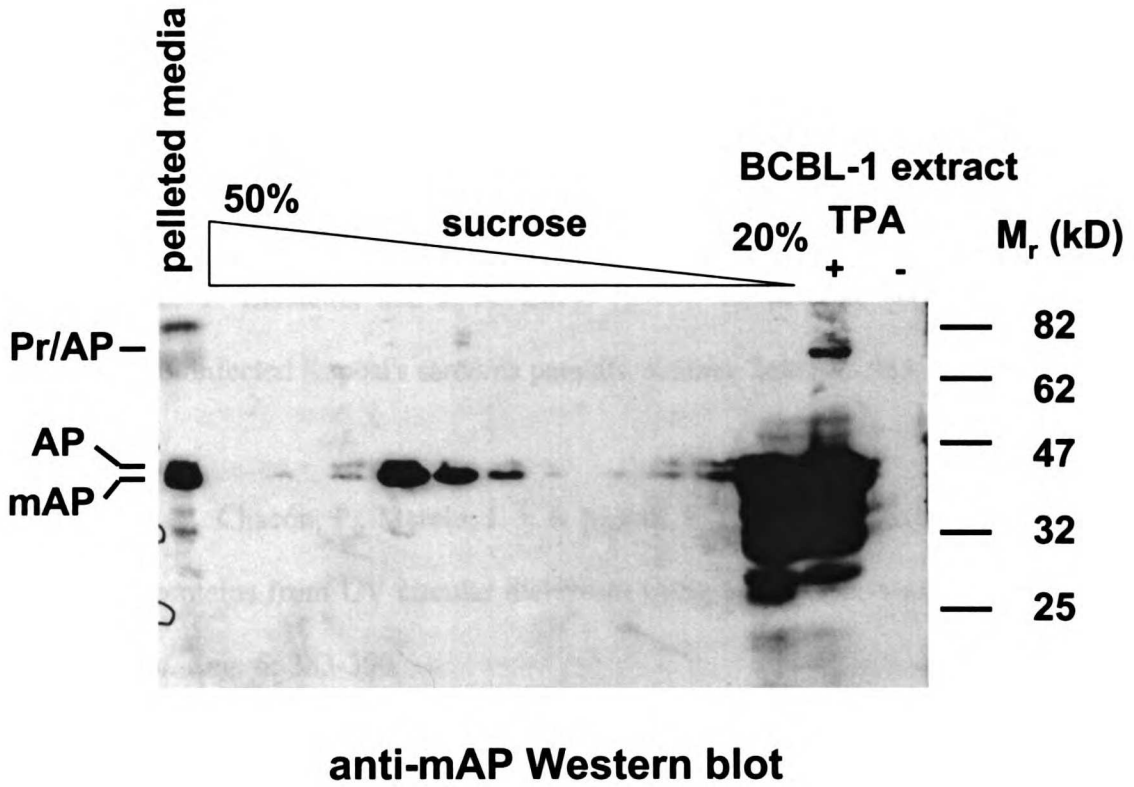


Figure 6-3: Analysis of Pr/AP processing in viral capsid species by sucrose gradient separation.



Bibliography

Albrecht, J. C., J. Nicholas, D. Biller, K. R. Cameron, B. Biesinger, C. Newman, S. Wittmann, M. A. Craxton, H. Coleman, B. Fleckenstein, and R. W. Hones. (1992). Primary structure of the herpesvirus saimiri genome. *J. Virol.* **66**:5047-5058.

Ambroziak, J. A., D. J. Blackbourn, B. G. Herndier, R. G. Glogau, J. H. Gullett, A. R. McDonald, E. T. Lennette, and J. A. Levy. (1995). Herpes-like sequences in HIV-infected and uninfected Kaposi's sarcoma patients. *Science* **268**:582-583.

Andrade, M. A., Chacón, P., Merelo, J. J. & Morán, F. (1993). Evaluation of secondary structure of proteins from UV circular dichroism using an unsupervised learning neural network. *Prot. Eng.* **6**: 383-390.

Ausubel, F. M., R. Brent, R. E. Kingston, D. D. Moore, J. G. Seidman, S. J.A., and K. Struhl. (1990). *Current protocols in molecular biology*. Wiley & Sons, New York, N.Y.

Babé, L. M., J. Rosé, and C. S. Craik. (1992). Synthetic "interface" peptides alter dimeric assembly of the HIV 1 and 2 proteases. *Protein Science* **1**:1244-1253.

Babe, L. M. & Craik , C. S. (1997). Viral proteases: evolution of diverse structural motifs to optimize function. *Cell* **91**: 427-430.

Backes BJ, Harris JL, Leonetti F, Craik CS, Ellman JA. (2000). Synthesis of positional-scanning libraries of fluorogenic peptide substrates to define the extended substrate specificity of plasmin and thrombin. *Nat Biotechnol.* **18**:187-93.

Baum EZ, Beberitz GA, Hulmes JD, Muzithras VP, Jones TR, Gluzman Y. (1993) Expression and analysis of the human cytomegalovirus UL80-encoded protease: identification of autoproteolytic sites. *J Virol.* **67**:497-506.

Beral, V. (1991). Epidemiology of Kaposi's sarcoma [published erratum appears in *Cancer Surv* 1992;12:following 225]. *Cancer Surv.* **10**:5-22.

Beral, V., T. A. Peterman, R. L. Berkelman, and H. W. Jaffe. (1990). Kaposi's sarcoma among persons with AIDS: a sexually transmitted infection? *Lancet* **335**:123-128.

Biggar, R. J., and Rabkin, C. S. (1996) *Hematol Oncol Clin North Am* **10**: 997-1010.

Bonneau, P. R., Grand-Maitre, C., Greenwood, D. J., Lagace, L., LaPlante, S. R., Massariol, M.-J., Ogilvie, W. W., O'Meara, J. A. & Kawai, S. H. (1997). Evidence of a conformational change in the human cytomegalovirus protease upon binding of peptidyl-activated carbonyl inhibitors. *Biochemistry* **36**: 12644-12652.

Boshoff, C., T. F. Schulz, M. M. Kennedy, A. K. Graham, C. Fisher, A. Thomas, J. O. McGee, R. A. Weiss, and J. J. O'Leary. (1995). Kaposi's sarcoma-associated herpesvirus infects endothelial and spindle cells. *Nat. Med.* **1**: 1274-1278.

Brunger, A. T., Adams, P. D., Clore, G. M., DeLano, W. L., Gros, P., Grosse-Kunstleve, R. W., Jiang, J. S., Kuszewski, J., Nilges, M., Pannu, N. S., Read, R. J., Rice, L. M., Simonson, T., and Warren, G. L. (1998) *Acta Crystallogr.* **D54**: 905-21.

Burck, P. J., D. H. Berg, T. P. Luk, L. M. Sassmannshausen, M. Wakulchik, D. P. Smith, H. M. Hsiung, G. W. Becker, W. Gibson, and E. C. Villarreal. (1994). Human cytomegalovirus maturational proteinase: expression in *Escherichia coli*, purification, and enzymatic characterization by using peptide substrate mimics of natural cleavage sites. *J. Virol.* **68**: 2937-2946.

Cantor, C. R. & Schimmel, P. R. (1980). *Biophysical Chemistry*, W. H. Freeman and Co., New York.

Chang J, Ganem D. (2000) On the control of late gene expression in Kaposi's sarcoma-associated herpesvirus (human herpesvirus-8). *J Gen Virol.* **81**:2039-47.

1. The first part of the document discusses the importance of maintaining accurate records of all transactions and activities related to the business. It emphasizes the need for transparency and accountability in financial reporting.

2. The second part of the document outlines the various methods and techniques used to collect and analyze data. It includes a detailed description of the experimental procedures and the tools used for data collection.

Chang, Y., E. Cesarman, M. S. Pessin, F. Lee, J. Culpepper, D. M. Knowles, and P. S. Moore. (1994). Identification of herpesvirus-like DNA sequences in AIDS-associated Kaposi's sarcoma. *Science* **266**:1865-1869.

Chen, P., Tsuge, H., Almassy, R. J., Gribskov, C. L., Katoh, S., Vanderpool, D. L., Margosiak, S. A., Pinko, C., Matthews, D. A. & Kan, C. (1996). Structure of the human cytomegalovirus protease catalytic domain reveals a novel serine protease fold and catalytic triad. *Cell* **86**: 835-843.

Chen P, Hochstrasser M. (1996). Autocatalytic subunit processing couples active site formation in the 20S proteasome to completion of assembly. *Cell*. **86**: 961-72.

Chuck, S., R. M. Grant, E. Katongole-Mbidde, M. Conant, and D. Ganem. (1996). Frequent presence of a novel herpesvirus genome in lesions of human immunodeficiency virus-negative Kaposi's sarcoma. *J. Infect. Dis.* **173**:248-251.

Cole, J. L. (1996). Characterization of human cytomegalovirus protease dimerization by analytical centrifugation. *Biochemistry* **35**: 15601-15610.

Collaborative Computational Project, N. (1994) *Acta Crystallogr.* **D50**: 760-763.

Condra JH, Schleif WA, Blahy OM, Gabryelski LJ, Graham DJ, Quintero JC, Rhodes A, Robbins HL, Roth E, Shivaprakash M, *et al.* (1995) In vivo emergence of HIV-1 variants resistant to multiple protease inhibitors. *Nature*. **374**:569-71.

Conte, L. L., Chothia, C., and Janin, J. (1999) *J Mol Biol* **285**, 2177-98.

Cowtan, K. (1994) *Joint CCP4 and ESF-EACBM Newsletter on Protein Crystallography*, 34-38.

Cox, G. A., M. Wakulchik, L. M. Sassmannshausen, W. Gibson, and E. C. Villarreal. (1995). Human cytomegalovirus proteinase: candidate glutamic acid identified as third member of putative active-site triad. *J. Virol.* **69**:4524-45248.

Craik, C. S., S. Rocznik, C. Largman, and W. J. Rutter. (1987). The catalytic role of the active site aspartic acid in serine proteases. *Science* **237**:909-913.

Dao-pin, S., Anderson, D. E., Baase, W. A., Dahlquist, F. W., and Matthews, B. W. (1991) *Biochemistry* **30**: 11521-9.

Darke, P. L., Cole, J. L., Waxman, L., Hall, D. L., Sardana, M. K. & Kuo, L. C. (1996). Active human cytomegalovirus protease is a dimer. *J. Biol. Chem.* **271**: 7445-7449.

Desai, P., S. C. Watkins, and S. Person. (1994). The size and symmetry of B capsids of herpes simplex virus type 1 are determined by the gene products of the UL26 open reading frame. *J. Virol.* **68**:5365-5374.

DiIanni CL, Mapelli C, Drier DA, Tsao J, Natarajan S, Riexinger D, Festin SM, Bolgar M, Yamanaka G, Weinheimer SP, *et al.* (1993). In vitro activity of the herpes simplex virus type 1 protease with peptide substrates. *J Biol Chem.* **268**:25449-54.

DiIanni, C. L., J. T. Stevens, M. Bolgar, D. R. O'Boyle, S. P. Weinheimer, and R. J. Colonno. (1994). Identification of the serine residue at the active site of the herpes simplex virus type 1 protease. *J. Biol. Chem.* **269**:12672-12676.

Donaghy, G. & Jupp, R. (1995). Characterization of the Epstein-Barr virus proteinase and comparison with the human cytomegalovirus proteinase. *J. Virol.* **69**: 1265-1270.

Eisenhaber, F., Lijnzaad, P., Argos, P., Sander, C., and Scharf, M. (1995) *Journal of Computational Chemistry* **16**: 273-284.

Emini, E. A., W. A. Schleif, D. J. Graham, P. J. Deutsch, F. Massari, H. Teppler, K. E. Squires, and J. H. Condra. (1994). Phenotypic and genotypic characterization of HIV-1

variants selected during treatment with the protease inhibitor L-735,524. Third International Workshop on HIV-1 Drug Resistance, Kauai, Hawaii, USA.

Ensoli, B., G. Barillari, and R. C. Gallo. (1991). Pathogenesis of AIDS-associated Kaposi's sarcoma. *Hematol Oncol Clin North Am.* **5**:281-295.

Evnin, L. B., J. R. Vasquez, and C. S. Craik. (1990). Substrate specificity of trypsin investigated by using a genetic selection. *Proc. Natl. Acad. Sci. USA* **87**:6659-6663.

Fersht, A. (1985). *Enzyme Structure and Mechanism*, 2nd edition. W. H. Freeman and Company. New York.

Ganem, D. (1994). Viruses, cytokines and Kaposi's sarcoma. *Current Biology* **5**:4693.

Ganem, D. (1997). KSHV and Kaposi's sarcoma: The end of the beginning? *Cell* **91**: 157-160.

Gao, M., L. Matusick-Kumar, W. Hurlburt, S. F. DiTusa, W. W. Newcomb, J. C. Brown, P. J. R. McCann, I. Deckman, and R. J. Colonno. (1994). The protease of herpes simplex virus type 1 is essential for functional capsid formation and viral growth. *J. Virol.* **68**:3702-3712.

Gao, S. J., L. Kingsley, M. Li, W. Zheng, C. Parravicini, J. Ziegler, R. Newton, C. R. Rinaldo, A. Saah, J. Phair, R. Detels, Y. Chang, and P. S. Moore. (1996). KSHV antibodies among Americans, Italians and Ugandans with and without Kaposi's sarcoma [see comments]. *Nat. Med.* **2**:925-928.

Gibson, W. (1981). Structural and nonstructural proteins of strain Colburn cytomegalovirus. *Virology* **111**:516-537.

Gibson, W., A. I. Marcy, J. C. Comolli, and J. Lee. (1990). Identification of precursor to cytomegalovirus capsid assembly protein and evidence that processing results in loss of its carboxy-terminal end. *J. Virol.* **64**:1241-1249.

Gibson, W., and B. Roizman. (1972). Proteins specified by herpes simplex virus. 8. Characterization and composition of multiple capsid forms of subtypes 1 and 2. *J. Virol.* **10**:1044-1052.

Gibson, W., A. R. Welch, and M. R. T. Hall. (1994). Assemblin, a herpes virus serine naturational proteinase and new molecular target for antivirals. *Perspectives in Drug Discovery and Design* **2**: 413-426.

Gibson, W. (1996). Structure and assembly of the virion. *Intervirolgy* **39**: 389-400.

Hall DL, Darke PL. (1995) Activation of the herpes simplex virus type 1 protease. *J Biol Chem.* **270**:22697-700.

Harris JL, Backes BJ, Leonetti F, Mahrus S, Ellman JA, Craik CS. (2000) Rapid and general profiling of protease specificity by using combinatorial fluorogenic substrate libraries. *Proc Natl Acad Sci U S A.* **97**:7754-9.

Hayes, D. B., Laue, T. & Philo, J. (1997). Sedimentation Interpretation Program version 1.01. Univ. of New Hampshire. <http://www.bbri.org/RASMB/rasmb.html>.

Holskin, B. P., Bukhtiyarova, M., Dunn, B. M., Baur, P., de Chastonay, J. & Pennington, M. W. (1995). A continuous fluorescence-based assay of human cytomegalovirus protease using a peptide substrate. *Anal. Biochem.* **227**: 148-155.

Holwerda, B. C., Wittwer, A. J., Duffin, K. L., Smith, C., Toth, M. V., Carr, L. S., Wiegand, R. C. & Bryant, M. L. (1994). Activity of two-chain recombinant human cytomegalovirus protease. *J. Biol. Chem.* **269**: 25911-25915.

Hong, Z., M. Beudet-Miller, J. Durkin, R. Zhang, and A. D. Kwong. (1996). Identification of a minimal hydrophobic domain in the herpes simplex virus type 1 scaffolding protein which is required for interaction with the major capsid protein. *J. Virol.* **70**:533-540.

Hoog, S. S., Smith, W. W., Qiu, X., Janson, C. A., Hellmig, B., McQueney, M. S., O'Donnell, K., O'Shannessy, D., DiLella, A. G., Debouck, C. & Abdel-Meguid, S. S. (1997). Active site cavity of herpesvirus proteases revealed by the crystal structure of herpes simplex virus protease/inhibitor complex. *Biochemistry* **36**: 14023-14029.

Hosfield CM, Elce JS, Davies PL, Jia Z. (1999) Crystal structure of calpain reveals the structural basis for Ca(2+)-dependent protease activity and a novel mode of enzyme activation. *EMBO J.* **18**:6880-9.

Huang, Y. Q., J. J. Li, M. H. Kaplan, B. Poiesz, E. Katabira, W. C. Zhang, D. Feiner, and A. E. Friedman-Kien. (1995). Human herpesvirus-like nucleic acid in various forms of Kaposi's sarcoma. *Lancet* **345**:759-761.

Hutchinson, E. G., and Thornton, J. M. (1996) *Protein Sci* **5**: 212-20.

Irmiere, A., and W. Gibson. (1985). Isolation of human cytomegalovirus intranuclear capsids, characterization of their protein constituents, and demonstration that the B-capsid assembly protein is also abundant in noninfectious enveloped particles. *J. Virol.* **56**:277-283.

Jacobson, L. P., Yamashita, T. E., Detels, R., Margolick, J. B., Chmiel, J. S., Kingsley, L. A., Melnick, S., and Munoz, A. (1999) *J Acquir Immune Defic Syndr* 21 Suppl 1: S34-41.

Joshua-Tor L, Xu HE, Johnston SA, Rees DC. (1995) Crystal structure of a conserved protease that binds DNA: the bleomycin hydrolase, Gal6. *Science*. 269: 945-50.

Junker, U., S. Escaich, I. Plavec, J. Baker, F. McPhee, J. R. Rosé, C. S. Craik, and E. Böhnlein. (1996). Intracellular expression of HIV-1 protease variants inhibits replication of wild-type and protease inhibitor resistant HIV-1 strains in human T cell lines. *J. Virol.* 70:7765-7772.

Kaiser E, Colescott RL, Bossinger CD, Cook PI. (1970). Color test for detection of free terminal amino groups in the solid-phase synthesis of peptides. *Anal Biochem.* 34:595-8.

Kedes, D. H., E. Operskalski, M. Busch, R. Kohn, J. Flood, and D. Ganem. (1996). The seroepidemiology of human herpesvirus 8 (Kaposi's sarcoma-associated herpesvirus): distribution of infection in KS risk groups and evidence for sexual transmission [see comments]. *Nat. Med.* 2:918-924.

Khan AR, James MN. (1998). Molecular mechanisms for the conversion of zymogens to active proteolytic enzymes. *Protein Sci.* 7:815-36.

King DS, Fields CG, Fields GB. (1990). A cleavage method which minimizes side reactions following Fmoc solid phase peptide synthesis. *Int J Pept Protein Res.* **36**:255-66.

Kleywegt G.J., J. T. A. (1994) *ESF/CCP4 Newsletter* **31**: 9-14.

Konig, W. & Geiger, R. (1970). [A new method for synthesis of peptides: activation of the carboxyl group with dicyclohexylcarbodiimide using 1-hydroxybenzotriazoles as additives]. *Chem. Ber.* **103**: 788-798.

Kraulis, P. K. (1991) *J. Appl. Cryst.* **24**: 946-950.

Ladbury, J. E., Wynn, R., Thomson, J. A., and Sturtevant, J. M. (1995) *Biochemistry* **34**: 2148-52.

Laemmli, U. K. (1970). Cleavage of structural proteins during the assembly of the head of bacteriophage T4. *Nature* **227**: 680-685.

Lagunoff M, Ganem D. (1997). The structure and coding organization of the genomic termini of Kaposi's sarcoma-associated herpesvirus. *Virology.* **236**:147-54.

Liang, P.-H., Brun, K. A., Field, J. A., O'Donnell, K., Doyle, M. L., Green, S. M., Baker, A. E., Blackburn, M. N. & Abdel-Meguid, S. S. (1998). Site-directed mutagenesis probing the catalytic role of arginines 165 and 166 of human cytomegalovirus protease. *Biochemistry* **37**: 5923-5929.

Liu, F., and B. Roizman. (1992). Differentiation of multiple domains in the herpes simplex virus 1 protease encoded by the UL26 gene. *Proc. Natl. Acad. Sci. USA* **89**:2076-2080.

Liu, F. Y., and B. Roizman. (1991). The herpes simplex virus 1 gene encoding a protease also contains within its coding domain the gene encoding the more abundant substrate. *J. Virol.* **65**:5149-5156.

Loutsch, J. M., N. J. Galvin, M. L. Bryant, and B. C. Holwerda. (1994). Cloning and sequence analysis of murine cytomegalovirus protease and capsid assembly protein genes. *Biochem. Biophys. Res. Commun.* **203**:472-478.

Margosiak, S. A., Vanderpool, D. L., Sisson, W., Pinko, C. & Kan, C. C. (1996). Dimerization of the human cytomegalovirus protease: kinetic and biochemical characterization of the catalytic homodimer. *Biochemistry* **35**: 5300-5307.

Matayoshi, E. D., Wang, G. T., Krafft, G. A. & Erickson, J. (1990). Novel fluorogenic substrates for assaying retroviral proteases by resonance energy transfer. *Science* **247**: 954-958.

Matusick-Kumar, L., McCann, P. J., 3rd, Robertson, B. J., Newcomb, W. W., Brown, J. C., and Gao, M. (1995) *J Virol* **69**: 7113-21.

McPhee, F., A. C. Good, I. D. Kuntz, and C. S. Craik. (1996). Engineering HIV-1 protease heterodimers as macromolecular inhibitors of viral maturation. *Proc. Natl. Acad. Sci. USA* **93**:11477-11481.

Merelo, J. J., Andrade, M. A., Prieto, A. & Morán, F. (1994). Proteinotopic feature maps. *Neurocomputing* **6**: 443-454.

Moore, P., L. Kingsley, S. Holmberg, T. Spira, P. Gupta, D. Hoover, J. Parry, L. Conley, H. Jaffe, and Y. Chang. (1995). Kaposi's sarcoma-associated herpesvirus infection prior to onset of Kaposi's sarcoma. *AIDS* **10**:175-180.

Moore, P. S., and Y. Chang. (1995). Detection of herpesvirus-like DNA sequences in Kaposi's sarcoma in patients with and without HIV infection. *N. Engl. J. Med.* **332**:1181-1185.

Moore, P. S., S. J. Gao, G. Dominguez, E. Cesarman, O. Lungu, D. M. Knowles, R. Garber, P. E. Pellett, D. J. McGeoch, and Y. Chang. (1996). Primary characterization of a herpesvirus agent associated with Kaposi's sarcoma. *J. Virol.* **70**:549-558.

Muller, K., Amman, H. J., Doran, D. M., Gerber, P. R., Gubernator, K., and Schrepfer, G. (1988) *Bull. Soc. Chim. Belg.* **97**: 655-667.

Nagase H, Fields CG, Fields GB. (1994). Design and characterization of a fluorogenic substrate selectively hydrolyzed by stromelysin 1 (matrix metalloproteinase-3). *J Biol Chem.* **269**:20952-7.

Navaza, J. (1994) *Acta Cryst.* **A50**: 157-163.

Navia, M.A., Fitzgerald, P.M.D., McKeever, B.M., Leu, C.-T., Heimbach, J.C., Herber, W.K., Sigal, I.S., Darke, P.L., & Springer, J.P. (1989). Three-dimensional structure of the aspartyl protease from human immunodeficiency virus HIV-1. *Nature* **337**: 615-620.

Nealon, K., Newcomb, W.W., Pray, T.R., Craik, C.S., Brown, J.C., and Kedes, D.H. (2000). Lytic replication of Kaposi's sarcoma-associated herpesvirus results in the formation of multiple capsid species - Isolation and molecular characterization of A, B and C capsids from a gammaherpesvirus. *J. Virol.* submitted.

Newcomb WW, Homa FL, Thomsen DR, Trus BL, Cheng N, Steven A, Booy F, Brown JC. (1999) Assembly of the herpes simplex virus procapsid from purified components and identification of small complexes containing the major capsid and scaffolding proteins. *J Virol.* 73:4239-50.

Nicholls, A., Sharp, K. A., and Honig, B. (1991) *Proteins* 11: 281-96.

Nicholson, P., C. Addison, A. M. Cross, J. Kennard, V.G. Preston and F. Rixon. (1994). Localization of the herpes simplex virus type 1 major capsid protein VP5 to the cell nucleus requires the abundant scaffolding protein VP22A. *J. Gen. Virol.* 75:1091-1099.

O'Boyle, D. R. II, Wager-Smith, K., Stevens, J. T. III & Weinheimer, S. P. (1995). The effect of internal autocleavage on kinetic properties of the human cytomegalovirus protease catalytic domain. *J. Biol. Chem.* 270: 4753-4758.

O'Boyle DR 2nd, Pokornowski KA, McCann PJ 3rd, Weinheimer SP. (1997). Identification of a novel peptide substrate of HSV-1 protease using substrate phage display. *Virology*. **236**:338-47.

O'Callaghan, D. J., and C. C. Randall. (1976). Molecular anatomy of herpesviruses: recent studies. *Prog. Med. Virol.* **22**:152-210.

Otwinowski, Z. (1993) *Data Collection and Processing*.

Pennington, M. (1994). HF cleavage and deprotection procedures for peptides synthesized using a Boc/Bzl strategy. In *Methods in Molecular Biology, vol 35. Peptide Synthesis Protocols* (Pennington, M. W. & Dunn, B. M., ed.), **35**: 41-62. Humana Press, Totowa, NJ.

Perona, J. J., and C. S. Craik. (1995). Structural basis of substrate specificity in the serine proteases. *Protein Sci.* **4**:337-360.

Pray, T. R., Nomura, A. M., Pennington, M. W., and Craik, C. S. (1999). Auto-inactivation by cleavage within the dimer interface of Kaposi's sarcoma-associated herpesvirus protease. *J Mol Biol* **289**: 197-203.

Preston, V. G., M. F. al-Kobaisi, I. M. McDougall, and F. J. Rixon. (1994). The herpes simplex virus gene UL26 proteinase in the presence of the UL26.5 gene product promotes the formation of scaffold-like structures. *J. Gen. Virol.* **75**:2355-2366.

Preston, V. G., J. A. Coates, and F. J. Rixon. (1983). Identification and characterization of a herpes simplex virus gene product required for encapsidation of virus DNA. *J. Virol.* **45**:1056-1064.

Preston, V. G., F. J. Rixon, I. M. McDougall, M. McGregor, and M. F. al Kobaisi. (1992). Processing of the herpes simplex virus assembly protein ICP35 near its carboxy terminal end requires the product of the whole of the UL26 reading frame. *Virology* **186**:87-98.

Qiu, X., Culp, J. S., DiLella, A. G., Hellmig, B., Hoog, S. S., Janson, C. A., Smith, W. W. & Abdel-Meguid, S. S. (1996). Unique fold and active site in cytomegalovirus protease. *Nature* **383**: 275-279.

Qiu, X., Janson, C. A., Culp, J. S., Richardson, S. B., Debouck, C., Smith, W. W. & Abdel-Meguid, S. S. (1997). Crystal structure of the varicella-zoster virus protease. *Proc. Natl. Acad. Sci. USA* **94**: 2874-2879.

Reiling, K.K., Pray, T.R., Craik, C.S., and Stroud, R.M. (2000). Functional consequences of the Kaposi's sarcoma-associated herpesvirus protease structure: Regulation of activity and dimerization by conserved structural elements. *Biochemistry*. **39**: 12796-12803.

Reitz, M. S., Jr., Nerurkar, L. S., and Gallo, R. C. (1999) *J Natl Cancer Inst* **91**: 1453-8.

Renne, R., W. Zhong, B. Herndier, M. McGrath, N. Abbey, D. Kedes, and D. Ganem. (1996). Lytic growth of Kaposi's sarcoma-associated herpesvirus (human herpesvirus 8) in culture. *Nat. Med.* **2**:342-346.

Rixon, F. J., A. M. Cross, C. Addison, and V. G. Preston. (1988). The products of herpes simplex virus type 1 gene UL26 which are involved in DNA packaging are strongly associated with empty but not with full capsids. *J. Gen. Virol.* **69**:2879-2891.

Roizman, B., Desrosiers, R. C., Fleckenstein, B., Lopez, C., Minson, A. C., and Studdert, M. J. (1992) *Arch Virol* **123**: 425-49.

Roizman, B. & Sears, A. E. (1996). Herpes simplex viruses and their replication. In *Fields Virology* 3 edit. (Fields *et al.*, ed.), pp. 2231-2295. Lippincott-Raven.

Russo, J. J., R. A. Bohenzky, M.-C. Chien, J. Chen, M. Yan, D. Maddalena, J. P. Preston Parry, D. Peruzzi, I. S. Edelman, Y. Chang, and P. S. Moore. (1996). Nucleotide sequence of the Kaposi sarcoma-associated herpesvirus (HHV8). *Proc. Natl. Acad. Sci. USA* **93**:14862-14867.

Sheaffer AK, Newcomb WW, Brown JC, Gao M, Weller SK, Tenney DJ. (2000). Evidence for controlled incorporation of herpes simplex virus type 1 UL26 protease into capsids. *J Virol.* **74**:6838-48.

Schalling, M., M. Ekman, E. E. Kaaya, A. Linde, and P. Biberfeld. (1995). A role for a new herpes virus (KSHV) in different forms of Kaposi's sarcoma. *Nat. Med.* **1**:705-706.

Schechter, I., and A. Berger. (1968). On the active site of proteases. 3. Mapping the active site of papain; specific peptide inhibitors of papain. *Biochem. Biophys. Res. Commun.* **32**:898-902.

Schmidt, U. & Darke, P. L. (1997). Dimerization and activation of the herpes simplex virus type 1 protease. *J. Biol. Chem.* **272**: 7732-7735.

Sherman, G., and S. L. Bachenheimer. (1988). Characterization of intranuclear capsids made by ts morphogenic mutants of HSV-1. *Virology* **163**:471-480.

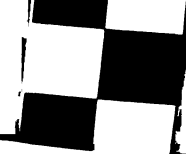
7
21
27

1. The first part of the document discusses the importance of maintaining accurate records of all transactions. It emphasizes that this is essential for ensuring the integrity and reliability of the financial data.

2. The second part of the document outlines the various methods used to collect and analyze data. It describes the different types of data sources and the techniques used to process and interpret the information.

3. The third part of the document provides a detailed overview of the results of the study. It includes a summary of the key findings and a discussion of their implications for the field.

4. The final part of the document concludes with a series of recommendations for future research. It suggests areas where further investigation is needed and provides guidance on how to design and conduct such studies.



Shieh, H., Kurumbail, R. G., Stevens, A. M., Stegeman, R. A., Sturman, E. J., Pak, J. Y., Wittwer, A. J., Palmier, M. O., Wiegand, R. C., Holwerda, B. C. & Stallings, W. C. (1996). Three-dimensional structure of human cytomegalovirus protease. *Nature* **383**: 279-282.

Sices HJ, Kristie TM. (1998). A genetic screen for the isolation and characterization of site-specific proteases. *Proc Natl Acad Sci U S A.* **95**:2828-33.

Sommerhoff CP, Bode W, Matschiner G, Bergner A, Fritz H. (2000). The human mast cell tryptase tetramer: a fascinating riddle solved by structure. *Biochim Biophys Acta.* **1477**: 75-89.

Soulier, J., L. Grollet, E. Oksenhendler, P. Cacoub, D. Cazals-Hatem, P. Babinet, M. F. d'Agay, J. P. Clauvel, M. Raphael, L. Degos, and *et al.* (1995). Kaposi's sarcoma-associated herpesvirus-like DNA sequences in multicentric Castleman's disease. *Blood* **86**:1276-1280.

Spolar RS, Record MT Jr. (1994) Coupling of local folding to site-specific binding of proteins to DNA. *Science.* **263**:777-84.

1. The first part of the document discusses the importance of maintaining accurate records of all transactions. It emphasizes that proper record-keeping is essential for the integrity of the financial system and for the ability to detect and prevent fraud.

2. The second part of the document outlines the specific requirements for record-keeping, including the need to maintain original documents and to keep copies of all transactions. It also discusses the importance of regular audits and the need to ensure that all records are up-to-date and accurate.

3. The third part of the document discusses the consequences of failing to maintain accurate records, including the potential for financial loss and the risk of legal action. It also discusses the importance of training staff on proper record-keeping procedures and the need to ensure that all staff are aware of the importance of accurate record-keeping.

4. The fourth part of the document discusses the importance of maintaining accurate records of all transactions, including the need to maintain original documents and to keep copies of all transactions. It also discusses the importance of regular audits and the need to ensure that all records are up-to-date and accurate.

5. The fifth part of the document discusses the consequences of failing to maintain accurate records, including the potential for financial loss and the risk of legal action. It also discusses the importance of training staff on proper record-keeping procedures and the need to ensure that all staff are aware of the importance of accurate record-keeping.

Stevens, J. T., C. Mapelli, J. Tsao, M. Hail, D. n. O'Boyle, S. P. Weinheimer, and C. L. Diianni. (1994). In vitro proteolytic activity and active-site identification of the human cytomegalovirus protease. *Eur. J. Biochem.* **226**:361-367.

Stites, W. E., Gittis, A. G., Lattman, E. E., and Shortle, D. (1991) *J Mol Biol* **221**: 7-14.

Tamura T, Tamura N, Cejka Z, Hegerl R, Lottspeich F, Baumeister W. (1996). Tricorn protease--the core of a modular proteolytic system. *Science.* **274**: 1385-9.

Thomsen, D. R., L. L. Roof, and F. L. Homa. (1994). Assembly of herpes simplex virus (HSV) intermediate capsids in insect cells infected with recombinant baculoviruses expressing HSV capsid proteins. *J. Virol.* **68**:2442-2457.

Thompson, J. D., Higgins, D. G., and Gibson, T. J. (1994) *Nucleic Acids Res* **22**: 4673-80.

Tigue, N. J., P. J. Matharu, N. A. Roberts, J. S. Mills, J. Kay, and R. Jupp. (1996). Cloning, expression and characterization of the proteinase from human herpesvirus 6. *J. Virol.* **70**:4136-4141.

7

18

2

3

4

5

6

7

8

9

10

11

12

13

14

15

16

17

18

19

20

21

22

23

24

25

26

27

28

Tong, L., Qian, C., Massariol, M., Bonneau, P., Cordingley, M. G. & Lagacé, L. (1996). A new serine protease fold revealed by the crystal structure of human cytomegalovirus protease. *Nature* **383**: 272-275.

Tong, L., Qian, C., Massariol, M. J., Déziel, R., Yoakim, C. & Lagacé, L. (1998). Conserved mode of peptidomimetic inhibition and substrate recognition of human cytomegalovirus protease. *Nat. Struct. Biol.* **5**: 819-826.

Ünal, A., Pray, T. R., Lagunoff, M., Pennington, M. W., Ganem, D. & Craik, C. S. (1997). The protease and the assembly protein of Kaposi's sarcoma-associated herpesvirus (human herpesvirus 8). *J. Virol.* **71**: 7030-7038.

Wang, G. & Krafft, G. (1992). Automated synthesis of fluorogenic protease substrates - design of probes for Alzheimers disease-associated proteases. *Bioorg. Med. Chem. Lett.* **2**: 1665-1668.

Welch, A. R., L. M. McNally, M. R. Hall, and W. Gibson. (1993). Herpesvirus proteinase: site-directed mutagenesis used to study maturational, release, and inactivation cleavage sites of precursor and to identify a possible catalytic site serine and histidine. *J. Virol.* **67**:7360-7372.

Welch, A. R., A. S. Woods, L. M. McNally, R. J. Cotter, and W. Gibson. (1991). A herpesvirus maturational proteinase, assemblin: identification of its gene, putative active site domain, and cleavage site. *Proc. Natl. Acad. Sci. USA* **88**:10792-10796.

Whitby, D., M. R. Howard, M. Tenant-Flowers, N. S. Brink, A. Copas, C. Boshoff, T. Hatzioannou, F. E. Suggett, D. M. Aldam, A. S. Denton, *et al.* (1995). Detection of Kaposi sarcoma associated herpesvirus in peripheral blood of HIV-infected individuals and progression to Kaposi's sarcoma. *Lancet* **346**:799-802.

Waxman L. and Darke P. L. (2000). The herpesvirus proteases as targets for antiviral chemotherapy. *Antivir Chem Chemother.* **11**:1-22.

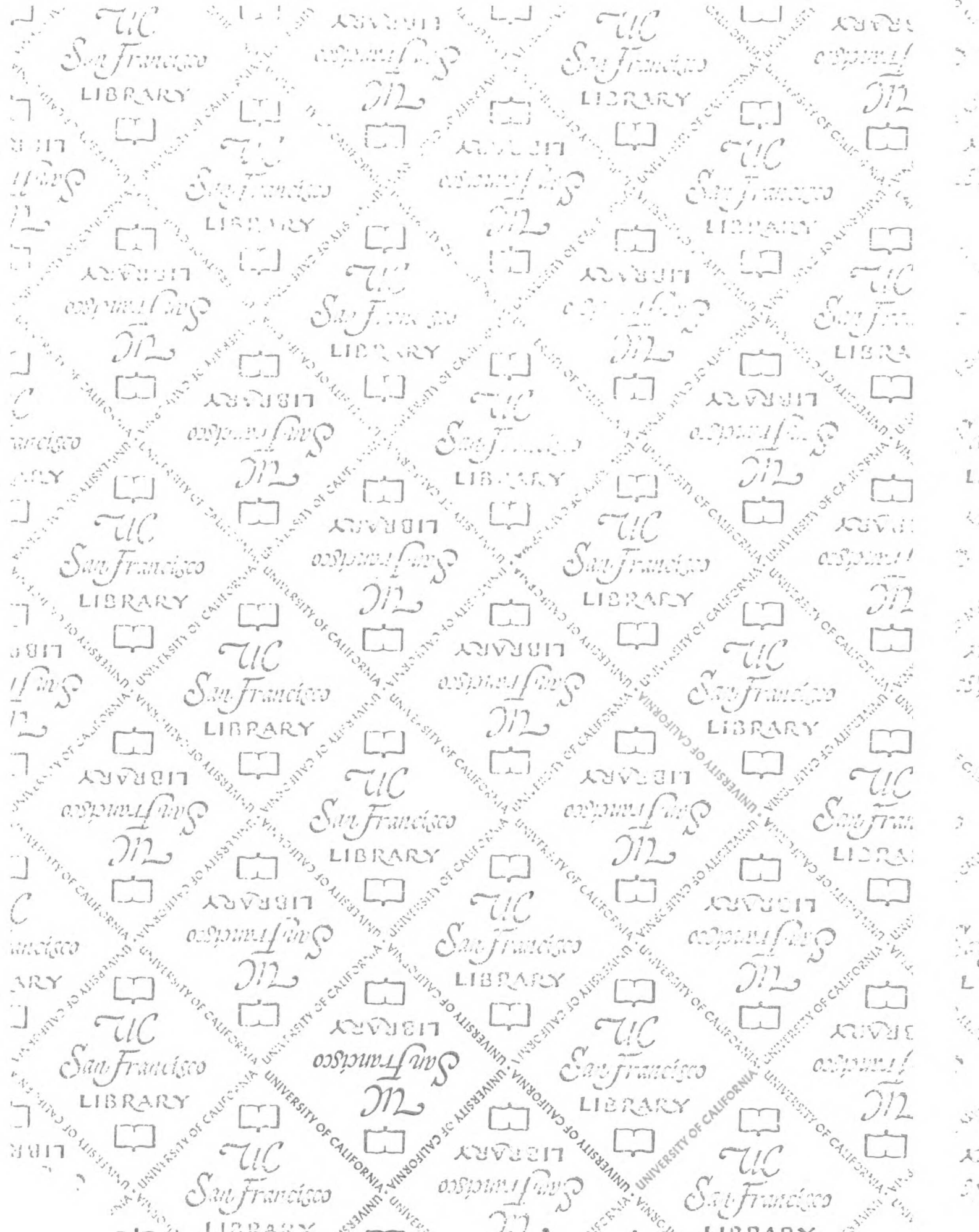
Wlodawer, A., Miller, M., Kaskolski, M., Sathyanarayana, B.K., Baldwin, E., Weber, I.T., Selk, L.M., Clawson, L., Schneider, J., & Kent, S.B.H. (1989). Conserved folding in retroviral proteases: Crystal structure of a synthetic HIV-1 protease. *Science* **245**: 616-621.

Wolf E, Kim PS, Berger B. (1997). MultiCoil: a program for predicting two- and three-stranded coiled coils. *Protein Sci.* **6**:1179-89.

Wood, L. J., M. K. Baxter, S. M. Plafker, and W. Gibson. (1997). Human cytomegalovirus capsid assembly protein precursor (pUL80.5) interacts with itself and

with the major capsid protein (pUL86) through two different domains. *J. Virol.* **71**:179-190.

Zhong, W., H. Wang, B. Herndier, and D. Ganem. (1996). Restricted expression of Kaposi sarcoma-associated herpesvirus (human herpesvirus 8) genes in Kaposi sarcoma. *Proc. Natl. Acad. Sci. USA* **93**:6641-6646.



For reference

Not to be taken
from the room.

7064580



3 1378 00706 4580

